

MODELLING AND APPLICATION OF A BIPEDAL MECHANISM

**A Thesis Submitted to the
Graduate School of Natural and Applied Sciences of Dokuz Eylül University
In Partial Fulfillment of the Requirements for the Degree of Doctor of
Philosophy in Mechanical Engineering, Machine Theory and Dynamics
Program**

**by
Özgün BAŞER**

**October, 2010
İZMİR**

Ph.D. THESIS EXAMINATION RESULT FORM

We have read the thesis entitled “**MODELLING AND APPLICATION OF A BIPEDAL MECHANISM**” completed by **ÖZGÜN BAŞER** under supervision of **PROF. DR. EROL UYAR** and we certify that in our opinion it is fully adequate, in scope and in quality, as a thesis for the degree of Doctor of Philosophy.

.....
Prof.Dr. Erol UYAR

Supervisor

.....
Prof.Dr. Hasan HAVITÇIOĞLU

Thesis Committee Member

.....
Assoc.Prof.Dr. Zeki KIRAL

Thesis Committee Member

.....

Examining Committee Member

.....

Examining Committee Member

Prof.Dr. Mustafa SABUNCU
Director
Graduate School of Natural and Applied Sciences

ACKNOWLEDGMENTS

I would like to show my gratitude to my supervisor Prof. Dr. Erol Uyar for his continuous encouragements, supports and valuable advices during this work. I would also like to thank to Prof. Dr. Hasan Havıtcıođlu and Assoc. Prof. Dr. Zeki Kırıl for their guidance in the discussions on the periodic meetings of this research.

I owe my deepest gratitude to Dr. Levent Çetin, who has made his support available in every part of the work.

I would like to thank Assist. Prof. Dr. Mutlu Boztepe for his supports in the design of electromechanical parts of the experimental setup. I would also like to thank Dr. Murat Akdađ and Taylan Maltaş who helped me very much to construct the mechanical parts of the experimental setup.

I am grateful to all my friends and all my colleagues from Dokuz Eylül University for their supports. I especially would like to thank Dr. Aytaç Gören and Onur Keskin for their technical suggestions about the work, Dr. Alpaslan Turgut and Yetkin Kader for maintaining electronic components for the experimental setup and Osman Korkut and Abdullah Adıyan for their supports in the computer aided design process.

Thanks to my father Prof. Dr. Güngör Başer who has supported me very much not only in this Ph.D. study but also in my whole life. I am also grateful to my brother Argun Başer, to my mother Assist. Prof. Dr. Neş'e Başer and to all my family. They encouraged me very much when I needed mental support and advice.

Finally, I am forever indebted to my wife Tuba Başer and my little son Kaan Başer. They gave me vitality, when I felt most depressed and exhausted. I would like to thank both of them for their patience and for giving me their endless love. This work is dedicated to my son, Kaan Başer whom I missed very much during the hours I was away from him in order to work on this thesis.

Özgün BAŞER

MODELLING AND APPLICATION OF A BIPEDAL MECHANISM

ABSTRACT

Bipedal walking is considered as one of the most important movements of human-being with full of synchronized relative motions of limbs, joints and muscles of both right and left legs with respect to each other, in changing walking velocities. Bipedal walking system is not only composed of dynamic mechanisms but it is also considered as a combination of these mechanisms with various control, sensory and actuator systems.

In this work, basic definitions about bipedal walking are given and based on these definitions, mathematical model of a bipedal walker in sagittal plane is derived. After the solutions for the system dynamics are obtained, model based control of the ankle and hip joint trajectories are achieved by using feed forward compensation methodology and simulation results are carried out.

Bipedal walking researches are not limited only with the two-legged walking robots and models. Walking aid devices are also related with these studies. For this reason a walking aid device which is an artificial hybrid leg having a polycentric knee joint is designed in this study. Polycentric knee joint considered here is a four bar mechanism. Theoretical background of the artificial leg model, including kinematic and dynamic analyses of the leg is explained and then an experimental setup is built. Two different trajectory control structures which are the point to point position control and the feed-forward compensation with disturbance rejection strategy are developed and experienced on the experimental setup. Results which show the performance of the control strategies are given at the end of the study.

Keywords: Bipedal walking, artificial hybrid leg, polycentric knee transfemoral amputation, point to point position control, feed forward compensation, disturbance rejection.

İKİ AYAKLI BİR YÜRÜME MEKANİZMASI MODELLEMESİ VE UYGULAMASI

ÖZ

İki ayaklı yürüme, hem sağ hem sol ayağın uzuvların, eklemlerin ve kasların birbirlerine göre değişik hızlarda senkronize hareket etmesi ile insan hareketlerinin en önemlilerinden bir tanesi olarak sayılmaktadır. İki ayaklı yürüme sistemi, istenen hareketleri yapabilmek için çeşitli kontrol, algılayıcı ve eyleyici sistemler ile birlikte çalışan bir mekanizmalar grubundan oluşmaktadır.

Bu çalışmada, iki ayaklı yürüme ile ilgili temel tanımlamalar verilmekte ve iki ayaklı bir mekanizmanın sajital düzlemde matematiksel modeli oluşturulmaktadır. Sistem dinamiği elde edildikten sonra ileri beslemeli kompanzasyon yöntemi kullanılarak kalça ve ayak bileği yörüngelerinin model tabanlı kontrolü yapılmış ve simulasyon sonuçları ortaya konulmuştur.

İki ayaklı yürüme çalışmaları sadece iki ayaklı yürüme modelleri ve iki ayaklı yürüyen robotlarla sınırlı kalmamaktadır. Yürümeye yardımcı cihazlar da bu çalışma alanı ile ilişkilidir. Bu nedenle, bu çalışmada çok merkezli bir diz eklemine sahip yapay hibrit bacak tasarımı yapılmıştır. Bahsedilen çok eksenli diz mafsalı bir dört kol mekanizmasıdır. Yapay ayak modelinin kinematik ve dinamik analizleri kapsayan teorik altyapı açıklanmış ve daha sonra da bir deney düzeneği kurulmuştur. Noktadan noktaya pozisyon kontrolü ve bozucu girdi etkisini yok eden ileri beslemeli kompanzasyonu şeklinde iki değişik yörünge kontrolü yapısı geliştirilmiş ve deney düzeneğinde denemeleri yapılmıştır. Çalışma sonunda kontrol stratejilerinin performanslarını gösteren sonuçlar verilmiştir.

Anahtar Kelimeler: İki ayaklı yürüme, yapay hibrit bacak, çok merkezli diz mafsalı, noktadan noktaya pozisyon kontrolü, ileri beslemeli kompanzasyon, bozucu girdinin yok edilmesi.

CONTENTS

	Page
Ph.D. THESIS EXAMINATION RESULT FORM	ii
ACKNOWLEDGEMENTS	iii
ABSTRACT	iv
ÖZ	v
CHAPTER ONE – INTRODUCTION	1
1.1 General Remarks	1
1.2 Bipedal Walking.....	3
1.3 Robotics and Historical Development of Bipedal Locomats	5
1.4 Medical Robotics in Bio-mechatronic Applications	13
1.4.1 Surgery Robotics	13
1.4.2 Rehabilitation Devices.....	14
1.4.3 Prosthetic Devices as Artificial Limbs	15
1.4.3.1 Hip Disarticulation.....	15
1.4.3.2 Above Knee Amputation	16
1.4.3.3 Below Knee Amputation.....	19
1.4.3.4 Knee Disarticulation	19
1.4.3.5 Foot Amputation	19
1.5 Aim of the Study	20
1.6 Outline of the Manuscript.....	21
CHAPTER TWO – MATHEMATICAL MODELLING OF BIPEDAL WALKING	23
2.1 Introduction	23
2.2 Mathematical Model of Locomotion.....	23

2.2.1 Inverse Kinematics of Bipedal Walker.....	25
2.2.2 Trajectory Planning for Hip and Knee Articulations in Related Phases ..	27
2.2.2.1 Hip Trajectory Generation	28
2.2.2.2 Ankle Trajectory Generation	29
2.2.3 System Dynamics of Bipedal Walker.....	31
2.2.3.1 Forward Computation	32
2.2.3.2 Backward Computation	33
2.2.4 Actuator Dynamics	35
CHAPTER THREE – MATHEMATICAL MODEL OF AN ARTIFICIAL LEG HAVING POLYCENTRIC KNEE MECHANISM TO BE USED FOR TRANSFEMORAL AMPUTATION.....	38
3.1 Transfemoral Amputation	38
3.1.1 Types of Knee Joint Used in Transfemoral Amputation.....	40
3.1.1.1 Single Axis Knee Joint.....	40
3.1.1.2 Polycentric Knee Joint	41
3.2 Mathematical Model of Artificial Leg Having Polycentric Knee Mechanism	42
3.2.1 Forward Kinematics to Obtain Workspace.....	44
3.2.2 Inverse Kinematics to Follow an Arbitrary Trajectory.....	46
3.2.3 Velocity and Acceleration Analysis	47
3.2.4 Dynamics of the Artificial Hybrid Leg.....	49
CHAPTER FOUR – CONTROL OF ARTIFICIAL HYBRID LEG.....	52
4.1 Introduction	52
4.2 Feed-forward Control	53
4.3 Disturbance Rejection Strategy	55
CHAPTER FIVE – ARTIFICIAL HYBRID LEG DESIGN.....	62
5.1 Introduction	62

5.2 Mechanical Subsystem	64
5.3 Electromechanical Subsystem	67
5.4 Computer Subsystem	69
5.4.1 Digital Input	70
5.4.2 Digital to Analog Conversion	71
CHAPTER SIX – EXPERIMENTAL SETUP	74
6.1 Introduction	74
6.2 Experimental Setup Parameters	75
6.2.1 Artificial Leg Parameters	75
6.2.2 Motor Parameters	77
6.3 Measuring Subsystem	78
6.3.1 Encoders	79
6.3.2 Potentiometer	81
6.3.2.1 Calibrating the Potentiometer	82
6.3.3 Vision-based Measuring Subsystem	83
6.4 Trajectory Generation	85
6.5 Real-Time Monitoring and Control	87
6.5.1 Controller	89
6.5.1.1 Position Control Architecture	89
6.5.1.2 Velocity Control Architecture for the Tracking Problem	93
CHAPTER SEVEN – RESULTS AND DISCUSSIONS	97
7.1 Results	97
7.1.1 Simulation Results of Bipedal Walker	99
7.1.2 Simulation Results of Artificial Hybrid Leg	102
7.1.3 Real-Time Point to Point Control Results of Artificial Hybrid Leg	110
7.2 Discussions and Conclusions	112
REFERENCES	117

CHAPTER ONE

INTRODUCTION

1.1 General Remarks

Locomotion is the basic movement of the animals which is performed in order to interact with the environment. All animals must move, somehow, from one location to another to achieve their daily activities like finding food, mates, or escaping from a predator, an intruder etc. This movement is very crucial for their living since, by changing the environment, they can have the ability to search for various food resources or shelters in other territories. The resulting change of location increases their chance of survival, when they encounter a problem or a dangerous circumstance in their habitat.

The movement of animals on land is called as “terrestrial locomotion”. Among terrestrial locomotion types, legged locomotion is considered as the most sophisticated and remarkable one in which animals move on appendages. The word “walking” is mostly used for this type of locomotion.

Imported aspects of legged locomotion are stance, functional structure of legs and feet, and a certain number of legs. According to these basic concepts, locomotion of animals differs among each other and these differences point to the secrets of the evolution of terrestrial animals from the very basic ones to the most complex one, the human being.

The importance of the stance is that it shows the way the body is supported on the legs. There are three main ways in which animals support themselves by their legs, “the sprawling stance, the semi-erect stance, and the fully erect stance”. The form of the stance of human-being is considered as the erect stance in which the legs are beneath the body. Although this form may not necessarily be the “most-evolved” stance, it is an important fact that by the evolution of fully erect stance human-beings

started to use their upper limbs, i.e. the arms, in a more efficient way by increasing their capacities and abilities of controlling and ruling their environment.

The leg and foot structure is supposed to have evolved in accord with different needs of animals. Mostly, legs of the terrestrial legged animals have the basic form with three joints, namely the shoulder, the knee and the ankle joints; but there are of course some differences in detail. These structural variations allow the animals to gain different abilities. Some may have the ability to move in statically stable manner while others can only move by hopping. Also, the foot structures vary according to the point on the foot where the animal's centre of weight is placed. Some animals use their heels and some of them move on their toes and all these forms have some advantages and disadvantages from the point of view of the stability of locomotion.

Number of legs is considered as the most important aspect of locomotion, since it affects both the stance types and the leg-foot structure of the animals. The number of locomotory limbs varies much between the animals and sometimes even the same living being uses different number of legs according to the circumstances that it encounters. Most of terrestrial animal groups, including most of the mammals, reptiles and amphibians usually use four legs, i.e. they are quadrupedal. A significant number of animals, mostly the insects, use six legs, i.e. they are hexapedals. There are also some other animals using more than six legs, spiders for example, having eight legs or some animals using fourteen legs, but those classifications are far away from the concern of this survey.

A number of animals use only two legs and they are called "bipedals". Most of the members of this group have hopping gait and only human-gait distinguishes from all these types with its alternative walking gait dynamics.

1.2 Bipedal Walking

In this dissertation, walking behaviour of bipedals is going to be studied in order to fully understand its dynamics; hence suitable walking gaits can be improved in various applications to control human-like bipedal locomotion of robotic devices.

The problem of controlling human-like locomotion, i.e. *bipedal locomotion* or *walking of human-being*, in artificial systems can be treated by taking inspiration from biological systems and applying these principles to the walking systems. This branch of robotics is called as *bio-inspired robotics*, and it is by definition, a broad field including synergies from different disciplines: neuroscience, biology, ethology and robotics (Webb & Consi, 2001). Robotics is also a multi-disciplinary field requiring engineering approach to mechanical and electronic systems and to computer science.

The main reason for the great interest of engineers in bio-inspired systems is the fact that bio-robotics provides suitable solutions for the design of efficient walking robots since the nature of the problems in walking that a human-being and a bipedal robot face with is the same. These solutions are very often based on common principles shared by a large variety of animals; so they appear as simple solutions to hard problems. Applications of principles of human walking on bipedal robots has become more feasible in recent days, since significant advances have been made by biologists in understanding human locomotion and at the same time they are interesting topics of study for biologists, since bio-robots are good and realistic instruments to verify a hypothesis regarding the biological model and a good source for new ideas (Frasca, Arena & Fortuna, 2004). Hence, studies done on bipedal locomotion must not only concentrate on engineering approaches to robotic systems, but also on the understanding of the nature of human walking so that the knowledge acquired may be adapted to robotics.

Bipedal walking is considered as one of the most important movement of human-being with full of synchronized relative motions of limbs, joints and muscles of both

right and left legs with respect to each other, in changing walking velocities. Bipedal walking system is composed of a group of mechanisms which work together with various control, sensory and actuator systems in order to make the desired movements. All these systems are biological and the relation between them is one of the most perfect interactions in nature. This perfection makes the bipedal locomotion hard to imitate with ordinary mechanical structures and control techniques. This may be the reason why bipeds attract much interest and are questioned so much in scientific circles.

The pendulum movement of leg around pelvis, which is made within the time interval that foot leaves the contacted surface and touches it again, is called a *step*. Bipedal walking is composed of these consequent steps. While one of the legs makes this pendulum movement (swing leg), the other leg (stance leg) rotates about a fixed point, called *zero moment point (ZMP)* on the ground to carry all load of the body (Katic & Vukobratovic, 2004). As the first step finishes and the second step starts, the legs interchange their duties and the leg previously considered as swing leg acts as stance leg. This continuous interchange gives people the ability to move from one place to another.

Bipedal walking is one of the earliest and effective specializations in humanoid evolution. With the specialization of bipedal walking, human-beings started to use their hands in a more efficient way, gaining the ability of manipulating or grasping objects, carrying food, infants, etc. while they are standing upright or walking on two legs. Also standing upright increases heat loss to air and it reduces the area directly exposed to the sun.

All humans spend most of their time standing on their two legs, which needs significant anatomical changes due to a shift in their posture. The pelvis has to locate the legs beneath the body, which causes the spine to become S-shaped in order to bring the centre of gravity to the appropriate position. The fore limbs, i.e. the arms, must also adapt to this shape making a swinging movement as a balancing aid in walking. In this vertical position, the rib cage must move up and down and it

becomes barrel-shaped in modern humans. Such major changes in anatomy have some consequences causing back problems that most people suffer. These conditions demonstrate that we are still far from being well adapted to an upright life (Darwin, 1871).

There are a number of states of movement associated with bipedal locomotion:

1. Standing: This is the position on both legs. In most bipeds, this position of human requires constant adjustment of the balance of the body maintained by the inner ear.
2. Walking: In this position, one foot is in front of the other. That means, at least one of the feet is on the ground (stance leg) at any time during walking.
3. Running: In this position, one foot is in front of the other as in the walking state. The difference is while running both feet are off the ground with periods.
4. Hopping: This movement is not done naturally by humans. It is described as moving by series of jumps with both feet moving together.

Note that the characteristics of mentioned locomotion states above differ in each circumstance, each describing different constraints and restrictions particularly for that walking type. This fact leads the researchers, biomedicians and engineers to present different dynamics for walking, running and hopping states. Standing is the common point in all these movements and it can be considered as the initial and final phase of each movement, i.e. as the stopping conditions.

1.3 Robotics and Historical Development of Bipedal Locomats

The fundamentals of bipedal locomats (bipedal walking machines) are based on development of the concepts of *robots* and *robotics*. All through history and technological progress, lots of researches have been made to design a “machine” that looks and behaves like human beings. This machine should help people in different fields, in houses as personal helper, in factories as process controllers, in hospitals as helper for the patients, etc. In modern times, it was Karel Capek (1921) who first

exposed the idea of a true artificial man, a robot in his play called *Rossum's Universal Robots (R.U.R)* in 1921, with the desire to create duty-driven devices capable of executing human tasks (the root of the word robot comes from the Czech word “robota” which means incumbent work). Since then, robotics has evolved to the point that different branches, such as industrial robots, mobile robots, legged transportation systems, bio-inspired robots, robots in medical applications in surgeries, medical prostheses, rehabilitation devices, micro-robotics as well as autonomous vehicles, have reached a remarkable level of maturity as evidenced by immense results and a variety of applications (Fukuda et.al., 2001). In Figure 1.1 can be seen some robotic applications.

Since the late 1950s, there has been a revolution in robotics and industrial automation, from the design of robots with no computing or sensory capabilities (first generation) to the design of robots with limited computational power and feedback capabilities (second generation) and to the most recent design of what may be considered as intelligent robots that possess diverse sensing capabilities (third generation). After the third generation, researches on bipedal robots could start to accelerate proportionally as the improvements in digital control systems with high rate processing capacities and in measuring devices started to increase. Hence, in recent years, bipedal walking machines have started to be considered as an important research area for high technology developers.

In an engineering point of view, bipeds have great advantages when they are compared with traditional wheeled mobile robots. The scientists have proved that diffusion based energy supply (metabolic energy) obtained from nutrients, is substantially less for legged transport on neutral terrain than for the conventional wheel transport. “Professor McNeill Alexander of Leeds University also stresses the economy of walking by likening it to a pendulum that needs very little input of energy to keep it swinging (Alexander, 1987)”. In fact, legged robots require much less energy than most people realize. In addition, their versatility in being able to go anywhere makes them ideal for many tasks impossible for more conventional wheeled designs. The engineering approach to the bipedal robots and to their control

has enormous potential for helping to test the control strategies that animals might employ and for suggesting new experiments.

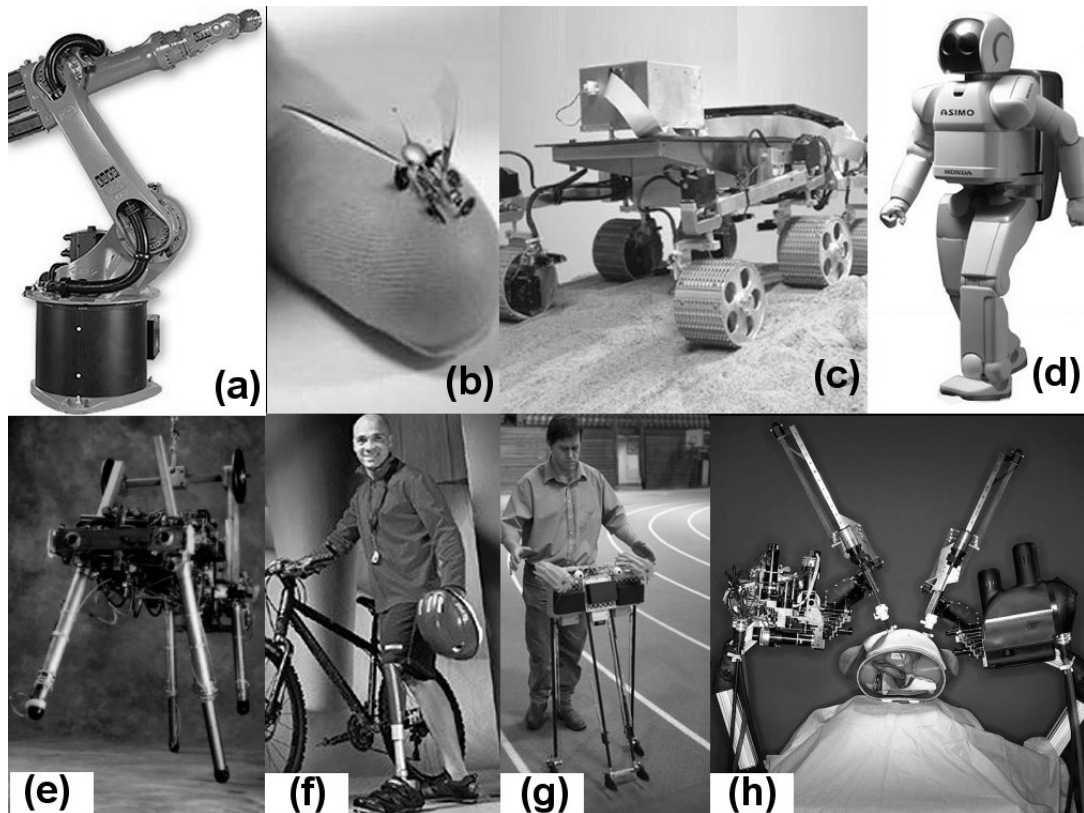


Figure 1.1 Various robotics applications: (a) Industrial Kuka robot, (b) Micro fly robot of Creative Research Center of Inha University, (c) Nasa's Mars Rover, (d) Honda's Asimo, (e) MIT's quadruped, (f) Otto Bock's C-leg, (g) Rehabilitation robot and (h) Raven mobile surgical robot.

In particular, researches done in 1960s and early 1970s provided the classical theoretical background for a biped walking machine (well-known concept of zero moment point) (Juricic & Vukobratovic, 1972; Vukobratovic, 1975). Research in multi-body dynamics, gave the solution to robotic arm dynamics, thus providing the theoretical foundation and background to the growing field of industrial robotics (Stepanenko, 1970; Vukobratovic & Stepanenko, 1973). The first industrial robot applications were aimed at specific manufacturing sectors, especially automotive industry, but the industrial robots changed essentially the entire manufacturing industry. In addition to these industrial robots, there has always existed a continuous research effort on problems of anthropomorphic robots, now called humanoid robots.

Major research was conducted at Waseda University that resulted in building the famous WABIAN RIV Humanoid (Carbone, Lim, Takanishi & Ceccarelli, 2009), while there was always a successful demonstration of the Honda humanoid, ASIMO.

Specific bipedal locomotion models, representing humans, have been simulated on the computer to investigate various gaits and stabilizing control schemes (Vukobratovic & Juricic, 1969; Alexander, 1984; Hurmuzlu & Moskowitz, 1987; McGeer, 1990; Raibert, Tzafestas & Tzafestas, 1993). In these locomotion models, two basic problems are tried to be solved:

1. Equilibrating or balancing the bipedal, both during standing phase and in progression phase (walking phase).
2. Making the walker track a desired trajectory within a desired time.

Equilibrium or balance problem of robots are analyzed according to walking type of the legged robots (whether they are balanced statically or dynamically). A fundamental distinction exists between statically and dynamically balanced machines (Raibert, Chepponis & Brown, 1986). A statically balanced system moves slowly in a manner that dynamical effects can be suppressed. It avoids tipping motions of the robot and the resulting horizontal accelerations, by keeping the projection of the Centre of Gravity (*COG*) of the system within the polygon formed by the supporting feet at all times. Such systems move with gait patterns that maintain this condition throughout the locomotion process, meaning that they work in or near a static equilibrium throughout their gait.

A two-legged robot should be dynamically balanced, during which the projected *COG* of the vehicle may not even lie on the support region. These bipeds are allowed to position their feet further away from the *COG*, which improves their mobility since they can attain higher forward velocities and can make steps with a greater length and height. The consequence is that dynamically balanced systems need very fast control action combined with short reaction time of actuators. Note that purely dynamically balanced systems demand continuous active actuation to maintain

balance. Systems moving with alternating static and dynamic stable phases during the gait cycle are called *quasi-static* or *quasi-dynamic* balanced systems. This kind of motion, where statically balanced moments are generally only interrupted for brief time intervals, are more stable than purely dynamically balanced systems but are unfortunately also slower.

To ensure dynamic stability, a parameter called *dynamic stability margin (DSM)* is calculated based on the concept of *zero moment point (ZMP)* (Vukobratovic, Brovac, Surla & Stokic, 1990; Vukobratovic, Frank & Juricic, 1970). The *ZMP* is a point lying on the ground about which the sum of all moments becomes equal to zero. It represents a point, at which the ground reaction force is being applied. To achieve a stable motion, the *ZMP* has to follow a certain trajectory. But, the *ZMP* may deviate from the prescribed trajectory, due to the disturbances or tracking errors which influence stability of the robot. Therefore, deviation of *ZMP* from prescribed trajectory has to be compensated. Seo & Yoon (1994) proposed the design of a robust dynamic gait of the biped using the concept of dynamic stability margin. According to them, gait failure occurred because of the discrepancy between the designed and the actual gait motions, which contributed to the changes in body forces. Thus, a gait can be considered to be robust, if it can sustain a fair magnitude of linear impulse applied at the mass centre of trunk, in the horizontal direction, for a certain amount of time. So, the minimum magnitude of that linear impulse was defined as the dynamic stability margin and the dynamic gait for a five link planar biped robot was designed by maximizing the dynamic stability margin. A parameter called foot strike time margin, representing the readiness of the foot strike, was also defined by them, which was supposed to have a close positive correlation with the dynamic stability margin. A robust gait with respect to the external disturbances was obtained by maximizing the foot strike time margin.

Although the above method lays down the foundation of the study of dynamically balanced two legged robot, it may not be suitable for on-line (real-time) implementations, due to its high computational complexity. Thus, suitable locomotion algorithms (adaptive in nature) are to be developed, which can negotiate

with unknown terrain also, on-line. Soft computing is an emerging technique, which consists of fuzzy logic, neural network, genetic algorithm, etc. and their different combinations, can handle real-world complex problems. Capi, Nasu, Barolli & Mitobe (2003) developed a method based on genetic algorithm to generate a human-like motion. Humanoid robot gait was generated using two different cost functions: minimum consumed energy and minimum torque change. In real-time situations, the robot has to change its gait according to the conditions of the terrain. But, as genetic algorithm is a time consuming tool, it was used to generate feasible optimal gaits, which were used to teach a radial basis function to the neural network. After getting trained, the neural network was used for real-time gait generation. Park & Chung (1999) developed a fuzzy logic-based *ZMP* trajectory generator, in which the leg trajectory was used as the input. The effectiveness of his algorithm was tested through computer simulations. The *ZMP* trajectory generated by his algorithm was able to increase the stability of the locomotion. The main drawback of his algorithm lies in the fact that the fuzzy logic-based controller may not be optimal, as no optimizer, such as a genetic algorithm or other tool, is used along with it. The studies still continue to overcome the problems encountered in the dynamical analysis of the bipedal robots.

As for the tracking problem, one of the most crucial aspects of motion control for bipedal robots is the design of reference trajectories for different joints. It is well known that arbitrarily defined trajectories can result in all kinds of difficulties like high energy consumption of the tracking actuators, possible instability of the robot caused by tipping over during the intermittent, unilateral contact phases with the supporting ground, etc. As correctly summarized by Sugihara, Nakamura & Inoue (2002), the previous works in motion generation for humanoid robots can be classified into two main approaches, being *trajectory replaying* and *real-time generation*, or roughly speaking off-line and on-line techniques. Although the latter group is far more promising from the point of view of high-mobility and autonomy of a humanoid, most walking trajectory generation methods successfully applied today belong to the first group. In general, off-line joint trajectories are calculated in advance and are applied to the real robot with no or little on-line modification.

Overall motion control is thus divided into two clearly distinct sub problems, namely planning and control of the trajectories.

The majority of bipedal locomotion researches explore the progression phase of the locomotion process, focusing primarily on the single support phase while ignoring the events of impact and transfer of the support. These phases of the locomotion process have been widely studied, owing to their periodic nature, which allows simplifying assumptions to be made in the modelling process. Commonly, the more complicated issues of impact and switching during the single support phase, initiation, stopping and standing/balance have been avoided because of their non-periodic nature. In general, most analytical and/or experimental bipedal locomotion studies have been limited to heavily linearized systems, with omission of the discontinuous or impulsive ground-contact events.

Only since the mid 1980s, researchers have begun to include impact in their models. Zheng & Hemami (1984) were the first to consider the effect of impact on locomotion system by considering the impact as a perturbation and not as a locomotion mechanism. Hurmuzlu & Moskowitz (1986, 1987) developed a nonlinear model for a bipedal locomotion system that included the events of impact and the transfer of support (switching). They demonstrated that the inclusion of the impact and switching phases into the locomotion model yielded a stable *limit cycle* in the phase space that the biped followed under steady progression. The events of impact and switching, which had in the past been ignored, were the stabilizing mechanisms for bipedal locomotion. McGeer (1990) compared bipedal walking with a rimless rolling wheel, where the contact between each spoke and the ground represented subsequent steps in the motion of the biped. He linearized step-to-step equations for passive walking down an incline, and showed that the motion was cyclic and stable. The models developed by Hurmuzlu & Moskowitz (1986, 1987) and McGeer (1990) were utilized to investigate the mechanisms responsible for stability of the locomotion systems for only the progression phase of the locomotion process. Little research has been devoted to the study of the transition phases of initiation and stopping, or the standing/balance phase of the bipedal locomotion process.

Bipedal gait initiation and stopping have been explored more often from a biological perspective rather than from an engineering viewpoint. Hirokawa (1989) addressed starting and stopping cases in his study, investigating human gait characteristics under temporal and distance constraints. He noted that two steps from starting and three steps before stopping characterized the starting and stopping phases, due to their acceleration and deceleration properties. Yamashita (1987) and after that Başer (2003) demonstrated that steady walking was achieved after the contact of the second swinging leg in gait initiation. Easton (1984) addressed human bipedal standing/balance from a physiological perspective, claiming that balance was a process comprised of several reflexes or automatic motor responses to specific sensory stimuli: a stretch reflex, a flexion reflex, a cross-extension reflex, a placing reflex, vestibular reflexes, and visual reflexes interact to achieve balance.

Paluska & Herr (2006) investigated the effects of series elasticity on actuator power and work output in bipedal walking applications. In their study, they stated: “the series elasticity changes the actuator operating point along its force–velocity curve and therefore affects the actuator work output over a fixed stroke length”. This fact can be well used in the force control of bipedal walker at the stance phase in which elasticity helps reducing the output impedance, acting like a mechanical low-pass filter to absorb shocks.

In recent years, with the improved actuating characteristics of pneumatic systems and their control systems, researchers have been trying to imitate human walking more precisely by using artificial muscles. Hosoda, Takuma, Nakamoto & Hayashi, (2008) used these artificial pneumatic muscles in order to control all moving states of a bipedal walker including walking, jumping (hopping) and running by designing an antagonistic joint mechanism and changing the compliance of robot for different locomotion types. Those kinds of studies are still persisting to achieve better result for bipedal walking machines.

1.4 Medical Robotics in Bio-mechatronic Applications

Because of the successes of robotics technology in industry, such as precise velocity and force control, rapidness, reaching the locations that human-being cannot, ability to have reasonably high output powers, correct self decision making, repeating the task without significant errors etc., new challenges to develop applicable and profitable robotic devices in other non-traditional fields of application were launched. One such challenge is the field of medical robotics. Medical robotics is a sub-branch of bio-mechanics, which is an interdisciplinary study of biology, mechanics and electronics, aiming the study of the interaction of biological organs with electro-mechanical systems. Medical robotics can be divided into three categories according to differences in applications as: (1) Surgery robotics, (2) Rehabilitation devices, and (3) Prosthetic devices as artificial limbs.

1.4.1 Surgery Robotics

Surgery robotics can be defined as the science which deals with the surgeries performed by robots. The first application was done by the robot PUMA 560, by Kwoh, Hou & Jonckheere (1985), to place a needle for brain biopsy using CT guidance and the results were published in 1988 (Kwoh, et. al., 1988). After some developments, including the *ROBODOC* (1992) from Integrated Surgical Systems used to mill out precise fittings in the femur for hip replacement and Da Vinci Surgical System composed of a surgeon's console, a patient-side robotic cart with 4 manipulators and a high definition 3-D system, the first unmanned surgery took place in Italy in May 2006.

In surgeries, perfection of precision and accuracy of the robots while using quantitative information taken from sensory sources cannot be reached by human operators. Also there are some applications which are beyond the abilities of human hands, like incising tiny scales and these can be performed by robotic devices. However, humans can collect the needed information from diverse sources of information obtained during surgery and can exercise a judgement, which still cannot

be made by a robot. For this reason, in today's surgery, current robots are generally restricted to simple procedures and assist human surgeons. Hence, Robotic systems are best described as "extending human capabilities" rather than "replacing human surgeons" (Howe, & Matsuoka, 1999).

1.4.2 Rehabilitation Devices

Rehabilitation devices are used in the field of rehabilitation engineering which can be defined as an engineering science to design, develop, adapt, test, evaluate, apply and find technological solutions to problems of individuals with disabilities. There are a many number of disabilities but the scope of this study covers only the orthopaedic problems encountered on the lower limbs of human body caused by spinal cord injuries or traumatic brain injuries. Main aim of rehabilitation devices is to assist the patients to restore some or all of his/her physical capacities that had been lost due to an injury, accident, illness or a disease. The importance of rehabilitation is that, it compensates the physical problems of the patient that cannot be fixed by medicine or surgery.

The basic rehabilitation method for orthopaedic problems is the physical therapy. It helps the patient restore the use of muscles, bones, and the nervous system through the use of heat, cold, massage, whirlpool baths, ultrasound, exercise, and by other techniques. It seeks to relieve pain, improve strength and mobility, and train the patient to perform important everyday tasks. Physical therapy may be prescribed to rehabilitate a patient after amputations, neurological problems, orthopaedic injuries, spinal cord injuries, stroke, traumatic brain injuries, and other injuries/illnesses. The duration of the physical therapy program varies depending on the injury/illness being treated and the patient's response to therapy.

1.4.3 Prosthetic Devices as Artificial Limbs

Design of prosthetic devices as artificial limbs is one of the significant research areas of medicine robotics, after recently accelerated developments of micro-electronics in the last two decades. By using motion and force controlled, electronically activated systems, more natural walking characteristics can be obtained not only on flat surfaces, but also on uneven surfaces, slopes or while climbing stairs. The progress on obtaining natural walking characteristics increases rapidly, because it directly affects the comfort of amputees for sustaining their daily life activities.

Throughout this study, artificial limbs used for amputation of lower extremities will be considered as the solution of walking problems of diverse orthopaedic disabilities. The awareness of importance of prostheses during World War I caused to set up an organization: the organization of the American Prosthetic and Orthotics Association. Artificial Limb Program was developed with sponsorship from Veteran Administration, Department of Health, Education, Welfare and armed forces. Today, a noticeable industrial branch for artificial limb construction has arisen and day by day the participants of this new industrial area increase all over the world. Thus, now, artificial limbs having complex control and sensory systems with various types of actuator can be manufactured according to amputation type. Lower limb amputations can be classified in five groups: Hip disarticulation, above knee amputation, below knee amputation, knee disarticulation and foot amputation (Figure 1.2).

1.4.3.1 Hip Disarticulation

Hip disarticulation can be defined as an amputation through hip joint capsule, removing the entire lower extremity, with the closure of the remaining musculature over the exposed acetabulum. It has been being performed with little variations in technique since it was first applied by Kirk (1943).

There is a number of prosthesis fitting protocols after hip disarticulation. One common approach is to use a temporary prosthesis in the first six months after discharge. Canadian hip disarticulation prosthesis is considered as an important permanently used prosthesis which is modified through the years as the technology has advanced into modern systems. It can be noted that new designs have advantages, including new material technologies like light weight metals or composites and being modular which means capability of easy adjustment. The results of latest studies show that hip disarticulation prostheses can be used together with intelligent knee prosthesis in order to decrease energy expenditure in place of constant friction knee joint with stance control.

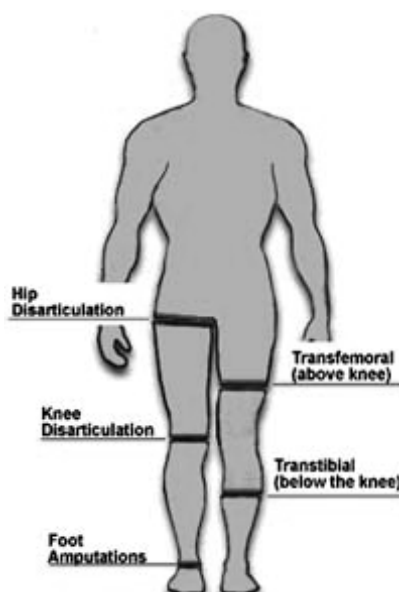


Figure 1.2 Types of lower limb amputation

1.4.3.2 Above-knee Amputation

Above knee amputation was the most commonly performed lower extremity amputation for vascular problems before 1960s. It has the advantage that 100% of patients can be healed with this method. These patients use transfemoral prostheses, which have an artificial knee joint. There are various kinds of transfemoral prostheses from the basic one having single axis of rotation to Otto Bock's C-Leg with a microcontroller unit to control both swing and stance phases. Type of the

prosthesis the patient will use, is chosen according to some criteria like the age of the patient, pre-amputation functional status and rehabilitation goals (Tang, Ravji, Key, Mahler, Blume & Sumpio, 2008) in order to meet the expectations of the patient.

Single axis knee is the most commonly used prosthesis type which is especially used in under-developed countries for the reason of being relatively cheaper than the other types. The swing phase control can be easily achieved by adjusting the stiffness of the spring and the friction cell pressed against the knee axle. Unfortunately, this system malfunctions when it is used on uneven surfaces. Despite the simplicity of design and limitations, the single axis knee is a surprisingly reliable and inexpensive design ideally suited to individuals with restricted access to regular health care and prosthetic maintenance (Michael, 1999).

More advanced prostheses use fluid swing-phase control mechanisms to overcome the problems encountered in the single axis prosthesis applications. These mechanisms can be either pneumatic or hydraulic systems according to patients' characteristics; Patients who need slow ambulatory speeds use pneumatic systems whereas higher speeds can be obtained with hydraulic elements. In new designs, turbulent flow is obtained to perform much higher speeds for the race walking applications.

There are some additional features incorporated to knee prostheses in order to meet the needs of different patients. Locked knee mechanisms are suitable for elder people, allowing higher walking speeds but lower cardiac effort. Patients who are totally unable to control the knee, such as the stroke patient, would also be suitable candidates for the locked knee mechanism. There are also some other types of prosthetic knees like Hans Mauch S-N-S cylinder, working in a similar way but giving high performance for only the patients with good muscular strength. Advantages and disadvantages of various knee prostheses are given in Table 1.1.

Newly developed polycentric knee mechanism is a four bar mechanism, allowing optimal control of swing and stance phases. An important feature of the polycentric

knee is better stance stabilization while maximizing ease of pre-swing knee flexion. When the knee flexes only a few degrees, the centre of rotation is shifted anteriorly, with subsequent ease of continued flexion accompanied by a mild decrease in prosthesis length. This ensures knee stability while the patient is walking at a moderate to brisk pace. In addition, toe clearance can be increased by up to 1 to 2 cm during mid-swing, leading to a less perceived risk of stumbling. This is preferred by patients who are in relatively good physical condition and require stance phase knee stability (Michael, 1999).

Advanced prosthetic knee mechanisms, “Intelligent” transfemoral microprocessor-controlled prostheses, can change the orifice size according to varying walking speeds to allow appropriate shin swing time. A knee joint sensor detects the swing speed and sends a signal to the stepper motor, which adjusts the valve size in the pneumatic cylinder (Buckley, Spence & Solomonidis, 1997).

There are several available types of microprocessor controlled prosthetic knees including the Endolite Intelligent Prosthesis Plus (Chas Blatchford & Sons), the Seattle Limb Systems Power Knee (Seattle Limb Systems), and the recently released C-Leg (Otto Bock). The C-Leg (Table 1.1) is an advanced processor-controlled prosthesis that uses a hydraulic cylinder to provide swing control and variable hydraulic stance phase control. The shin includes numerous sensors that accumulate biomechanical data such as vertical loading amplitude and sagittal knee movement, and can also determine the direction and angular acceleration of the knee joint. A software analysis system optimizes prosthetic characteristics through a process of data sampling and calculations of up to 60 times in a 1.2- second gait cycle. When examined using the swing-phase treadmill test, the C-Leg clearly demonstrates superiority at higher walking speeds when compared with mechanical hydraulic knees such as the Otto Bock 3R45 and 3R80. The C-Leg has demonstrated greatest efficiency in the areas of flexion angle, flexion speed, and extension speed. It is more beneficial at higher ambulation speed in physically fit patients, with one report documenting a walking speed of up to 6.67 km per hour with the C-Leg (Pinzur & Bowker, 1999).

1.4.3.3 Below-knee Amputation

Because of a number of advancements, the proportion of below-knee amputation compared with above knee amputations is increased. Revascularization techniques have been being developed which result in salvage of threatened limbs or allow a more distal level of amputation. Increasing the distal level of amputation decreases the energy expenditure; hence this method is preferred to other amputation applications (Pinzur, Gold & Schwartz, 1992).

1.4.3.4 Knee Disarticulation

Knee disarticulation has significant theoretic advantages over conventional above knee amputation, including simplicity of technique, minimal blood loss, residual limb balanced by strong muscles, and less energy expenditure with a longer femoral stump. In patients with poor rehabilitation potential, a knee disarticulation provides more optimal sitting balance, bed mobility and transfer compared with an above knee amputation (Pinzur, Slosar, Reddy & Osterman, 1992).

1.4.3.5 Foot Amputation

Mid-foot and transmetatarsal amputations are performed typically for digital gangrene, osteomyelitis of the forefoot, or non-healing ulcerations of the forefoot. Custom moulded shoes and inlays, which are off-load and support excessive pressure areas, are often prescribed postoperatively once the patient has completely healed the amputation (Tang, et. al., 2008).

Table 1.1 Overview of lower extremity prostheses (Tang et. al. 2008)

MODEL	ADVANTAGES	DISADVANTAGES	INDICATIONS
Otto-Bock Modular Endoskeletal Hip Prosthesis	Light weight, flexibility of use with interchangeable components	High energy expenditure, slow ambulation	Able bodied patients post hip disarticulation
Single Axis Friction Controlled Knee Prosthesis	Inexpensive Very reliable	One cadence, difficult to use on uneven surfaces	Restricted acces to regular health care
Fluid Swing Controlled Locked Knee Mechanism	More stable, lower energy expenditure, lower heart rate	Lower ambulation speeds	Weaker amputees such as elderly or stroke patients
Fluid Swing Controlled Open Knee Mechanism Hans Mauch S-N-S Cylin.	Faster ambulation, Wide range of walking speeds	Higher energy expenditure, Higher heart rate	Patients in good physical condition with higher exercise demands
Intelligent Transfemoral Microcontrolled Processor Controlled Knee Mechanism	Able to adjust swing speed according to perceived ambulation speeds	Expensive, patients with average physique derive little benefit	Patients in excellent physical condition desiring a high exercise capacity
Four BarLinkage Polycentric Knee Joint	Prosthetic knee bends on sitting at same level as contra lateral native knee	Higher cost	Ambulatory patients post knee disarticulation

1.5 Aim of the Study

The first aim of the thesis is to understand deeply the meaning of walking from an engineering point of view. As it is discussed in the introduction chapter, bipedal walking is the most efficient and sophisticated walking type which gives a great freedom of movement to the walkers. It is believed that there remain only little steps for the walking robots to take the place of wheeled ones in the fields of military, industry, service sector as well as in the field of medicine. The biggest problem in these studies is the non-linear characteristics of walking machines and apparatuses, since they are designed as serial and parallel manipulators, the dynamics of which are highly non-linear. Hence, solution techniques for inverse and forward kinematics/dynamics problems of bipedal walkers are included in this work.

The second and the major aim of the study is to design an artificial hybrid leg which can be used by transfemoral amputees. Transfemoral amputation can be defined as the amputation of the lower limb between hip and knee articulation. There are various reasons for this kind of amputations; the most conspicuous ones being vascular problems and disabilities occurred in traffic accidents or in military services.

When a person loses his/her lower limb together with the knee articulation, his/her body dynamics totally change. Knee joint is especially very important, because walking capability of a walker increases with the existence of knee joint, particularly in running and in climbing stairs. Even when walking on flat surfaces, because of the obstacles, amputees encounter great problems which are not realized by the healthy people. For this reason, it is believed that the researches like this one have great importance for the humanity.

Artificial hybrid leg discussed here has a polycentric knee which is a four bar mechanism. As it is mentioned in the related chapter, with a good polycentric knee design, the amount of the torque to be exerted by the actuators can be reduced which enables the usage of smaller motors with low power capacities, making the design more compact and easy to use.

It must be noted that, artificial knee designed in this research is a prototype and yet it has not been tested by transfemoral amputees. However, different control algorithms are developed with an introduction to experimental setup in order to choose the best method which gives a comfortable and stable walking for the patients.

1.6 Outline of the Study

In Chapter one, which is the introduction to the study, general remarks about bipedal walking are given. Firstly, basic definitions and information about robotics are given and then application areas of robotics, in the special case bipedal walkers and walking aiding devices, are determined briefly. The state of art is also presented in this chapter.

Chapter two is related with the mathematical model of a bipedal walker in sagittal plane. Trajectories for stance and swing leg phases are determined and by inverse

kinematics method, related joint parameters are found. After inverse kinematical analysis, dynamics of the walker and the motors which excite the walker are given.

In Chapter three, mathematical model of an artificial leg having a polycentric knee mechanism is derived. Types of knee mechanisms are discussed and it is stated that polycentric knee mechanism is the most efficient and reliable mechanism for the transfemoral amputees. Workspace of the artificial leg is found and its dynamics is derived.

In Chapter four, the control theory developed for the purpose of the work is explained. As the control method, feed-forward compensation with disturbance rejection strategy is introduced. Feed-forward control is supported by a feedback loop in order to guarantee the system to track the reference signal and to suppress unmeasured and undetermined disturbances.

Chapter five is about the design of the hybrid artificial leg. Three subsystems, mechanical subsystem, electromechanical subsystem and computer subsystem are introduced and general design properties are given.

In Chapter six, experimental setup is introduced. Experimental setup is the artificial hybrid leg, which is designed in Chapter five. It is mentioned here that a standard PC is used as the control unit. Monitoring and control tasks are all achieved by using the software MATLAB and its Real-Time Windows Target toolbox. Two control strategies are introduced.

Chapter seven is devoted to results and discussions. In this chapter, firstly, simulation results for the control of a bipedal walker in sagittal plane are given. Secondly, the results of the experiments in which two control strategies are used are described. Discussions about the results and suggestions about future studies are given at the end of the chapter.

CHAPTER TWO

MATHEMATICAL MODELLING OF BIPEDAL WALKING

2.1 Introduction

In the analysis and control of bipedal walking, the first thing to do is to obtain the mathematical model of the system. The mathematical model gives the researchers the characteristics of the system and it associates the real world with mathematical expressions. It is a set of equations which includes the system variables, type of the system, whether it is time variant or not, stable or not, etc. Only by having this kind of information, the actuator system and measurement devices can be chosen and control structures can be constructed.

Bipedal walking system is a dynamic system the variables of which are time dependent joint variables and it can be represented by differential equations. System is composed of two serial manipulators and four actuators mounted to the joints so that the mathematical model is composed of not only serial manipulator dynamics, but it includes also the dynamics of actuators, which are chosen as permanent magnet direct current motors.

In this chapter, mathematical model of bipedal walking system is derived. For this purpose, first, kinematic analyses are made and after obtaining pose, velocity and acceleration expressions, dynamics of the system are obtained.

2.2 Mathematical Model of Locomotion

Mathematically, bipedal walking can be modelled as a combination of two serial manipulators, namely stance leg and swing leg, having two revolute type joints (two R-R type serial manipulators). This is the simplest model corresponding to walking with two legs, i.e. human-like motion. Referring to Figure 2.1, system has two degrees of freedom, since ankle joints are assumed to be fixed on the ground for the simplicity.

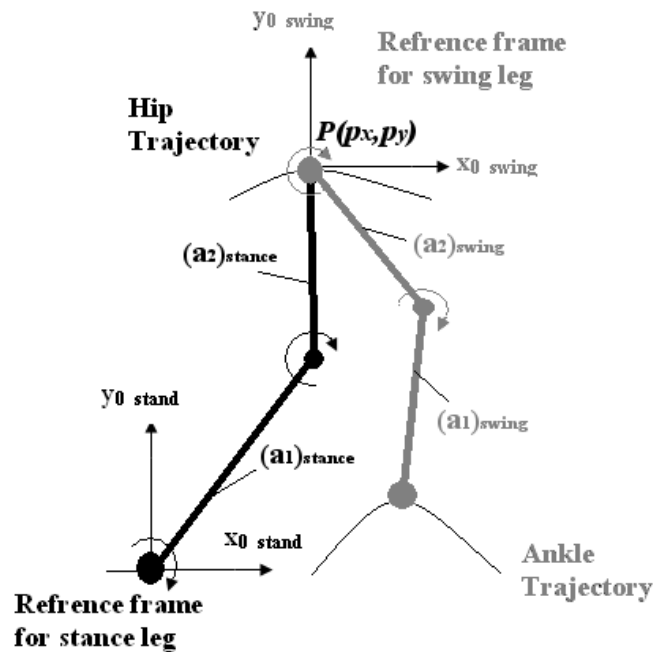


Figure 2.1 Bipedal walking model

During motion, each leg changes its state from stance leg to swing leg periodically and it is assumed that the legs can only be in the same phase (stance leg phase) at the beginning and at the end of the motion. Each three joints of the legs can be actuated (hip joint, knee joint and ankle joint) but it is important to note that only two of these three joints are actuated simultaneously according to the phase of walking. This means, in the stance leg phase, the ankle and knee joints are actuated while in the swing leg phase, the ankle joint stands still but hip joint becomes the active articulation. The walker parameters can be chosen from the measured body parameters of a typical human-being (Table 2.1).

Reference frames attached to swing leg and stance leg of the walker have some distinctive features. Pose of the reference frame of stance leg remains fixed to the ground, while that of swing leg moves along an arbitrary trajectory as the hip joint changes its position and orientation with the movement of stance leg. For this reason, pose of reference frame related to this motion must be calculated for each instant of time according to the movement of stance leg in the given trajectory during swing leg phase.

Table 2.1 Body Parameters of the bipedal walker based on the parameters of a man having 77 kg weight and 175 cm height

Robot Body Part	Weight (kg)	Length (cm)
Upper legs (a_2)	11	50
Lower legs (a_1)	12	52
Upper Body	54 (<i>lumped at point P</i>)	73 (<i>not shown in Figure 2.1</i>)

2.2.1 Inverse Kinematics of Bipedal Walker

To derive the mathematical model of the walker, the joint variables must be calculated, i.e. inverse kinematic analysis for the system must be done. Inverse kinematics is a mathematical method of finding the degrees of freedom of a system subject to kinematic constraints. In robotics, more briefly, it is the process of determining the joint parameters of a manipulator (a serial manipulator in this case) in order to achieve a desired pose.

For the walking model, joints variables are defined distinctly for swing leg and stance leg phases. In the swing leg phase, joint variable θ_1 represents hip joint variable and θ_2 that of the knee joint, whereas in stance leg θ_1 is the ankle joint variable and θ_2 is again the variable for the knee articulation as in the swing phase.

The first step for the inverse kinematic analysis of bipedal walker is to write down the equation for hip trajectory corresponding to the desired pose of the bipedal as a sequence in Cartesian coordinates. This leads us to the information of position and orientation of hip joint in every instant of time along the walking process. Coordinates attached to hip joint is considered as the coordinate frame for the end-effector in stance leg phase. Hence, methods used for the inverse kinematics analysis of serial manipulators become ideal for this analysis of walking process, since there is an analogy between the structures of both systems. By using this analogy, pose of a joint can be represented by the following vector equation:

$${}^o\mathbf{P}_{0,2} = {}^o\mathbf{P}_{0,1} + {}^o\mathbf{P}_{1,2} \quad (2.1)$$

where ${}^0\mathbf{p}_{i,j}$ is the vector from the origin of frame i attached to the i^{th} joint to the origin of frame j attached to the j^{th} joint as seen from the reference frame. Using basic trigonometric relations, x and y components of the two vectors, ${}^0\mathbf{p}_{l,2}$ and ${}^0\mathbf{p}_{u,2}$ can be found. Substituting these relations in Eq.(2.1), the geometric model can be obtained as follows for the stance phase:

$$\left\{ \begin{array}{l} p_x = a_1 \cdot c\theta_1 + a_2 \cdot c\theta_{12} \\ p_y = a_1 \cdot s\theta_1 + a_2 \cdot s\theta_{12} \end{array} \right\}_{s \text{ stance}} \quad (2.2)$$

where a_1 , a_2 are the length of lower and upper leg respectively and $\{\mathbf{P}(p_x, p_y)\}_{s \text{ stance}}$ is the position of hip articulation with respect to the reference base frame of stance leg.

Taking the derivatives of Eq.(2.2), the instant velocity expressions of hip joint for stance leg phase can be obtained as:

$$\left\{ \begin{array}{l} v_x \\ v_y \end{array} \right\}_{s \text{ stance}} = \left[\begin{array}{cc} -a_1 \cdot s\theta_1 - a_2 \cdot s\theta_{12} & -a_2 \cdot s\theta_{12} \\ a_1 \cdot c\theta_1 + a_2 \cdot c\theta_{12} & a_2 \cdot c\theta_{12} \end{array} \right] \cdot \left\{ \begin{array}{l} \dot{\theta}_1 \\ \dot{\theta}_2 \end{array} \right\}_{s \text{ stance}} = \mathbf{J} \cdot \left\{ \begin{array}{l} \dot{\theta}_1 \\ \dot{\theta}_2 \end{array} \right\} \quad (2.3)$$

where the first term on right hand side represents the Jacobian Matrix, \mathbf{J} . Joint variables can be obtained by multiplying both sides of Eq.(2.3) by inverse of the Jacobian:

$$\mathbf{J}^{-1} \cdot \mathbf{v} = \dot{\theta} \quad (2.4)$$

Differentiating Eq.(2.3) with respect to θ_1 and $\theta_1 + \theta_2$, and joint variables with respect to world frame (coincident with stance leg base reference frame), the acceleration term can be found as:

$$\begin{aligned} \begin{bmatrix} \ddot{\theta}_1 \\ \ddot{\theta}_1 + \ddot{\theta}_2 \end{bmatrix} &= \frac{1}{a_1 a_2 \cdot s\theta_2} \cdot \begin{bmatrix} a_2 c\theta_{12} & a_2 s\theta_{12} \\ -a_1 c\theta_1 & -a_1 s\theta_{12} \end{bmatrix} \cdot \begin{bmatrix} \dot{v}_x \\ \dot{v}_y \end{bmatrix} \\ &+ \frac{1}{a_1 a_2 \cdot s\theta_2} \cdot \begin{bmatrix} a_1 a_2 c\theta_2 & a_2^2 \\ -a_1^2 & -a_1 a_2 c\theta_2 \end{bmatrix} \cdot \begin{bmatrix} \dot{\theta}_1^2 \\ (\dot{\theta}_1 + \dot{\theta}_2)^2 \end{bmatrix} \end{aligned} \quad (2.5)$$

Reference frame for swing leg phase is not fixed to any point, but it changes its location as the hip joint moves along its trajectory mentioned in stance leg movement. Thus, for each time sequence in swing leg phase, ankle position must be obtained by using the following inverse transformation matrix which represents the coordinate transformation from world frame to swing leg reference frame:

$$\{P_{ankle}\}_{swing} = {}^{swing}T_{stance} \{P_{ankle}\}_{stance} \quad (2.6)$$

All equations for motion in swing leg phase are derived according to this manipulation. Eq. (2.6) is called as *phase transition equation* and for every epoch of motion, this calculation must be done in order to derive the correct poses for knee and ankle joints in swing phase .

2.2.2 Trajectory Planning for Hip and Knee Articulations in Related Phases

A trajectory is the path followed by the manipulator, plus the time profile along the path. Trajectories can be planned either in joint space (directly specifying the time evolution of the joint angles) or in Cartesian space (specifying the position and orientation of the end frame). Issues in trajectory planning include attaining a specific target from an initial starting point, avoiding obstacles, and staying within manipulator capabilities.

In walking phenomenon, trajectories of hip and knee articulations have great importance for the reason that they guarantee the synchronized movement of the joints yielding a stable walking characteristic. These trajectories are time dependent periodic functions in Cartesian space (in world coordinates) or in joint space, so that

the time and position constraints defined due to the walking phase plays important roles while forming these trajectories. Below, is given a short description of trajectory planning procedure and detailed analyses will be discussed in consequent sections.

- First, the space curve which passes through all of the desired points along hip trajectories are specified. In literature, this task is called as *path planning task for robot manipulators*.
- Then, parameters of hip trajectory curve are specified to assure that the hip tracks this curve in the desired fashion, i.e. with the decided velocity. This is where the trajectory planing concept arises.
- Corresponding joint variables are calculated in time domain.
- For ankle trajectory, three critical points corresponding to extremum poses of bipedal walker must be defined. These are the start point, mid-point and end point of one step motion. Each have important characteristics which will be discussed later.
- By solving kinematic equations of the bipedal walker, the joint angles of the swing and stance legs are obtained for the given poses.
- Time dependent angular position parameters are calculated in configuration space.

By following these steps, both hip and ankle trajectories are derived for the given constraints defined pertinent to the walking phase.

2.2.2.1 Hip Trajectory Generation

In bipedal walking of human-being, hip articulation traces a trajectory which is very similar to a parabola in Cartesian coordinates. The equation of the curve can be given as:

$$y_h(t) = A \cdot [x_h(t) - a] \cdot [x_h(t) - b] \quad (2.7)$$

where y_h and x_h are the Cartesian coordinate components of hip trajectory, The parameters A, a, b define the characteristics of walking and they are calculated according to the boundry conditions of hip articulation as:

$$\text{start point constraints} \Rightarrow P_1(-L_{gait}/4, 0)$$

$$\text{mid point constraints} \Rightarrow P_2(0, L_{leg} + h_{max})$$

$$\text{end point constraints} \Rightarrow P_3(L_{gait}/4, 0)$$

Here, L_{gait} is the gait length, L_{leg} is the total length of the leg and h_{max} is the maximum displacement in y direction. Note that, midpoint is considered as axis of symmetry for hip joint where maximum height of hip articulation is reached.

Since trajectories are time-dependent, time dependent constraint including some initial conditions must also be chosen in order to obtained the path with desired velocity profiles. For time dependent constraints, the statements $x_{hip}(t=0) = -L_{gait}/4$ and $x_{hip}(t=t_{gait}) = L_{gait}/4$ give the constraints for positions and $\dot{x}_{hip}(t=t_{gait}) = 0$ gives the velocity of the walker, as the time interval for walking is $(0, t_{gait})$. Hence, time dependent variation of $x_{hip}(t)$ will be:

$$x_{hip}(t) = A_t \cdot \sin^2(b_t \cdot t) + C \quad (2.8)$$

where A_t, b_t, C are the time domain parameters and they are to be found for the given time dependent constraints. After x component of the trajectory is obtained, y component can be calculated from Eq.(2.7).

2.2.2.2 Ankle Trajectory Generation

Trajectory of ankle joint is especially important in the control of swing leg phase for climbing a stair, walking on inclined planes or for obstacle avoidance applications. The leg must be rised to a proper height within a certain period of time

without loosing the stability of the walker. For this reason, pose of ankle joint and foot, which depends on the ankle movement, must be determined according to the movement of upper and lower legs actuated by hip and knee joint actuators, respectively.

Different from the hip trajectory, trajectory of the ankle joint in swing leg motion will be generated in the joint space, since algorithmic computation of the trajectory of swing leg seems to be easier. In the trajectory planning of ankle joint, *critical points* are the *extremum* points of the trajectory and they define the boundary conditions for start point as $(-L_{gait}/2, 0)$, for end point as $(L_{gait}/2, 0)$ and also midpoint constraint at the point $(0, L_{lower}/2)$. L_{lower} represents the lower leg length. These constraints are given in task space in a such manner that they satisfy the poses corresponding to ankle joint positions of swing leg when stance leg has a certain pose to track hip trajectory. Algorithm used to generate the ankle trajectory can be given as follows:

- Reference swing leg position with respect to moving reference frame attached to hip joint is calculated by using the inverse stance leg transformation given in Eq. (2.6).
- For the given *critical points*, inverse kinematics equations are solved. Hence, joint space constraints are obtained from the world space coordinates.
- Since joint variables are time dependent, the polynomial given in Eqs. (2.9) and (2.10) are used to obtain desired motion.

$$\theta_{hip}(t) = a_{hip} \cdot t^2 + b_{hip} \cdot t + c_{hip} \quad (2.9)$$

$$\theta_{knee}(t) = a_{knee} \cdot t^2 + b_{knee} \cdot t + c_{knee} \quad (2.10)$$

Parameters in Eqs. (2.9) and (2.10) are selected properly to satisfy the configuration space constraints.

2.2.3 System Dynamics of Bipedal Walker

Inverse kinematic analysis is the first step which describes the motion of the system without considering the causes leading to the motion. However, in order to fully control a system, the causes are important and system dynamics approach must be introduced to the model in a proper way.

Dynamical analyses include force and torque relations, caused by the motion of the system and many methods can be used to derive these relations. Researchers, who deal with robotics and mechatronic applications, mostly deal with *Recursive Newton-Euler Computation* to derive the dynamics of bipedal walking system in sagittal plane. This method combines all the forces acting on the individual links of the walker, two links in this case. In Figure 2.2, the forces and moments acting on a link of a serial manipulator are shown. The notations can be given below:

- $\mathbf{f}_{i,i-1}$: resulting forces exerted on link i by link $i-1$
- \mathbf{f}_i^* : inertia forces exerted at the center of mass of link i
- \mathbf{I}_i^i : Inertia matrix of link i about its center of mass expressed in link i frame.
- $\mathbf{n}_{i,i-1}$: resulting moment exerted on link i by link $i-1$
- \mathbf{n}_i^* : moment exerted at the center of mass of link i
- \mathbf{p}_i : position vector of the origin of link i with respect to the base frame
- \mathbf{p}_{ci} : position vector of the center of mass of link i with respect to the base frame
- \mathbf{r}_i : position vector of the origin of the link i frame with respect to link $(i-1)$ frame
- \mathbf{r}_{ci} : position vector of the center of mass of the link i frame with respect to the i th link frame
- $\mathbf{v}_i, \dot{\mathbf{v}}_i$: linear velocity and acceleration of the origin O_i
- $\mathbf{v}_{ci}, \dot{\mathbf{v}}_{ci}$: linear velocity and acceleration of center of mass of link i
- $\mathbf{w}_i, \dot{\mathbf{w}}_i$: angular velocity and acceleration of link i
- \mathbf{z}_i : unit vector pointing along z_i axis

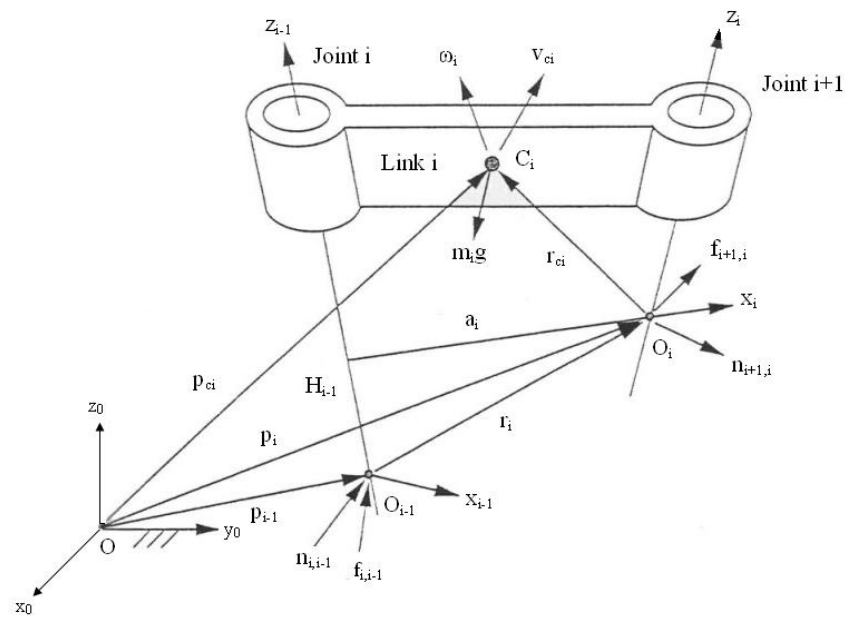


Figure 2.2 Forces and moments exerted on link i.

Recursive Newton-Euler Computation method consists of a *forward computation* of the velocities and accelerations of each links, followed by a *backward computation* of the forces and moments in each joint.

2.2.3.1 Forward Computation

In this method, linear and angular velocities of each link in terms of its preceding link must be calculated. Since it is forward computation, these computations start with the first moving link and end at the second one. The initial conditions for the stance leg are $\mathbf{v}_0 = \dot{\mathbf{v}}_0 = \mathbf{w}_0 = \dot{\mathbf{w}}_0 = 0$. The velocity and acceleration of the origin and the center of mass of the first and second link can be evaluated from the equations of rigid body dynamics. The required homogenous transformations must be done to obtain these values.

2.2.3.2 Backward Computation

Once the velocity and acceleration of the links are derived, the joint forces can be computed one link at a time starting from the end effector link and ending at the base link. It is important to note that once the reaction force and moment are computed in the i th link frame, they must be converted into the $(i-1)$ th link frame by the following transformation:

$${}^{i-1}\mathbf{f}_{i,i-1} = {}^{i-1}\mathbf{R}_i \cdot {}^i\mathbf{f}_{i,i-1} \quad (2.11)$$

$${}^{i-1}\mathbf{n}_{i,i-1} = {}^{i-1}\mathbf{R}_i \cdot {}^i\mathbf{n}_{i,i-1} \quad (2.12)$$

where,

$${}^i\mathbf{R}_{i-1} = \begin{bmatrix} c\theta_i & s\theta_i & 0 \\ -c\alpha_i s\theta_i & c\alpha_i c\theta_i & s\alpha_i \\ s\alpha_i s\theta_i & -s\alpha_i c\theta_i & c\alpha_i \end{bmatrix} \quad (2.13)$$

This rotation matrix is derived from the Denavit-Hartenberg Homogenous transformation matrix. θ_i represents joint variables and α_i represents the angle about which the current x-axis is rotated.

After resulting forces and moments are obtained, it is easy to find the joint torques by projecting the forces of constraint onto their corresponding joint axes;

$$\tau_i = {}^{i-1}\mathbf{n}_{i,i-1}^T \cdot {}^{i-1}\mathbf{z}_{i-1} \quad (2.14)$$

where \mathbf{z}_i is unit vector pointing along z_i axis of the i th joint. At the end of the Newton-Euler recursive computation, the dynamics of the stance leg of the biped in generalized coordinates is derived as follows:

$$\mathbf{D}(q)\ddot{q} + \mathbf{C}(q, \dot{q})\dot{q} + \mathbf{G}(q) + \mathbf{F}(q) + \tau_e = \tau \quad (2.15)$$

Here,

- $q \in \mathfrak{R}^k$ is a k -vector angular positions called *the vector of generalized coordinates*.
- $F(q)$ is a k -vector with applied and external forces and/or torques called *the vector of generalized forces*.
- $\mathbf{D}(q)$ is a $k \times k$ non-singular symmetric positive-definite matrix called *the mass matrix*.
- $\mathbf{C}(q, \dot{q})$ is a $k \times k$ matrix sometimes called *the centrifugal/Coriolis/friction matrix*.
- $G(q)$ is a k -vector called *the vector of conservative forces* or *vector of gravitational forces*
- τ_e is the end effector moment expression which arise due the weight and the movements of the upper body.

Sometimes, Eq.(2.15) is written in the scalar form to identify the Coriolis and centrifugal and friction effects individually. Eq. (2.15) can be re-written as:

$$\tau_k = \sum_{j=1}^n d_{kj}(q)\ddot{q}_j + \sum_{i=1}^n \sum_{j=1}^n c_{ijk} \dot{q}_i \dot{q}_j + g_k \quad (2.16)$$

In the above equation, there are three types of terms. The first type involves the second derivative of the generalized coordinates. The second type involves quadratic terms in the first derivatives of q , where the coefficients may depend on q . These latter terms are further classified into those involving a product of the type \dot{q}_i^2 and those involving a product of the type $\dot{q}_i \dot{q}_j$ where $i \neq j$. Terms of the type \dot{q}_i^2 are called **centrifugal**, while terms of the type $\dot{q}_i \dot{q}_j$ are called **Coriolis** terms. The third type of terms are those involving only q but not its derivatives. The third type arises from differentiating the potential energy. The terms c_{ijk} in Eq.(2.16) are known as **Christoffel symbols** (of the first kind).

In swing leg phase, It is assumed that there are no external forces acting on the system, since the forces which effect the motion of the ankle arise from the swing leg dynamics only. When the manipulations given by Eq. (2.6) are made, swing leg dynamics in generalized coordinates can be obtained from Eq. (2.15) as:

$$\mathbf{D}_{swing}(q)\ddot{q} + \mathbf{C}_{swing}(q, \dot{q})\dot{q} + \mathbf{G}(q) = \tau \quad (2.17)$$

where $\mathbf{D}_{swing}(q)$ and $\mathbf{C}_{swing}(q, \dot{q})$ are obtained by using Recursive Newton-Euler computation method.

2.2.4 Actuator Dynamics

The task in the system of bipedal walker is to determine the time history of joint inputs required to cause the hip joint to execute a commanded motion. Execution of motion is done by actuator systems so the dynamical characteristics of the actuators must be obtained and they must somehow be associated with manipulator dynamics.

The motion of the robot is given in Eqs. (2.15) and (2.16). In these equations, $\tau = T_d$ represents the torque disturbance acting at the joints to the actuators which are caused due to the dynamics of walking model and the torques which are necessary for tracking the given trajectories under the effect of these disturbances are produced by two permanent magnet direct current (PMDC) motors. From the electrical and mechanical characteristic of PMDC motor, the state space representation of the actuator can be obtained as follows:

$$\frac{d}{dt} \begin{bmatrix} i_a \\ \omega_a \end{bmatrix} = \begin{bmatrix} -\frac{R_a}{L_a} & -\frac{K_b}{L_a} \\ \frac{K_M}{J_a} & -\frac{B_a}{J_a} \end{bmatrix} \cdot \begin{bmatrix} i_a \\ \omega_a \end{bmatrix} + \begin{bmatrix} \frac{1}{L_a} & 0 \\ 0 & -\frac{1}{J_a} \end{bmatrix} \cdot \begin{bmatrix} V_a \\ T_d \end{bmatrix} \quad (2.18)$$

$$\begin{bmatrix} y_1 \\ y_2 \end{bmatrix} = \begin{bmatrix} 0 & 1 \\ 0 & 0 \end{bmatrix} \cdot \begin{bmatrix} i_a \\ \omega_a \end{bmatrix} \quad (2.19)$$

where variables $i_a, R_a, L_a, K_b, \omega_a, V_a, K_M, J_a, B_a, T_d$ are: armature current, armature resistance, inductance of armature coil, velocity constant, rotational velocity of the armature, armature voltage, torque constant, inertia of the rotor, damping coefficient of mechanical system and torque of mechanical load, respectively. Simulink model of the actuator system is given in Figure 2.3. The effect of torque produced at knee joint is considered as a disturbance for the actuator at the ankle joint.

When actuator dynamics is considered analytically, it is seen that equivalent moment of inertia of the ankle is a time dependent parameter. This fact turns the equation of mechanical part of the actuator transfer function into a time variant system given as:

$$J_a = \frac{M_1}{3} L_1^2 + \frac{M_2}{3} (L_1^2 + L_2^2 + L_1 L_2 \cos \theta_2) \quad (2.20)$$

where $\theta_2 = \theta_2(t)$.

After modelling the system, control structure which fullfills the desired trajectory of hip and ankle articulations in the related walking phases can be decided. Also by making stability analysis using the mathematical model, the system guarantees the secure walking conditions. These matters will be discussed in the following chapters.

CHAPTER THREE
MATHEMATICAL MODEL OF AN ARTIFICIAL LEG HAVING
POLYCENTRIC KNEE MECHANISM TO BE USED FOR
TRANSFEMORAL AMPUTATION

3.1 Transfemoral Amputation

There are various types of bipedal walking problems which occur due to neural problems in brain, cerebellum or in some part of neural network, due to muscular and orthopedic problems like malfunctioning of joints and limbs or loss of walking organs because of some kinds of diseases.

Transfemoral amputation is one of the most important walking problems encountered by lower limb amputees. It can be defined as the amputation of the lower limb between hip and knee articulation. The reasons for transfemoral amputation are mostly the vascular problems and disabilities occurred in military service. This operation is preferred by the surgeons because 100 % of the patients are healed after the operation. Despite the recovery success of the process, it has the disadvantage that walking characteristics of the patients change significantly, since they have lost one limb and one articulation, that is the knee.

In the case of transfemoral amputation, the patient uses an artificial leg with an artificial knee joint. To walk with this combination, which is called an *artificial leg*, is quite difficult because the patient must adapt his/her body posture by changing his/her body position and orientation or by adjusting the stiffness of the muscles of his/her legs in order to meet the needs of this new circumstance. Although rapidly developed artificial knee mechanisms and newly improved actuators, which have high efficiencies with good control modules improved specially for that kind of actuator, allow the walkers to move more comfortably, studies showed that amputees still have to consume 45 % more energy than the people having healthy walking anatomy do (Boonstra, Schrama, Fidler & Eisma, 1994). Today, studies are focused

on the aim of reducing this amount of energy consumption, but still more has to be done by the researchers.

The improvements in the field of artificial knee joints and artificial legs started at the last decade of nineteenth century with newly established companies which manufactured artificial limb products. In these artificial limb structures, control of walking speeds and gait length could only be achieved by mechanical components, since in those years there was much to do to develop electronics technology for use in the intelligent systems. Especially during World War II, countries started to spend more money for artificial limb and joint researches due to the increasing number of war veterans. Hence, it can be said that in those years, mechanical design of these products reached its most developed state. In the last decades of the twentieth century, like in all other technological improvements, there occurred some developments on the field of artificial limbs and joints. After microprocessor controlled knee joints had been introduced in 1993, these studies started to find their way on the field of biomechatronics. In 1997, the company Otto-Bock introduced a new design C-Leg, a single axis knee with electronically controlled hydraulic swing and stance phases (Perry, Burnfield, Newsam & Conley, 2004). In the year 2000, Otto-Bock introduced C-Leg Compact, a newer, safer and more reliable product. Today there are lots of companies like, Otto-Bock, Endolite, Nabtesco, Össur, etc. who deal with electronically controlled artificial legs having knee joint and it is believed that in the coming decade, more technology will be introduced by them on this area of biomechatronics.

Like bipedal walking system, artificial leg is also a dynamic system, the variables of which are time dependent joint variables and it can be represented by differential equations. In this chapter, in order to derive the mathematical model of artificial leg, kinematic analyses are made first, and after obtaining pose, velocity and acceleration information, dynamics of the system is derived.

3.1.1 Types of Knee Joints Used in Transfemoral Amputation

Basically two types of knee joints are used in the artificial leg design in transfemoral amputation cases. These are single axis and poly-centric knee joints. Both designs have some advantages and disadvantages, when compared with each other, and for this reason, the suitable knee axis type must be chosen altogether with the patient, doctor and the physiotherapists in order to obtain suitable and comfortable walking characteristics for the amputee.

3.1.1.1 Single Axis Knee Joint

For the patients suffering from transfemoral amputation, single axis knee joint is widely used (Figure 3.1). In this mechanism, flexion and extension occur around only one axis. This type of knee joint has some advantages when compared with other types of joints. Advantages are its reliability, simplicity, low maintenance, and low cost. This is a simple prosthetic knee that is rarely used except in poorer and developing countries.



Figure 3.1 Single axis friction knee of Hosmer Corporation.

<http://www.hosmer.com/products/knees/index.html>

One of the most important design advancements for the prosthesis is control of the swing phase. The initial prototype was a friction based system in which an adjustable friction cell was pressed against the knee axle, resulting in a certain degree of swing control. An elastic or spring loaded mechanism is also frequently provided

to promote full leg extension before heel strike. Unfortunately, the friction swing control mechanism functions well in only one cadence and it is difficult to use it on irregular surfaces. Despite the simplicity of design and limitations, the single axis knee is a surprisingly reliable and inexpensive design ideally suited to individuals with restricted access to regular health care and prosthetic maintenance.

3.1.1.2 Polycentric Knee Joint

In different walking conditions and walking phases (swing and stance phases), an increment in the stability of walker can be achieved by polycentric knee mechanism (Figure 3.2). A polycentric knee mechanism consists of four points of rotation, each connected by a linkage bar. This allows optimal control of swing and stance phases. Another feature of the polycentric knee is better stance stabilization while maximizing ease of pre-swing knee flexion.

The stance stability of the prosthetic polycentric knee changes with the changing position of the instant centre of rotation. Instant centre of rotation can be described as a point where, for a very small change in the angle of knee flexion, the thigh section rotates about a point on an extension of the shank which appears to be temporarily fixed.

For prosthesis having a polycentric knee joint, instant centre of rotation is always located at the intersection of centre lines of the anterior and posterior links connecting the socket section to the shank section of the prosthesis. As the knee flexion angle is increased, the instant centre takes a series of positions. In the studies made in 1994 (Radcliffe, 1994), it is proved that for a stable prosthetic knee mechanism which has no actuators and control systems, this instant centre must lie within an acceptable zone, called “the stability zone”. An elevated and posterior location of instant centre increases the knee stability.

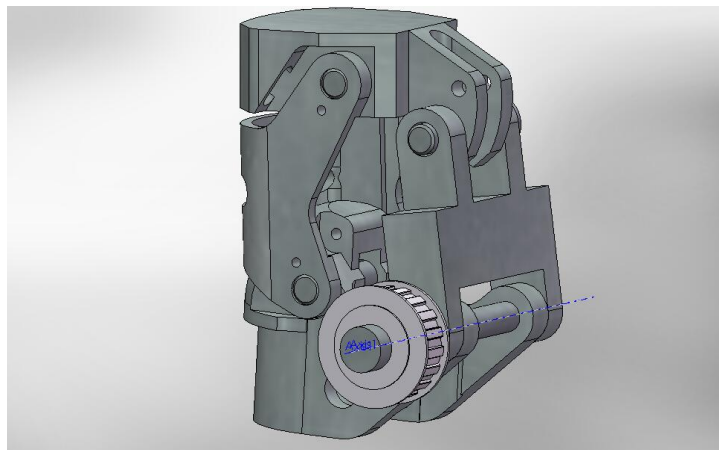


Figure 3.2 Solidworks model of polycentric knee based on NI-C411 intelligent knee model of Japanese firm Nabtesco. The intelligent knee is modified in order to be actuated by permanent magnet D.C. motors.

The choice of the lengths of anterior and posterior links of a polycentric knee changes the position of the instant centre of rotation, which leads to a change in the stability of the system. Definitely, an optimization must be made for the link lengths. If the instant centre is elevated very much, the system becomes extremely stable and this makes the system to behave as a locked mechanism at fully extension. If it is lowered very much, this time the system is over stabilized and the patient loses his/her control of walking and starts to have difficulties in doing daily activities like sitting from a standing position, stair descent etc. For this reason, instant centre must be in a proper position allowing the patient to control his/her motion through all walking period.

3.2 Mathematical Model of Artificial Leg Having Polycentric Knee Mechanism

Geometry of artificial leg with polycentric knee is quite different from most of the walking mechanisms. In walking robots and some prosthetic devices used in transfemoral amputation applications, single axis joints are widely used and mathematical models are derived using the methodologies which can be found in the literature for serial manipulator dynamics problems. Distinctive feature of the artificial leg having polycentric knee is that it is a serial manipulator, one of the

joints (the knee joint) of which is designed as a close chain (Figure 3.3). For this reason, standard analyses fail to obtain the dynamics of this kind of system.

The model of artificial leg is considered as a *hybrid artificial leg* having two degrees of freedom; one at the ankle joint, *Joint O* and one at *Joint A* of the four bar mechanism. By activating the system with motors mounted on these two joints, hip joint can track an arbitrary path which complies with the conditions of natural walking.

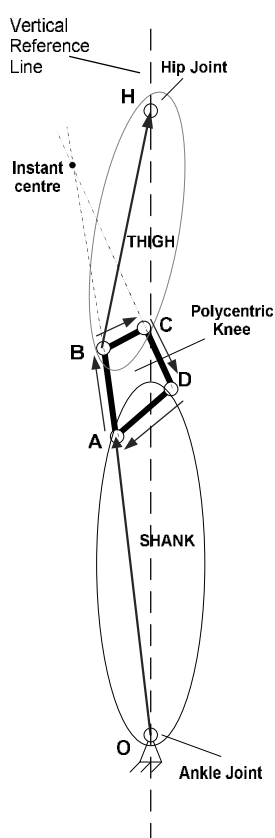


Figure 3.3 Hybrid Artificial leg model is considered as a serial manipulator with a polycentric knee joint.

In the design of artificial leg having polycentric knee joint, the important point is that, at every instant of walking at stance phase, moment demand of the system is as small as possible. To obtain stability, the instant centre must be elevated and it must also lie behind the force line, the line along which the equivalent single force acts on

prosthesis and it is directed from hip joint to the ankle. This type of knee has typically a long anterior link and a short posterior link. Thus, such kind of a knee joint allows the usage of smaller and less powerful motors in the design.

As for the serial manipulator characteristic of artificial leg, the ankle joint is considered as the joint where the reference plane of the system is attached. Hip joint axis is the centre of the end effector and the trajectory of the end effector must be followed correctly to obtain a correct walking characteristic.

Mathematical modelling of artificial knee starts with obtaining the workspace of the system. Workspace of a robot manipulator represents all the possible values of joint variables. After workspace of the manipulator is determined, inverse kinematic analysis is made in order to obtain the joint variables for a given trajectory.

Having made the whole kinematic analysis, which means finding velocity and acceleration terms for the joint variables, dynamics of the system can then be derived. By the use of the mathematical model, control algorithms can be improved and model-based real-time control of artificial leg can be achieved.

3.2.1 Forward Kinematics to Obtain the Workspace

Forward kinematics can be defined as computation of the position and orientation of robot's end effector as a function of joint angles. Since all the possible values of joint angles are taken into consideration, the workspace of artificial leg can be derived by this method. Note that, for the hip joint to track the arbitrarily selected hip trajectory, the joints need not take all the possible angular values, but the trajectory must definitely lie within the workspace in order that the end effector, i.e. the hip joint, reach some point at the trajectory. This means that the trajectory results in accord with some mathematical solution which gives the posture and orientation knowledge of the joints.

If the kinematic equations of the close chain $ABCD$ and open chain $OABH$ are written, then by forward kinematics, all the positions of hip joint, i.e. the workspace, can be derived (Figure 3.4).

For the close chain $ABCD$, equations are given as follows:

$$l_2 \cdot e^{i(\theta_a + \theta_2)} + l_3 \cdot e^{i\theta_3} - l_4 \cdot e^{i\theta_4} - l_1 e^{i\theta_1} = 0 \quad (3.1)$$

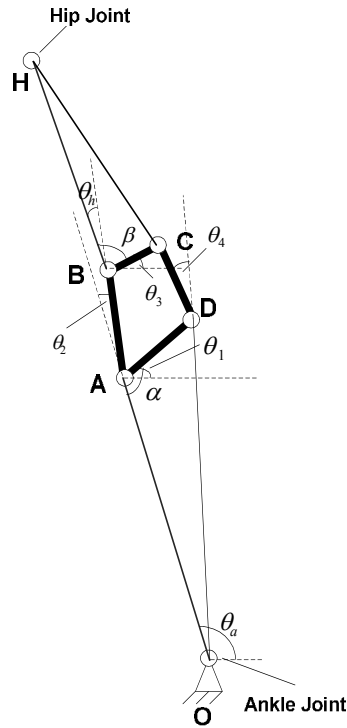


Figure 3.4 Hybrid artificial knee and joint variable representations in flexion.

Here l_2 , l_3 , l_4 and l_1 are the length of the links AB , BC , CD and DA , respectively. θ_a is the angle of the ankle joint, $\theta_1, \theta_2, \theta_3$ and θ_4 are the joint variables for the joints D , A , B and C respectively. From the geometry, θ_1 can be found as:

$$\theta_1 = \alpha - 180^\circ - \theta_a \quad (3.2)$$

where, α is the constant angle of the lower rigid body. In Eq. (3.1), θ_a and θ_2 are known variables, since they are reference inputs. Hence, joint variables θ_3 and θ_4 of

the four bar mechanism can be found from this equation. As for the position of hip joint, the following open chain equation can be used:

$$P_H = l_a \cdot e^{i\theta_a} + l_2 \cdot e^{i(\theta_a + \theta_2)} + l_h \cdot e^{i\theta_h} \quad (3.3)$$

Here, l_a and l_h are the lengths of the lower and upper rigid body vectors. θ_h is the joint variable for hip joint. Again, from the geometry, θ_h can be found as:

$$\theta_h = \theta_3 + \beta - (\theta_a + \theta_2) \quad (3.4)$$

where, β is the constant angle of lower rigid body. Since θ_a and θ_2 are the inputs and θ_3 is to be found from Eq. (3.1), the position of the hip can be found from Eq. (3.3).

3.2.2 Inverse Kinematics to Follow an Arbitrary Trajectory

Inverse kinematics is the process of determining joint parameters of a kinematic chain in order to achieve a desired pose. After obtaining the workspace from forward kinematics, a suitable trajectory which lies within the workspace of the system must be chosen and joint variables must be derived according to this trajectory. Trajectory of end effector can be determined from the studies of Başer, Çetin and Uyar (2007), by choosing the needed parameters as follows:

$$L_{leg} = 1.01 \text{ m}$$

$$L_{lower} = 0.5 \text{ m}$$

$$L_w = 0.2 \cdot L_{leg}$$

$$T_w = 1 \text{ sec}$$

$$h_{max} = 0.01 \text{ m}$$

Here, L_{leg} is the length of the leg, L_{lower} is the length of the lower leg (i.e. shank), L_{gait} is the gait length, T_{gait} is the time for one step and h_{max} is the maximum

displacement of hip joint in y direction. To obtain the values of joint variable of hybrid artificial knee at every point of the trajectory, iterative solutions must be considered since joint variables of close chain four bar mechanism can only be found by solving nonlinear Eq. (3.1) and (3.3) for the given end effector pose.

3.2.3 Velocity and Acceleration Analysis

The velocity of end effector, which is the hip joint, on the trajectory can be obtained by using the concept of Jacobian matrix. The velocity problem in this study is considered as inverse velocity problem. For the inverse velocity problem, velocity state of the end effector is given and input joint rates required to produce the desired velocity are found.

For the robot manipulators, the Jacobian matrix is defined as the matrix that transforms the joint rates in the actuator space to the velocity state in the end effector space. This can be represented as:

$$\mathbf{V}_H = \mathbf{J} \cdot \dot{\mathbf{q}} \quad (3.5)$$

where \mathbf{V}_H represents the velocity of end effector, $\dot{\mathbf{q}}$ is the vector that represents the joint variables and \mathbf{J} is the Jacobian matrix. As a remark, it must be noted that the Jacobian matrix derived here is quite different from the Jacobian matrices obtained both in serial manipulator and parallel manipulator mechanisms, since the system mentioned here is a hybrid system composed of both open and close chains. Equations representing the velocity equalities are given as:

$$2\vec{w}_t \times \vec{r}_H + \vec{w}_2 \times \vec{r}_{H/A} + \vec{w}_f \times (\vec{r}_{H/C} + \vec{r}_{H/B}) + \vec{w}_5 \times \vec{r}_{H/D} = \vec{V}_H \quad (3.6)$$

$$\vec{w}_2 \times \vec{r}_{B/A} + \vec{w}_f \times \vec{r}_{C/B} - \vec{w}_5 \times \vec{r}_{C/D} - \vec{w}_t \times \vec{r}_{B/C} = \mathbf{0} \quad (3.7)$$

where w_t and w_f are the angular velocities of tibia and femur, respectively. Eqs. (3.6) and (3.7) can be written in matrix form to obtain the Jacobian matrix as:

$$\mathbf{J} = \begin{bmatrix} -(r_{B/C})_y & -(r_{C/B})_y & -(r_{B/A})_y & (r_{C/D})_y \\ (r_{B/C})_x & (r_{C/B})_x & (r_{B/A})_x & -(r_{C/D})_x \\ 2(r_H)_y & -(r_{H/C} + r_{H/B})_y & -(r_{H/A})_y & -(r_{H/D})_y \\ 2(r_H)_x & (r_{H/C} + r_{H/B})_x & (r_{H/A})_x & (r_{H/D})_y \end{bmatrix} \quad (3.8)$$

where components trajectory velocity vector and joint variable terms are given as:

$$\mathbf{V}_H = \begin{bmatrix} 0 & 0 & (\mathbf{V}_H)_x & (\mathbf{V}_H)_y \end{bmatrix} \quad (3.9)$$

and

$$\dot{\mathbf{q}} = \begin{bmatrix} w_t & w_f & w_2 & w_5 \end{bmatrix}^T \quad (3.10)$$

Acceleration of joint variables can be calculated by taking the derivatives of Eqs. (3.6) and (3.7) with respect to time. Equations of acceleration are given below:

$$\begin{aligned} & 2\vec{\alpha}_t \times \vec{r}_H + \vec{\alpha}_f \times (\vec{r}_{H/C} + \vec{r}_{H/B}) + \vec{\alpha}_2 \times \vec{r}_{H/A} + \vec{\alpha}_5 \times \vec{r}_{H/D} \\ &= \vec{a}_H - 2\vec{w}_t \times (\vec{w}_t \times \vec{r}_H) - \vec{w}_f \times \left[\vec{w}_f \times (\vec{r}_{H/C} + \vec{r}_{H/B}) \right] - \vec{w}_5 \times (\vec{w}_5 \times \vec{r}_{H/D}) \\ & - \vec{w}_2 \times (\vec{w}_2 \times \vec{r}_{H/A}) \end{aligned} \quad (3.11)$$

$$\begin{aligned} & \vec{\alpha}_t \times \vec{r}_{B/C} + \vec{\alpha}_2 \times \vec{r}_{B/A} + \vec{\alpha}_f \times \vec{r}_{C/B} - \vec{\alpha}_5 \times \vec{r}_{C/D} = \\ & - \vec{w}_t \times (\vec{w}_t \times \vec{r}_{B/C}) - \vec{w}_2 \times (\vec{w}_2 \times \vec{r}_{B/A}) + \vec{w}_5 \times (\vec{w}_5 \times \vec{r}_{C/D}) \end{aligned} \quad (3.12)$$

Here, the joint variables vector representing the joint accelerations are given as:

$$\ddot{\mathbf{q}} = \begin{bmatrix} \alpha_t & \alpha_f & \alpha_2 & \alpha_5 \end{bmatrix}^T \quad (3.13)$$

Note that, these values must be calculated in every instant of time as the position of hip joint changes through the walking process. After finding the values of all joint variables and their derivatives according to the given trajectory pose, velocity and acceleration, dynamics of the system can be derived.

3.2.4 Dynamics of the Artificial Hybrid Leg

To control the motion of the artificial hybrid leg for the purpose that hip joint traces a desired trajectory satisfying a natural walking for the amputee, the control system has to decide and produce torques at the joints via the actuator system. Hence, forces which arise due to the system dynamics can be balanced by the produced joint torques.

The problem mentioned on this study is the problem of *inverse dynamics*, which is the calculation of required joint torques for the computed joint positions, velocities and accelerations in the inverse kinematics analysis. For this reason, an accurate modeling of inverse dynamics is quite important since design of the controller is related with the model.

As mentioned in Chapter two, gravity torques which arise from the gravitational force exerted on the links, external forces/torques which are applied to the end effector and three types of dynamic torques which arise from the motion of a manipulator act on the hybrid artificial leg. Dynamic torques include inertial, centripetal and Coriolis effects. Inertial torques are proportional to joint accelerations pertinent to Newton's second law. Centripetal torques arise from the centrifugal forces which constrain a body to rotate about a point. They are directed towards the centre of the uniform circular motion and are proportional to the square of joint velocity. As for the Coriolis torques, they arise from vortex forces derived from the interaction of two rotating links (McKerrow, 1991). The dynamical equation of hybrid artificial leg covers all these effects and it can be derived by using Newton-Euler formulation.

According to Figure 3.5, net torque acting on point B of the upper leg can be expressed as:

$$\vec{\tau}_B = \vec{\tau}_{ext} + \vec{r}_{G_3/B} \times m_3 \cdot \vec{a}_{G_3} + \vec{r}_{H/B} \times \vec{f}_{ext} - \vec{r}_{G_3/B} \times m_3 \cdot \vec{g} + I_3 \cdot \vec{\alpha}_f \quad (3.14)$$

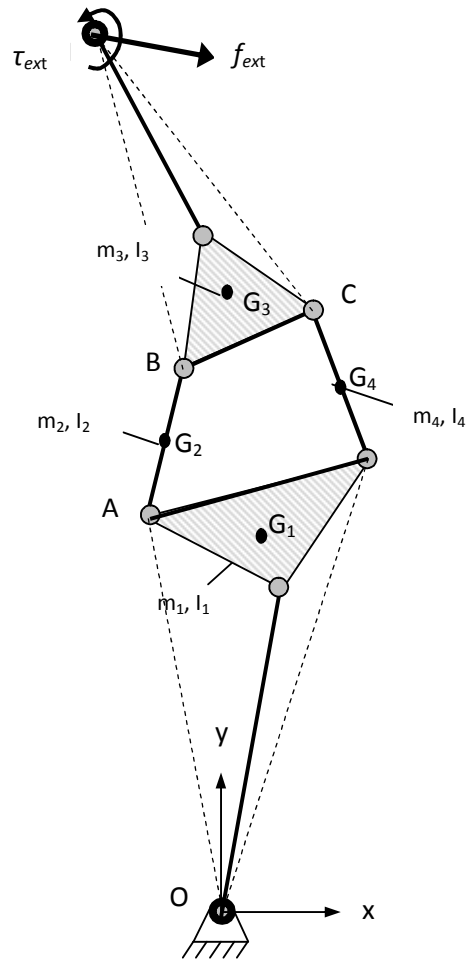


Figure 3.5 Representation of acting forces and torques on the hybrid artificial leg.

where $\vec{\tau}_{ext}$ is the external torque exerted to the hip joint, m_3 is the weight of the upper leg, \vec{f}_{ext} is the external force acting at hip joint and I_3 is the mass moment of inertia of the upper leg. As the joint velocities and accelerations are given in Eqs. (3.11) and (3.12), acceleration term \vec{a}_{G_3} can be easily calculated from these expressions and can be substituted into Eq. (3.14).

As for the point A , not only the gravitational and dynamic torques act on the body, but also the torques arisen from the movement of upper leg and calculated in Eq.(3.14) must also be taken into consideration.

$$\vec{\tau}_A = \vec{\tau}_B + \vec{r}_{G_2/A} \times m_2 \cdot \vec{a}_{G_2} - \vec{r}_{G_2/A} \times m_2 \cdot \vec{g} + I_2 \cdot \vec{\alpha}_2 \quad (3.15)$$

Eq.(3.15) represents the basic torque needed which will be supplied by the direct current motor attached to this joint of the leg. Since the second motor will be attached to the ankle joint (point O), the net torque effect acting on point O must be computed as

$$\vec{\tau}_O = \vec{\tau}_D + \vec{\tau}_A + \vec{r}_{G_1} \times m_1 \cdot \vec{a}_{G_1} - \vec{r}_{G_1} \times m_1 \cdot \vec{g} + I_1 \cdot \vec{\alpha}_1 \quad (3.16)$$

Here, $\vec{\tau}_A$ is the torque component which is found by Eq.(3.15), $\vec{\tau}_D$ is the torque component which acts on point D and it can be found as:

$$\vec{\tau}_D = \vec{\tau}_C + \vec{r}_{G_4/D} \times m_5 \cdot \vec{a}_{G_4} - \vec{r}_{G_4/D} \times m_5 \cdot \vec{g} + I_4 \cdot \vec{\alpha}_4 \quad (3.17)$$

where,

$$\vec{\tau}_C = \vec{\tau}_{ext} + \vec{r}_{G_3/C} \times m_3 \cdot \vec{a}_{G_3} + \vec{r}_{H/C} \times \vec{f}_{ext} - \vec{r}_{G_3/C} \times m_3 \cdot \vec{g} + I_3 \cdot \vec{\alpha}_f \quad (3.18)$$

After obtaining the torques acting on the joints A and D, the control system supplying a stable walking for hybrid artificial leg can be constructed to reduce the disturbance torque effects on the motors attached to these joints. These disturbance torques arise from the dynamics of the leg which is discussed in this chapter. In the next chapter, control of the hybrid artificial leg will be discussed, briefly.

CHAPTER FOUR
CONTROL OF ARTIFICIAL HYBRID LEG HAVING POLYCENTRIC
KNEE MECHANISM

4.1 Introduction

Mechatronic system design deals with integrated and optimal design of a physical system including subsystems like sensors, actuators, electronic components and digital control systems in order that system behaves in a desired manner with the desired characteristics. Since a physical system is a dynamic system the behavior of which changes with time, response of the system to a given input varies according to the system dynamics. To ensure the output to be stable and to track the reference trajectory with a good system performance, mechatronic system must be supported with control architecture.

In mechatronic systems, control subsystems sometimes have inputs that do not participate in feedback control. This means that although the reference input is compared with the feedback signal (which is the measured or computed output signal), some input signals like undesired disturbances or load effects caused by external factors cannot be presented in the feedback control structure. These undesired and/or unavoidable inputs affect the performance of the control systems in a negative manner. Hence, if they can be included in the control structure somehow before they affect the output of the process, performance of the system can be improved significantly. To include the disturbance signals into control structure and use this information in order to generate the control signals, disturbances must be either computed or they must be measured correctly (if they are to be known).

4.2 Feed-forward Control

In feed forward control, unknown inputs are measured and that information, along with the desired inputs, is used to generate control signals that can reduce the errors due to these unknown inputs and/or to their variations.

The reason for calling this method “feed forward control” stems from the fact that the associated measurement and control (and compensation) concern the input, not the output, and it takes place in the forward path of the control signal (De Silva, 2005). Note that in feedback control systems outputs are measured and they are fed back in order to be compared with the reference value to form the error signal.

It is another fact that feed forward control is always used along with feedback control because a feedback control system is required to track set point changes and to suppress unmeasured disturbances that are always present in any real process (Brosilow & Joseph, 2002). A block diagram representation of feed forward and feedback control is given in Figure 4.1. In this system, in addition to feedback control, disturbance input is also fed into the controller. Here, the controller is a modified version of the standard feedback controller having no feed forward effect and it reduces, i.e. compensates, the disturbance effects. Design of the controller is the main interest of this chapter.

Today, there are still great discrepancies between newly improved control systems and the ones used in industrial robotic applications. In industrial applications, usually simple linear joint controllers are used because of the fact that more sophisticated control algorithms are time-consuming structures and they are not suitable for real-time working systems. Although control systems based on linear joint control are sufficient for applications that require only high position accuracy, they lead to non-acceptable deviations for applications requiring high path accuracy, e.g., laser-cutting (Grotjahn & Heimann, 2002). The reasons of these deviations are the non-linearities which arise from gear friction and/or non-linear dynamics of robot manipulators.

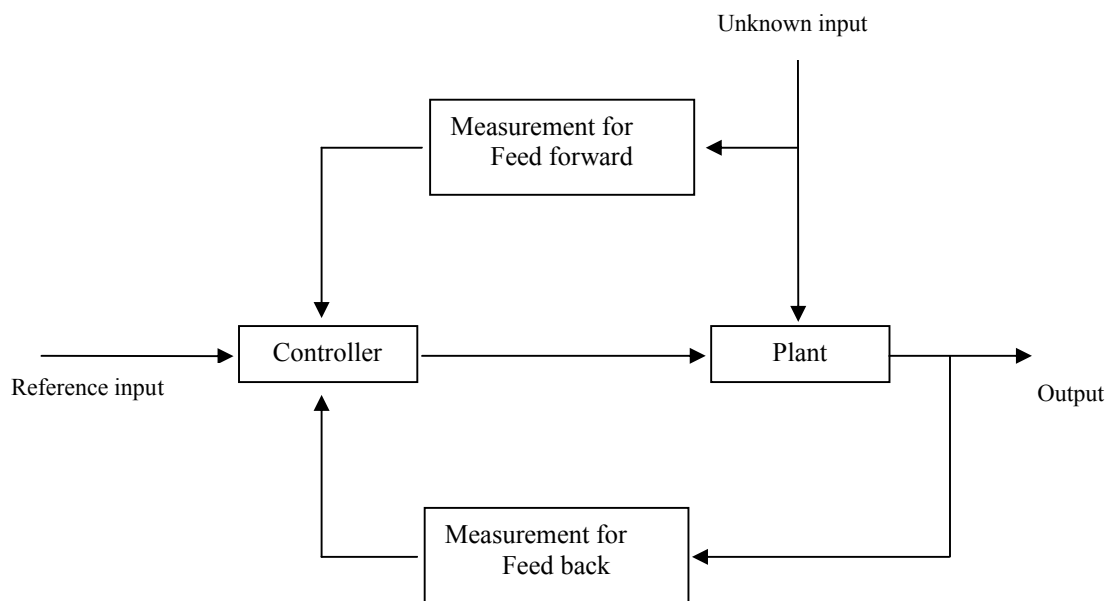


Figure 4.1 System with feed forward and feedback control

Non-linear effects due to system dynamics can be compensated in several ways. One of these methods is the computed torque methodology developed in robotics research some years ago (Sciavicco & Siciliano, 1996). The computed torque control structure is a non-linear control law which results linear decoupled tracking error dynamics. Provided that the parameters of the bipedal robot are known accurately, this controller will provide accurate tracking of the desired path, if the joint positions and velocities are measured accurately. In this method a feedback loop is constructed in order to cancel the dynamic torques and gravity torques.

Computed torque methodology is very successful. However, the necessity of torque interface, which is not employed in industrial systems, stands as a milestone in real-time applications. For this reason, Grotjah, Heimann, & Heimann (1999) proposed another approach, called non-linear pre-correction. In this method, as in computed torque method, the inverse dynamics of the robot is used to calculate the expected torques from the desired joint motions. Since no torque interface is available for feed forward control, the resulting values are transferred into trajectory corrections by an inverted controller model.

Feed-forward control is also used in parallel manipulator mechanisms, since they have highly non-linear, coupled dynamic behaviour. In the study of Wang & Wu (2008), a model based control is achieved integrating the non-linear system dynamics into the control design with a feed forward controller. In dynamic feed-forward control, each chain of a parallel manipulator is regarded as an independent control object, and the control system for each chain is designed as based on the dynamic model of the chain. Moreover, the feed-forward compensator is added to the control system of each chain to compensate for the load torque of each chain. Although the dynamic feed-forward control increases the number of independently controlled systems, it has some advantages as such: (1) anti-disturbance capability of the closed-loop control subsystem can be used to decrease the influence of inaccurate dynamic model on the motion precision; (2) the dynamic control subsystem and closed-loop control subsystem can be regarded as independent systems such that they can be designed independently (Wang, Wu, Wang, & You, 2008). The basic disadvantage of this control method is that it is computationally intensive and this makes it to be unsuitable for real-time applications.

Another approach to solving the tracking problem of robot manipulators is the use of disturbance rejection strategy together with the feed-forward compensation. This method can be applied, if the disturbance can be measured or computed correctly. Since system dynamics of the artificial hybrid leg is derived in Chapter 3, disturbance rejection method can be used as the main control strategy for artificial hybrid leg system.

4.3 Disturbance Rejection Strategy

In a control system, the plant (or sometimes called the process) is to be controlled by an input to the plant, which is called the *manipulated input* or the *reference input*. Reference input gives the desired value or desired values of a sequence to a system, the output of which differs from this input due to the system dynamics. In order to reduce this discrepancy as much as possible, a controller which has the task of

obtaining a desired effect on the output of the system by eliminating steady state errors must be designed.

Any control system can have some inputs other than the reference input, which cannot be controlled by feedback loop but influence the process output. Such inputs are called as *disturbance signals* and one of the aims of the control structure is usually to minimize the effects of these unwanted inputs on the process output.

Control problem discussed in this manuscript is the trajectory control of two permanent magnet direct current motors (PMDC motors) which drive an artificial hybrid leg having a polycentric knee mechanism. Here, velocity control task is to be achieved for the given velocity profiles as reference input to the motors. Although, the dynamic characteristics of PMDC motors are well known, disturbance effects which arise due to dynamical structure of hybrid artificial leg are unknown. As it is mentioned in the previous parts of this chapter, these disturbances must be computed or measured before they affect the outputs of motors.

General block diagram of a PMDC motor is given in Figure 4.2. Here, K_M is the motor constant, K_b is the back electromotive force, L_a is the armature inductance, R_a is the armature resistance, J_a is the inertia of the rotor and B_a viscous friction occurring in the rotor bearings.

Both motors attached to ankle and knee joints of the hybrid artificial leg have the same characteristic given in Figure 4.2 with only one distinctive feature, which is the difference between torque disturbance expressions. Disturbance torques arise from the dynamics of the system which are derived in chapter three. The motor which is mounted on the knee joint carries the dynamical load caused by upper leg motion and this disturbance torque input is given in Eq. 3.17.

The second motor at the ankle joint carries not only the torque load that arises from upper body motion, but also the torque caused by the lower leg. This expression is given in Eq. 3.18. Note that the ankle motor does not carry the weight of the knee

joint motor, since this motor is physically mounted to the foot and the power is transmitted through combined belt-pulley mechanism. When considering motor dynamics, these differences in the disturbance input signals must be taken into account.

In the control architecture, feedback control is to be used to compare the measured joint inputs with the reference values. Any error between the feedback signal and the reference signal is amplified to provide power to the actuator. But the existence of the disturbances causes the system to produce a certain steady state error. Therefore, the effect of these disturbances must be compensated.

State space representation of PMDC motor was introduced in chapter two with Eqs. (2.18) and (2.19) which can be rewritten in closed form as:

$$\dot{\mathbf{x}} = \mathbf{A} \cdot \mathbf{x} + \mathbf{B} \cdot \mathbf{u} \quad (4.1)$$

$$\mathbf{y} = \mathbf{C} \cdot \mathbf{x} \quad (4.2)$$

In Eqs. (4.1) and (4.2), \mathbf{x} is the state vector, \mathbf{u} is the input vector, \mathbf{A} is the system matrix, \mathbf{B} is the input matrix and \mathbf{C} is the output matrix of the actuator system. The mathematical expressions for the state and input vectors are as follows:

$$\mathbf{x} = \begin{bmatrix} i_a \\ \omega_a \end{bmatrix} \quad (4.3)$$

$$\mathbf{u} = \begin{bmatrix} V_a \\ T_d \end{bmatrix} \quad (4.4)$$

Overall transfer function of PMDC motor can be computed as:

$$\mathbf{G}(s) = \mathbf{C} \cdot (s\mathbf{I} - \mathbf{A})^{-1} \cdot \mathbf{B} \quad (4.5)$$

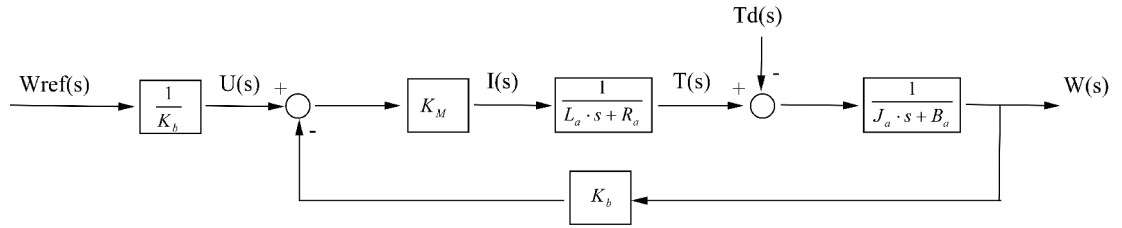


Figure 4.2 General characteristics of a permanent magnet direct current motor with the given torque disturbance input. The output of the system is angular velocity of the motor shaft and the reference input denoted by $W_{ref}(s)$ is the angular velocity reference value. Note that the armature feeding voltage $U(s)$ and $W_{ref}(s)$ are directly proportional with a constant of $1/K_b$.

Note that, $G(s)$ is the combination of two inputs, namely reference input which is the armature angular velocity (i.e. $w_a(s) = w_{ref}(s)$) and the disturbance input ($T_{La}(s)$). Hence, referring to Figure (4.2) and taking $K_b=1$ for simplicity, which give the result $W_{ref}(s)=U(s)$, the output of the system yields:

$$y(s) = \begin{bmatrix} G_{ref}(s) & G_{dis}(s) \end{bmatrix} \cdot \begin{bmatrix} \omega_{ref}(s) \\ T_d(s) \end{bmatrix} \quad (4.6)$$

Here,

$$G_{ref}(s) = \frac{\omega(s)}{\omega_{ref}(s)} = \frac{K_M}{(L_a s + R_a)(J_a + B_a) + K_b K_M} \quad (4.7)$$

$$G_{dis}(s) = \frac{\omega(s)}{T_{La}(s)} = \frac{-(L_a s + R_a)}{(L_a s + R_a)(J_a + B_a) + K_b K_M} \quad (4.8)$$

The block diagram of the PMDC motor with disturbance input due to artificial leg dynamics is given in Figure 4.3. Note that Figure 4.3 shows an uncontrolled system; it only demonstrates the input output relations given by the Eqs. (4.3) through (4.8).

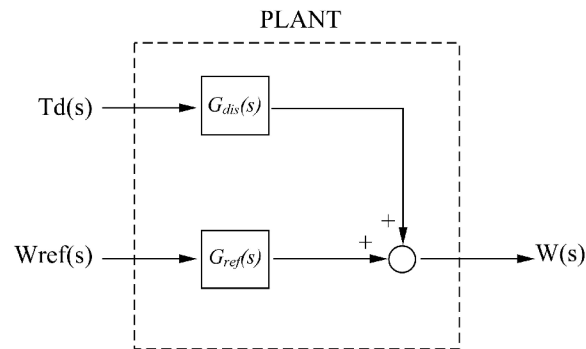


Figure 4.3 Uncontrolled plant with disturbance input due to artificial leg dynamics.

If a closed-loop control (i.e. feedback control) system for a PMDC motor is presented, its block diagram is given as in Figure 4.4. Controlled output expression can be written as follows:

$$W(s) = \frac{G_c(s) \cdot G_{ref}(s)}{1 + G_c(s) \cdot G_{ref}(s) \cdot H(s)} \cdot R(s) + \frac{G_{dis}(s)}{1 + G_c(s) \cdot G_{ref}(s) \cdot H(s)} \cdot Td(s) \quad (4.9)$$

Here, $G_c(s)$ is the transfer function block of the controller and $H(s)$ is the transfer function of an angular velocity transducer (for example, an encoder).

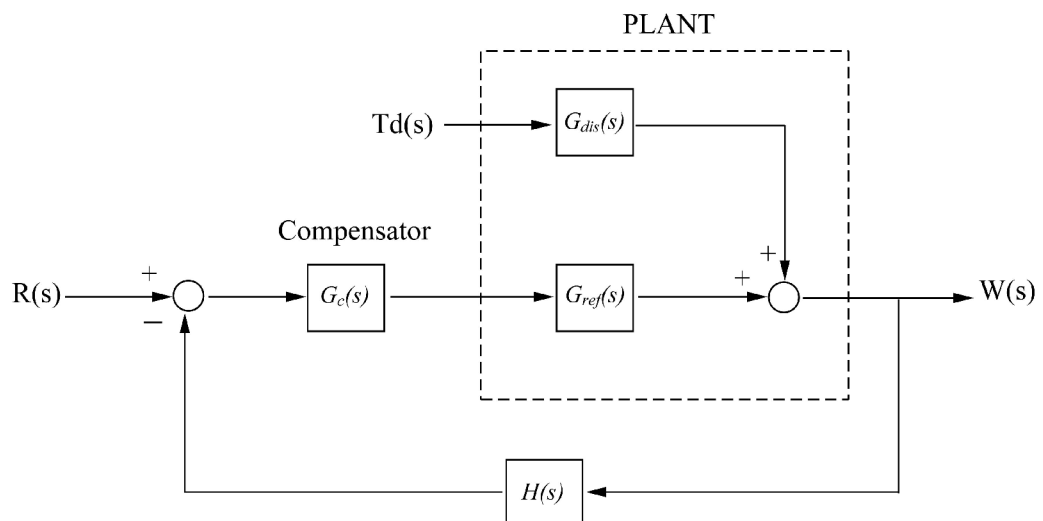


Figure 4.3 Feedback control scheme of a PMDC motor with disturbance input. $G_c(s)$ is the controller and $H(s)$ is the angular velocity transducer (for example, an encoder).

In order to reject the disturbance effect, feed-forward compensation methodology can be applied to the system. Block diagram representation of feed-forward compensation with the feedback loop is given in Figure 4.4.

When classical feed-forward scheme is adopted (Figure 4.4), the overall output of the system will be,

$$W(s) = \frac{G_c G_{ref}(s)}{1 + G_c G_{ref} H(s)} \cdot R(s) + \frac{G_{dis}(s) - G_{cd} G_c G_{ref}(s)}{1 + G_c G_{ref} H(s)} \cdot Td(s) \quad (4.10)$$

where $G_c(s)$ is the transfer function of the compensator for reference input. Here, the controller can be selected as a P or a PI controller to achieve a successful reference tracking, if the controller parameters are chosen carefully.

In the figure, $G_{cd}(s)$ represents the transfer function of the feed-forward compensator for disturbance. It is seen from Eq. (4.10) that, when the numerator of the disturbance term is set to zero, the disturbance effects can be cancelled out. For this purpose, feed-forward compensator $G_{cd}(s)$ must be selected to ensure the disturbance transfer function to be equal to zero. Hence,:

$$G_{cd}(s) = \frac{G_{dis}(s)}{G_c G_{ref}(s)} \quad (4.11)$$

It is important to note that, for systems with time variant parameters, control paradigms based on transfer function manipulations, which are developed for constant parameter systems, are invalid. As a solution to this problem a sequential control method is adopted. At any control sequence, time dependent system parameters are calculated first, from joint variables of the previous sequence and then, parameters of both compensators are re-calculated and the developed control law is executed.

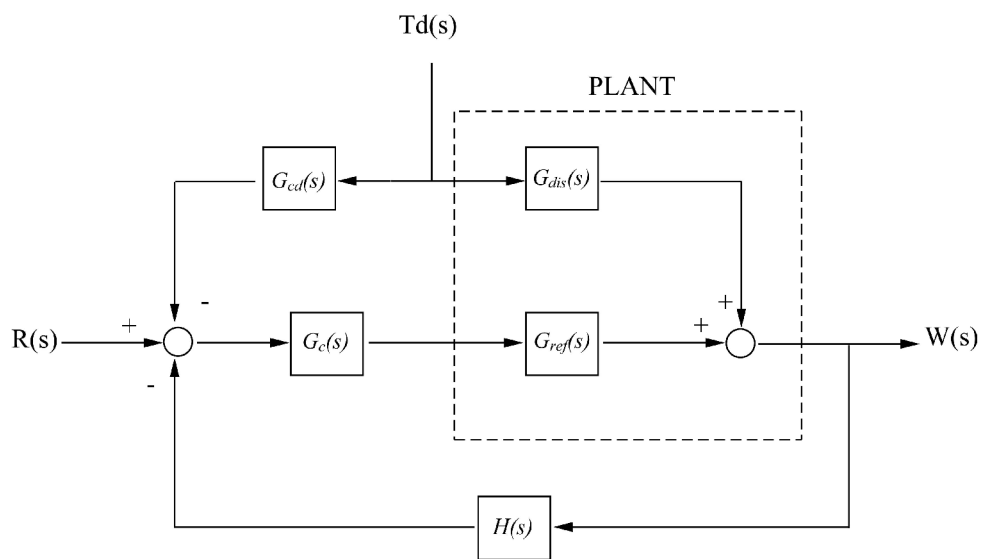


Figure 4.4 Feed-forward compensation scheme with a feedback loop. Disturbance torques are fed-forward in order to take them into account in the control architecture.

CHAPTER FIVE

ARTIFICIAL HYBRID LEG DESIGN

5.1 Introduction

In today's world, design of walking robots, walking aid apparatuses and devices are considered as important topics of various research groups, who deal with the usage of mechatronic products in human's daily life for the purpose of making the life easier. Among these topics, design of walking aid devices may be one of the most significant one, since people having walking problems come across lots of other difficulties which are not even realised by healthy people.

In transfemoral amputation, patient needs a device which has a knee joint together with an ankle joint. Performance of the device increases as much as it provides a stable, comfortable, natural walking for the amputees and at the same time it consumes less energy. Increase in the stability and control performance of the system can be realized by the design of an *artificial hybrid leg*, which is the main scope of this chapter.

The term *hybrid* means something having two kinds of components that produce the same or similar results. In this study, the hybrid characteristic comes from the mechanical structure of the system. Mechanical subsystem is composed of a serial manipulator and a closed-loop four-bar knee mechanism, which connects the upper-leg with the lower-leg. Since the artificial knee is a polycentric type joint, the whole artificial leg exhibits the characteristics of both serial and parallel manipulators.

Like all other mechatronic systems, hybrid leg is a mechatronic system which is the synergistic application of mechanics, electronics, control and computer engineering in the development of an electromechanical product, namely the artificial leg, through an integrated design approach. This means that, electrical, mechanical, structural and electronic components of this system operate as an integrated system under real-time computer monitoring and control with interface for

operator supervision and direction (Necsulescu, 2002). In a true mechatronic sense, design of this mixed multi-component system requires simultaneous consideration, integration and design of all its components, which is the distinctive characteristics of mechatronic systems when compared with classical mechanical systems. By using integrated design approach, an *intelligent* system satisfying normal walking conditions can be produced.

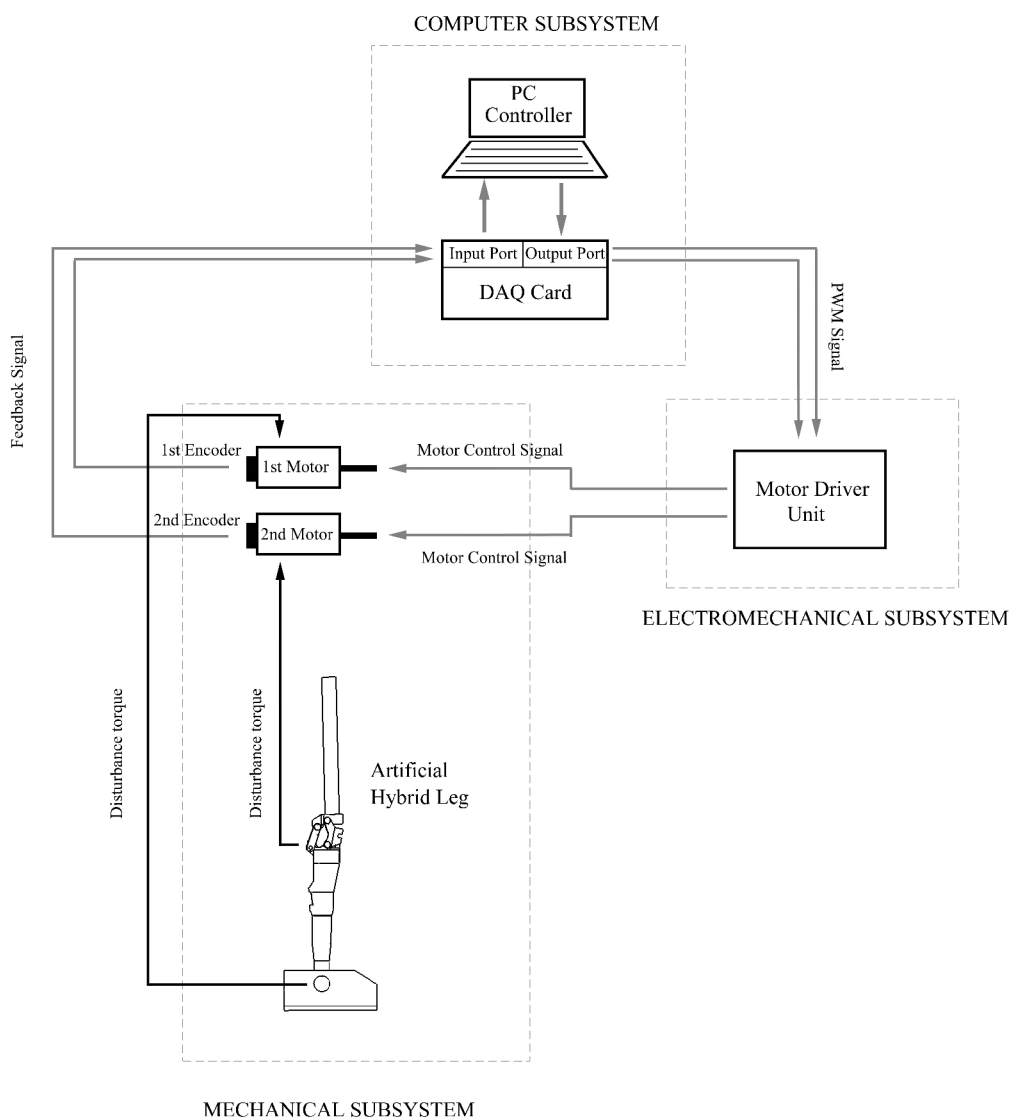


Figure 5.1 Representation of data transmission for hybrid artificial leg. Mechanical subsystem is composed of two D.C. Motors which are mounted to two joints of artificial hybrid leg. Computer subsystem acts as the control unit and electromechanical subsystem associates the control unit with the mechanical subsystem.

Artificial hybrid leg mentioned in this thesis has three subsystems. These are: mechanical subsystem, electromechanical subsystem and computer subsystem (Figure 5.1). Interaction of inputs and outputs of these subsystems enables the realization of natural walking characteristics with a desired control performance for transfemoral amputees.

5.2 Mechanical Subsystem

A mechanical system is a combination of mechanical parts like chassis, hull of robotic system, actuators or power transmission components, which interact mechanically in order to fulfil a specific objective.

In the research area of mechatronics, there exist a vast number of mechanical structures, including serial manipulators, parallel manipulators, mobile robots and humanoid systems, which are the fundamental parts in robotic systems. According to the task to be achieved, type of the mechanical structure must be chosen carefully in order to fully derive the benefits from that part of the whole system.

Since serial manipulators are widely used in the design of bipedal walking mechanisms and walking aiding devices, solutions of trajectory planning, obstacle avoidance and stable walking problems of such structures can be frequently found in the literature. Serial manipulator is a mechanical arm structure, i.e. a serial chain of rigid links connected by revolute or prismatic joints, forming a shoulder, an elbow and a wrist. Type of the joints and degrees of freedom of these systems can be changed, but the solution methodologies remain the same.

Especially in recent years, research groups started to investigate and develop polycentric knee joints to be used in the area of prosthetic device design. A polycentric knee joint is a multi-axes mechanism, having one degree of freedom. Because of the advantages of this type of mechanism discussed in Chapter two, it seems to be a reasonable and applicable knee joint design for these patients as it allows stable walking of the amputees with less energy consumption.

This study focuses on design of an artificial leg having a polycentric knee joint for transfemoral amputees. The intelligent leg is a *hybrid* system and it is composed of a serial manipulator structure having a closed-loop chain (a four bar mechanism) at the knee joint (Figure 5.2). Different from the traditional four bar mechanisms, there are no fixed links in the knee mechanism since all the links moves within 2-D space in arbitrary trajectories as the two driving joints (one at knee and one at ankle joint) give the system the desired motion in the stance leg phase.

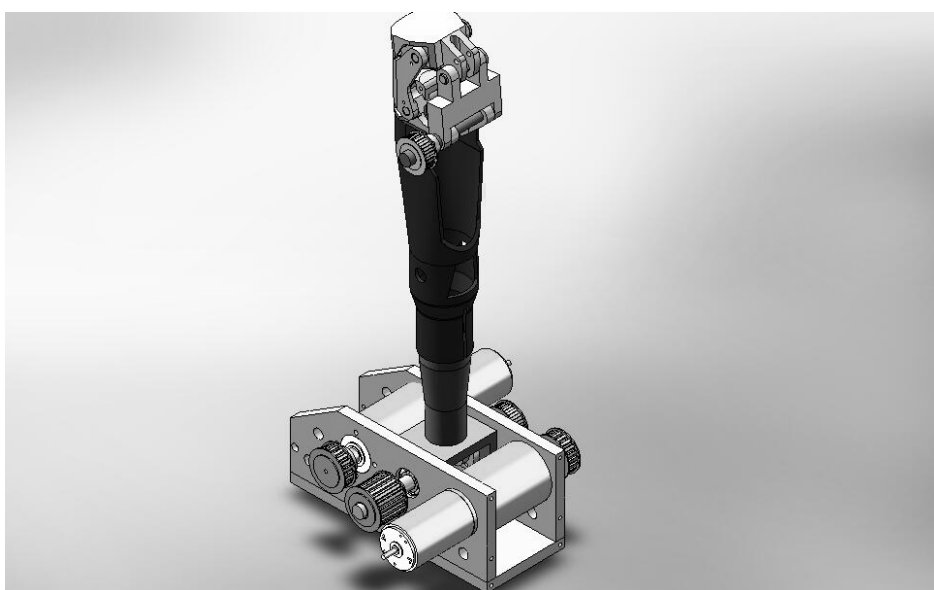


Figure 5.2 Artificial hybrid leg design. System has two degrees of freedom, one at ankle joint, another at polycentric knee joint. Design is a lower leg design with a knee joint and a socket part which connects the upper leg of the patient with the mechanism to be constructed according the physical properties of the amputee.

Polycentric knee joint is designed based on the intelligent knee product NI-C411 of the firm Nabtesco with some modifications: the length of the posterior link is changed to obtain the desired workspace of the system. Also, two timing pulley and belt mechanisms which will transmit the torque generated by the actuators to the joint axes are mounted to the polycentric knee (Figure 5.3).

Artificial hybrid leg has two degrees of freedom, one at ankle joint and the other at knee joint; and two permanent magnet D.C. motors produce the torques which are

needed to drive the system. The motors are mounted to the foot (Figure 5.4) for the purpose of keeping the centre of gravity of the whole system as low as possible. Lowering the centre of gravity has a positive effect on stability on stance phase as the mechanism needs less torque because of the reduction of inertia moments due to the low height of the point of centre of gravity.

The motor which is mounted behind the ankle rotating axis generates torque for ankle joint while the D.C. motor which is in front of the rotation axis rotates the knee joint. Five pulleys are used in order to transmit the generated torques. Two of these pulleys are coupled with the motors, one with the ankle joint and the other with the knee joint. The last one is an idle pulley, rotating freely around ankle joint axis but it rotates together with one of the motors and the knee joint, thus transmitting the motor torque to the knee joint.

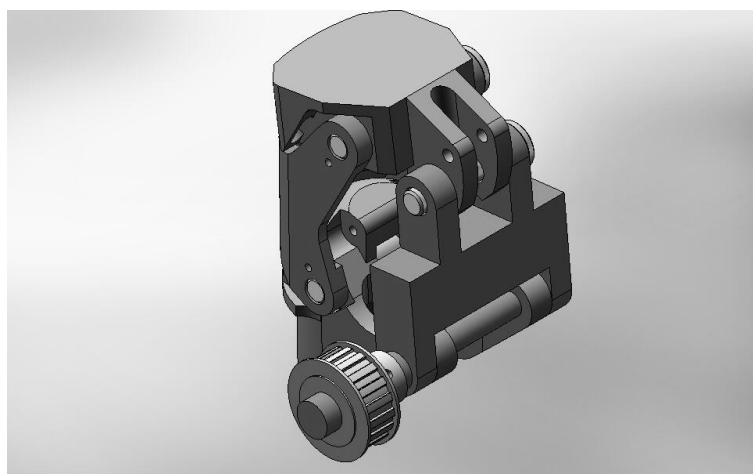


Figure 5.3 Polycentric knee mechanism. It connects the upper leg and lower leg of the amputee. It is a closed-loop mechanism and it gives to the system parallel manipulation characteristic.

In the design, it is desired to choose light-weight materials having high durability in order to reach the sound leg parameters of a human-being. Most of the parts of the artificial hybrid leg, the foot, the knee joint and the timing pulleys are made of duralumin. Pylon is made of carbon fibre, which gives a high stress resistance property to the system. The pins representing rotating axes of knee and ankle joints

are made of AISI-1020 steel, since they have to carry dynamic loads without bending.

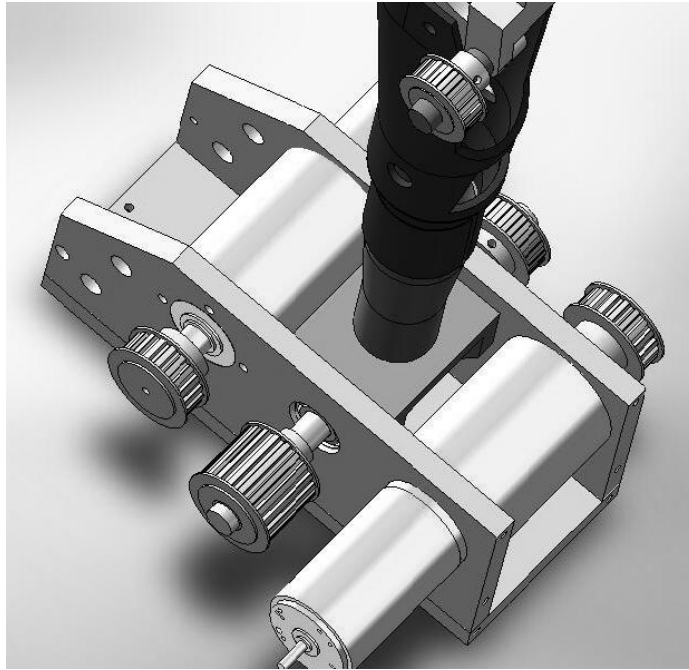


Figure 5.4 Foot design of artificial hybrid leg. Motors exciting the system are mounted here in order to keep centre of gravity of the intelligent leg as low as possible for the purpose of stabilizing the leg. Power is transmitted to the system through timing pulleys and belt mechanism.

5.3 Electromechanical Subsystem

Electromechanical subsystem is one of the most important parts of a robotic system, since it functions both as a data communication device and as an actuator driver unit allowing the system to perform certain tasks defined by the designer. This system comprises of an integrated circuit application card and two permanent magnet motors. Together, they integrate the actuator to the system and implement low level control tasks, like encoder data reading and motor driving.

The first objective of electromechanical subsystem is to transmit the sensory data from encoders of motors to main control unit. Transmitted data is the position information and by its evaluation (taking derivative of positions with respect to time), instant motor velocities are also obtained and taken into consideration as a part of sensory input. Sensory input is then compared with the reference values in the controller subsystem.

The second objective of the subsystem is to receive the control signal produced within the control loop at the main controller, which is the computer. Rating this signal as reference, electromechanical subsystem acts as a low level controller and produces actuator signal, i.e. pulse width modulation signal (P.W.M.), to drive the motors.

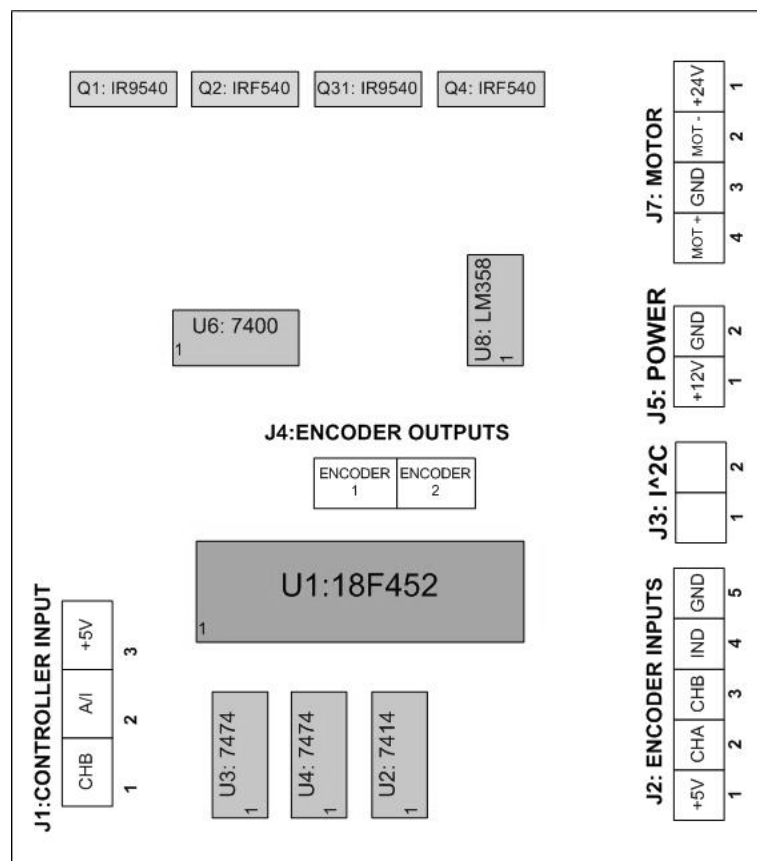


Figure 5.5 Schematic representations of data transmission unit and motor driver card with the pin numbers given

Schematic representation of the electronic card which is designed for integrated circuit application is given in Figure 5.5. In the scheme, jumper and pin numbers for the inputs and output ports are shown. Note that the electromechanical subsystem contains two electronic cards, one for each motor. Motor is mounted to the subsystem through J7 terminals while data from the encoder is received through J2 terminals. Position and motor rotation direction information is processed through 74F74 dual type flip-flops and 7414 type logic gate (U2, U3 and U4 integrated circuits). After that, this data is transmitted to the main controller through the main low-level controller unit, PIC18F452 from encoder output port, namely J4 terminal.

As for the second objective of the card, controller subsystem output transmitted to the electronic card through J1 terminals is evaluated at PIC18F452 microchip and the pulse width modulation signal is generated. P.W.M. output of PIC18F452 must be amplified in the power amplifier level of the card in order that the system gives the proper power to the motors.

5.4 Computer Subsystem

Computers can be exploited in mechatronic systems as controllers if they are equipped with suitable peripheral devices like serial, parallel ports, or data acquisition cards (DAQ cards) which can interact with low level controllers and/or with motor driver units. High computational speeds and wide compatibility of operating systems are the main advantages of computers in control systems. However, employment of some of computer's processing source by the operating system and need of the compatibility of special peripheral devices with the operating system sometimes give trouble in employing the computer as control unit.

If a standard PC is to be considered as a part of the artificial hybrid leg, it can perform the standard tasks of a digital computer which is used as integral controller of mechatronic systems. A digital computer is commonly incorporated in the form of micro processors and single-board computers together with components such as signal processors.

The reason for using a standard PC instead of a digital computer in order to achieve the control purpose is that, there are available some software programs like MATLAB or LabVIEW having the advantages of easy system installation and automatic recognition of input/output ports and DAQ cards. These software programs can achieve the control task for real-time applications by communicating with peripheral devices automatically so that system designers do not need to deal with interfacing process. In this way, any standard PC which fulfils the system requirements to install these software programmes can be used as the control unit. As for digital computers, either computer interface must be constructed by the system designer or it must be bought from control unit suppliers, which causes loss of time and extra budget.

In artificial hybrid leg system, like in all other mechatronic systems, computer is interfaced with mechanical and electromechanical subsystems via analog and digital input/output ports. Signal activities through these ports allow the information flow from or to the controller. By evaluating these signals, the designed control unit can decide the regulations to be done according to the error signal automatically and it adjusts the system output.

5.4.1 Digital Input

Input signal entering the controller unit, i.e. the computer, is the sensory feedback signal of the system. Referring to Figure 5.1, feedback signal comes from two encoders which are mounted to two motors which drive ankle and knee joints. During one full rotation of 360 degrees, each encoder generates 256 pulses but due to the gear ratio of 1:81, each encoder generates $81 \times 256 = 20736$ pulses for one whole turn of the motor. The amount of sensory input signal received from the encoders depends on the rotation speed of the motors and the working duration of the system. The control system must be designed in a manner that it can follow the encoder output signal, which is 81 times faster than the motor rotation speed.

Feedback signal entering the input channels of the controller comes from the encoder as pulses having 5V of amplitude. Each encoder has two output channels, each corresponding to one way of rotation of the encoder shaft, either in clockwise or in counter-clockwise direction. This means that the computer input signal is supposed to be the clock signal, which can be described as a signal oscillating between a high state (5V) and a low state (0V). These clock signals are then processed in the controller unit in order to obtain the angular position and rate of rotation of the encoder shaft. Obtaining the rotation way and the rotation speed of the encoders will be discussed in the next chapter, while giving information about the experimental rig.

5.4.2 Digital to Analog Conversion

Output signal from the computer is a digital signal, so it must first be converted to an analog signal before sending it to electromechanical subsystem in order to accomplish the motor driving task. In this way, controller output can be compatible with those of the actuators.

Computer output is a sequence of digital words, which is in the straight binary form. Each binary digit (bit) of information may be present as a state of two-stage logic device, which can generate a voltage pulse or a voltage level to represent that bit (De Silva, 2005). The “absence” of a voltage pulse or in some cases a “low level” voltage signal represents binary 0, while “presence” of a voltage pulse or a “high level” voltage signal represents binary 1. The sequential combination of these bits forms the digital word and this is sent to the data register (DAC register) of the digital to analog converter. Digital word in DAC register corresponds to some numerical values and DAC generates the voltage for those numerical values at its output port. Since a voltage signal cannot be arbitrarily large or small for practical reasons, some form of scaling would have to be employed in the DAC process. This scale depends on the reference voltage used in the particular DAC circuit (De Silva, 2005).

In this thesis, a standard PC, equipped with a multifunction DAQ card is used as supervisory controller. The DAQ card mentioned here is Advantech's PCI-1710 multifunction card which is designed to be connected to the PCI bus of the computer. Its advanced circuit design provides higher quality and more functions, including five most desired measurement and control functions as: 12 bit analog to digital (A/D) conversion, digital to analog (D/A) conversion, digital input, digital output and counter/timer functions. PCI-1710 multifunction card has 2 analog output channels, 16 digital inputs and 16 digital output channels.

Basic control algorithms are generated and activated by using a special software application called "Matrix Laboratory" (MATLAB), in order to achieve the task of trajectory control in stance leg phase.

MATLAB is a high performance language for numerical computation and visualization. It integrates computation, visualization and programming in the same environment where problems and solutions are expressed basically by Matrix notations, which means that various computations can be done easily in MATLAB, if data can be arranged as arrays. By the use of MATLAB, following operations can be done easily:

- Mathematical operations and computation
- Algorithm development
- Modelling and simulation
- Data analysis, exploration and visualization
- Scientific and engineering graphics.

Note that, all above operations have great importance in the control problem of mechatronic systems. Besides these advantages, MATLAB can recognize various peripheral devices like sensors or data transmission elements (e.g. DAQ cards) which are widely used in mechatronic systems for real-time control applications.

MATLAB features a family of application-specific solutions called toolboxes. Being very important to most users of MATLAB, toolboxes allow you to *learn* and *apply* specialized technology. Toolboxes are comprehensive collections of MATLAB functions (M-files) that extend the MATLAB environment to solve particular classes of problems. Areas in which toolboxes are available include signal processing, control systems, neural networks, fuzzy logic, wavelets, simulation, and many others.

In this thesis, real-time windows target toolbox of MATLAB is used in order to construct the control algorithms for the trajectory control of artificial hybrid leg in stance phase. Details of this control application and the toolbox will be given in the next chapter while introducing the experimental rig.

CHAPTER SIX

EXPERIMENTAL SETUP

6.1 Introduction

In the previous Chapters, modelling of an artificial hybrid leg having a polycentric knee mechanism is discussed. Control theory for the system is developed and a system design is proposed and constructed. In this chapter, it is aimed to apply two kinds of control algorithms in order to compare the performance of the artificial leg with different control architectures. For this reason an experimental setup has been designed and built. The setup is given in Figure 6.1.

It is seen in the Figure that the experimental setup is composed of an artificial leg which is planned to be controlled, an electromechanical subsystem to drive the motors, a DAQ terminal and a DAQ card which is mounted on the PCI slot of a PC (the connection is shown), the PC itself as the controller, a camera which is a part of measuring subsystem and of course the power supply. A laptop computer is also used for the execution of vision-based control algorithms.

It must be noted that this experimental setup is designed to investigate the performance of the artificial leg in stance-phase only; swing leg control is not considered. Stance phase control has a great meaning especially for the transfemoral amputees because while they are walking, synchronized motion of two hip joints together makes the patients to feel comfortable and confident. Swing leg motion is important for passing over the obstacles and climbing the stairs, but these are not included in this work. Hence, performance of the artificial leg is only experienced for walking applications on a flat surface with different walking rates.

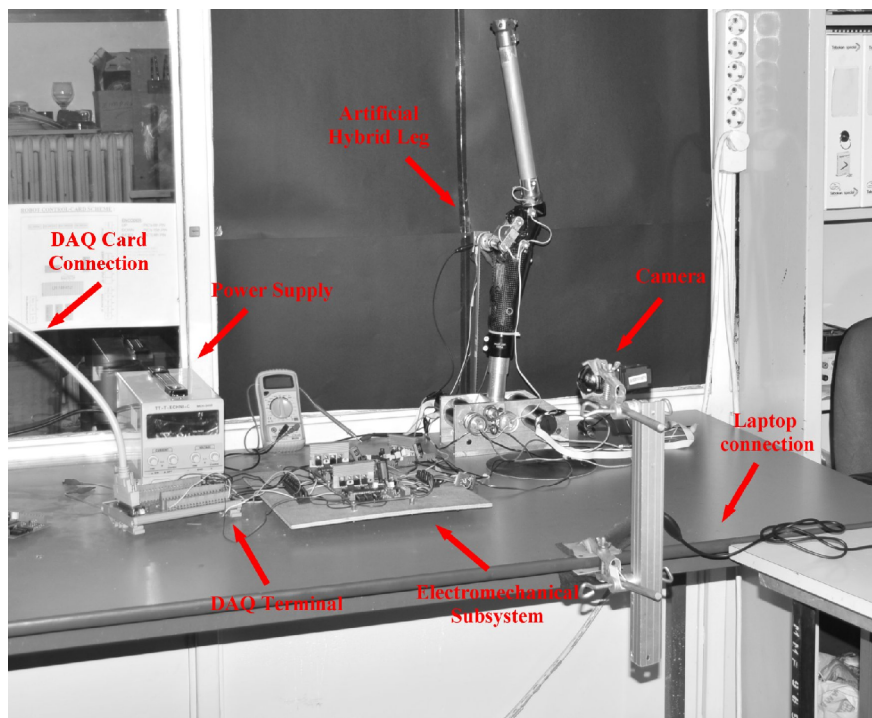


Figure 6.1 Experimental setup which is used to apply different control theories for the purpose of hip joint trajectory following. With this setup, only stance phase control application is introduced.

6.2 Experimental Setup Parameters

For the performance of the experimental setup, parameters must be chosen properly in order to achieve realistic solutions. Parameters of the manipulator which is an artificial hybrid is important for the system dynamics, since torques are computed according to these parameters. Also, motors are the components which generate the torques to the system; so the characteristics of the motors, with the gear boxes, change the behavior of the system.

6.2.1 Artificial Leg Parameters

Artificial leg is made up of different kinds of materials (composite, steel, aluminum) which have different densities. Total system has a weight of 5360 grams. The foot weighs much more than the other parts, therefore the centre of mass of the system is in a quite low level.

The most important parameters are the lengths of the limbs and the working range of the joint variables which indicates the maximum and minimum reachable angular values for each variable. Lengths of the limbs are given in Table 6.1 and the range of joint variables in 6.2.

In Table 6.1, the given length for the lower leg is the magnitude of the vector that connects the ankle joint with the exciting joint of the knee mechanism and the upper leg length is the magnitude of the vector that connects the four bar mechanism with the hip joint. The lengths of these vectors are used in the computation of artificial leg dynamics. They represent the length of lower and upper legs.

Note that in Table 6.2, θ_a and θ_2 are the inputs to the system and $\theta_2, \theta_3, \theta_4$ and θ_h are obtained from the geometry.

Table 6.1 Structural parameters of the artificial hybrid leg. The limbs are named according to the notations given in Figure 3.3.

<i>Limb</i>	<i>Length (m)</i>	<i>Explanation</i>	<i>Limb</i>	<i>Length (m)</i>	<i>Explanation</i>
OA	0.310 m	Lower leg	DC	0.056 m	Anterior link
BA	0.050 m	Posterior link	AD	0.036 m	4-bar lower link
CB	0.026 m	4-bar upper link	HB	0.290 m	Upper leg

Table 6.2 Range of the joint variables: θ_a and θ_2 are the ankle and knee joint variables respectively and they are inputs to the system. A range of the other variables are obtained from these values by using the Eqs. 3.1 through 3.4.

<i>Variable</i>	<i>Start value (°)</i>	<i>End Value (°)</i>	<i>Variable</i>	<i>Start value (°)</i>	<i>End Value (°)</i>
θ_a	131°	82°	θ_3	65°	2°
θ_2	-15°	-40°	θ_4	18°	2°
θ_1	43°	-42°	θ_h	-40°	-62°

6.2.2 Motor Parameters

In the experimental setup, two DC Maxon motors having 150 watts of power are used. The specifications of the motors and the gearboxes are given in Table 6.3. Gear boxes are attached to the output shafts of the motors.

Motors are placed on the foot and torques are transmitted to the related joints via belt-pulley mechanisms. One belt-pulley mechanism is used between ankle shaft and first motor shaft. Between the knee and the second motor shaft, there are two belt-pulley mechanisms. The torques are transmitted first to the ankle shaft and then to the knee shaft.

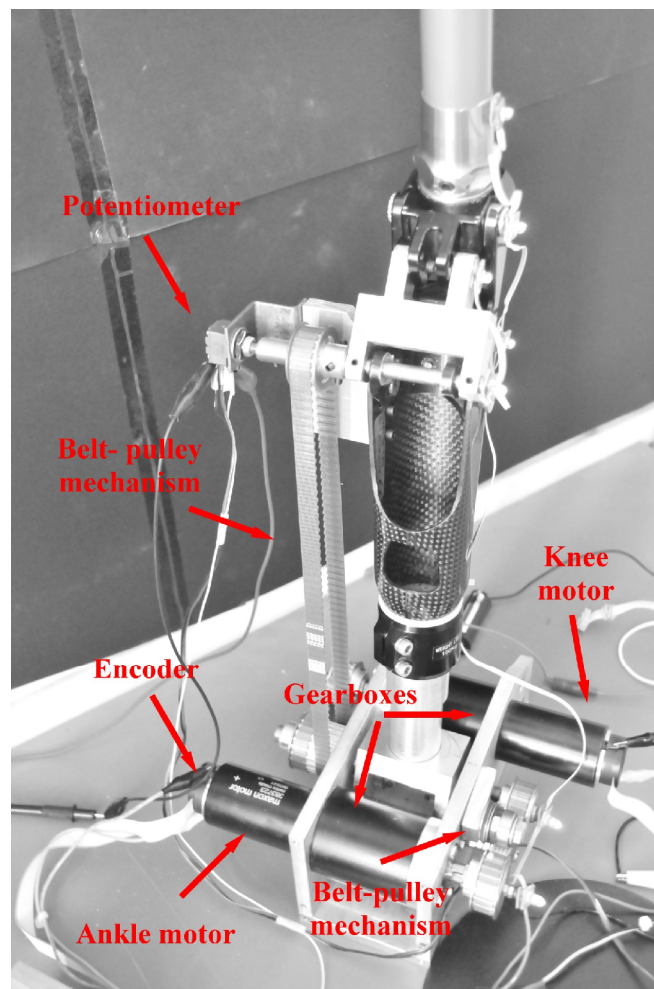


Figure 6.2 Assembly of the motors. Two belt-pulley mechanisms are used. Positions of the encoder and potentiometer are also shown in the figure.

Table 6.3 Motor and gearbox parameters.

<i>Motor Specifications</i>		<i>Gearbox Specifications</i>	
Power	150 W	Reduction	81:1
Nominal voltage	48 V	Max. Continuous torque	30 Nm
No load speed	1420 min ⁻¹	Max. Efficiency	75%
Terminal resistance	37.1 Ohms	Weight	770 gr
Terminal inductance	9.31 mH (negligible)		
Torque constant	321 mNm/A ⁻¹		
Rotor inertia	120 gcm ²		
Weight	480 gr		

6.3 Measuring Subsystem

Measuring devices are the key features of a system to be considered as a mechatronic system. Sensory feedback information allows the system to become aware of its environment and by the use of this information, controllers can decide the way of actuating the system.

Sensors can be used in a mechatronic system for different purposes. Sensors used in the feedback loop measure the output signals. This is common for all automatically controlled systems.

In some systems, like in the system measured in this study, input signals are also measured for feed-forward control. As the theory behind feed forward control is discussed in Chapter 4, position and velocity information coming from encoders and the potentiometer is used to compute the dynamic torques, which is then fed forward to the system. In fact, this is a special case for this system, since disturbance input is not measured directly, but it is computed through position and velocity inputs. In other words, encoders and potentiometer attached to the proper parts of the artificial hybrid leg are used for output measurement for the feedback control as well as the disturbance input computation for the feed forward control.

In addition to above purposes, input and/or output signals can be measured in system monitoring, tuning and supervisory control. These measurements are usually done in the design process manually by the designer in order to optimize the system and make the necessary changes and corrections for real-time applications. For those purposes, scopes, multimeters for voltage and current measurements, cameras and some other sensors can be used.

Like all experimental setups, artificial hybrid leg experimental setup designed has a measuring system. The measuring system is composed of position and velocity sensors as well as a vision-based measuring device which is a standard webcam. Specifications of these measuring devices, calibration methods and system mounting will be discussed in the following part.

6.3.1 Encoders

Encoders are digital transducers which produce a digital output as pulses. The pulses can be counted and angle of rotation of the encoder shaft can be computed. Angular velocities can be obtained by differentiating the angular changes with respect to time.

Computation of angle of rotation (i.e. angular position) and angular velocity can be done via an electronic circuit or pulses can be transmitted to computer through DAQ cards and calculations can be done in PC.

Using encoders as measuring devices has some advantages. Computers are digital platforms and they always use digital information. Any signal coming to the ports of a computer must either be digital or it must be converted into digital form via D/A converters. Since output signal of an encoder is digital in nature, there is no need to convert it to any other digital form. For this reason no quantization error occurs and angular position and velocity can be calculated precisely.

Digital signals are affected less from noise, disturbance or parameter variation in instruments than the analog transducers are. Also, high reliability in the system can be achieved by minimizing the usage of analog components in the system. These are the other advantages of the encoders which make the encoder to be a good choice for the measuring system of artificial hybrid leg.

Artificial hybrid leg system designed has two encoders attached to the motors which drive knee and ankle joints (Figure 6.2). One of the encoders generates pulses for the ankle rotation while the other one has output signal as the knee joint rotates. Since motors are not direct drive, which means that power transmission components (belt-pulley mechanisms) are used to convey the torque generated to the relevant joints, encoders measure the angular position and velocity of the motor shaft, not those of the knee or ankle joint.

At the ankle joint, a pulley (a wheel) having 20 teeth is attached to the one end of the ankle pin (Figure 6.2). The wheel which is attached to the relevant motor has 21 teeth. Besides, gearboxes which have gear ratios of 1:81 are mounted on shafts of each motor. This means that there is a certain gear ratio between motor shaft (which is encoder shaft at the same time) and the motor output shaft. So, the relation between rotation of the first encoder and the ankle joint can be derived as follows:

$$\frac{\theta_{e1}}{\theta_{m1}} = \frac{81}{1} \quad (6.1)$$

$$\frac{\theta_{m1}}{\theta_{a1}} = \frac{20}{21} \quad (6.2)$$

$$\frac{\theta_{e1}}{\theta_{a1}} = \frac{\theta_{e1}}{\theta_{m1}} \cdot \frac{\theta_{m1}}{\theta_{a1}} = \frac{81}{1} \cdot \frac{20}{21} = 77.14$$

Here θ_{e1} is the rotation of the first encoder, θ_{m1} is the rotation of the first motor *output* shaft and θ_{a1} is the rotation of the ankle joint which is provided by the related wheel.

As for the knee joint, calculations are a little bit different because there are two belt-pulley mechanisms to convey the torque from the motor to the knee joint. At the other end of ankle pin a wheel, which is an idle wheel having 21 teeth, is attached. At the knee joint, another wheel having 18 teeth is attached (Figure 6.2). So, the relation between rotation of the second encoder and the knee joint can be derived as follows:

$$\frac{\theta_{e2}}{\theta_{m2}} = \frac{81}{1} \quad (6.3)$$

$$\frac{\theta_{m2}}{\theta_{a2}} = \frac{21}{21} \quad (6.4)$$

$$\frac{\theta_{a2}}{\theta_k} = \frac{18}{22} \quad (6.5)$$

$$\frac{\theta_{e2}}{\theta_k} = \frac{\theta_{e2}}{\theta_{m2}} \cdot \frac{\theta_{m2}}{\theta_{a2}} \cdot \frac{\theta_{a2}}{\theta_k} = \frac{81}{1} \cdot \frac{21}{21} \cdot \frac{18}{22} = 66.28$$

Here θ_{e2} is the rotation of the second encoder, θ_{m2} is the rotation of the first motor *output* shaft, θ_{a2} is the rotation of the idle wheel and θ_k is the rotation of the knee joint. When receiving angular position and velocity information from the encoders, these gear ratios are taken into consideration to obtain the real joint angular positions and velocities.

6.3.2 Potentiometer

Potentiometer is an analog transducer which has an output in volts. Like encoder, potentiometer is used to measure position and velocity. Type of the potentiometer considered here is the rotary potentiometer and it measures angular position and angular velocity of the shaft on which it is mounted.

The output voltage changes according to the input voltage with the given relation:

$$\frac{v_o}{v_i} = \left[\frac{(\theta / \theta_{\max}) \cdot (R_L / R_C)}{(R_L / R_C + (1 - R_L / R_C) \cdot (\theta / \theta_{\max}) - (\theta / \theta_{\max})^2)} \right] \quad (6.6)$$

Here, v_i is the input voltage, v_o is the output voltage, R_C is the total resistance of the potentiometer coil, R_L is the load resistance, θ_{max} is the maximum angle that can be measured by the potentiometer and θ is an arbitrary angular position. Eq. (6.6) shows that there is a non-linear relation between output and input voltages, but if load resistance is increased and measurements are done within a small range, the loading error can be reduced and the potentiometer can work in a linear region.

Although the usage of encoder has many advantages (since it is a digital transducer), a high precision potentiometer is used for angular position and angular velocity measurements of the knee joint of the hybrid leg. Encoder which is planned to measure angular changes of the knee joint is mounted on the motor shaft. In construction, this motor is placed at the foot and, as mentioned before, the torque generated by the motor is conveyed to the knee joint through belt-pulley mechanisms (Figure 6.2). It is a fact that, the more transmission components are used, the less precisely the encoder reading is obtained.

Also, when two motors run together, the knee joint motor is affected by the motion of the ankle joint motor and this causes an error in encoder reading. Calculating the encoder errors due to these two effects is quite difficult. Errors in encoder reading cause problems in the control system, since obtaining the feedback signal precisely is the crucial point for a good control system design. For this reason a potentiometer is directly coupled to the knee joint for reading position and velocity information. By doing so, a trustable feedback signal can be taken from this joint.

6.3.2.1 Calibrating the Potentiometer

Potentiometer output is a voltage signal and this signal corresponds to an angular position. Potentiometer attached to the knee joint works in a small range of angular change so it can be regarded that there is a linear relation between the voltage and the angular position. As it is given in Table 6.2, knee joint rotates in an angular range of 12° to 40° . Potentiometer is calibrated in a manner that 12° corresponds to 2.61 Volts

and 40° to 4 Volts. Other values within the range are considered to be distributed linearly with the given equation:

$$\theta = 20.14 \cdot V - 72 \quad (6.7)$$

Here, V is the voltage output of the potentiometer in Volts and θ is the corresponding angular value in degrees.

6.3.3 Vision-based Measuring Subsystem

To measure the response of the artificial hybrid leg to the controller output, a vision-based control system is used. The system is composed of a camera, which is a standard web-cam having a resolution of 800x600 pixels, a laptop for implementing software for the measurements and seven markers which are attached on the proper parts of the artificial hybrid leg.

Six markers are attached to the rotating axes of the artificial hybrid leg. These markers are light emitting diodes (LEDs) and they are powered by an independent power source. In Figure 6.3, they are named as L1, L2, L3, L4, L5, L6 and L7.

The first two LEDs, L1 and L2 are used to indicate the horizontal reference axis. All the calculations are carried out according to this reference horizontal axis. L2 is an important LED, since it is attached on the ankle joint of the artificial hybrid leg.

L3, L4, L5 and L6 are used to represent the four-bar knee mechanism joints. Angular changes in three joints are measured by using these markers. Note that L3 is placed on the joint axis through which the knee joint is excited by the knee motor.

The seventh LED, L7, is attached to an arbitrary point on the upper leg. Since the vision range of the camera is not wide enough to see the whole mechanism, this marker cannot be attached on the hip joint, but on some other place within the camera range and orientation of the upper leg. Thus, the position of the hip joint can

be calculated according to this point, since the upper leg is a rigid body and all the points on it rotate in a same manner.

As artificial hybrid leg moves, the camera captures frames in a rate of 6 Hz. In each frame, values of joint parameters which define the movement of the mechanism are calculated. Joint parameters are defined in Chapter 3, in the kinematic analysis of artificial hybrid leg (refer to Figure 3.4).

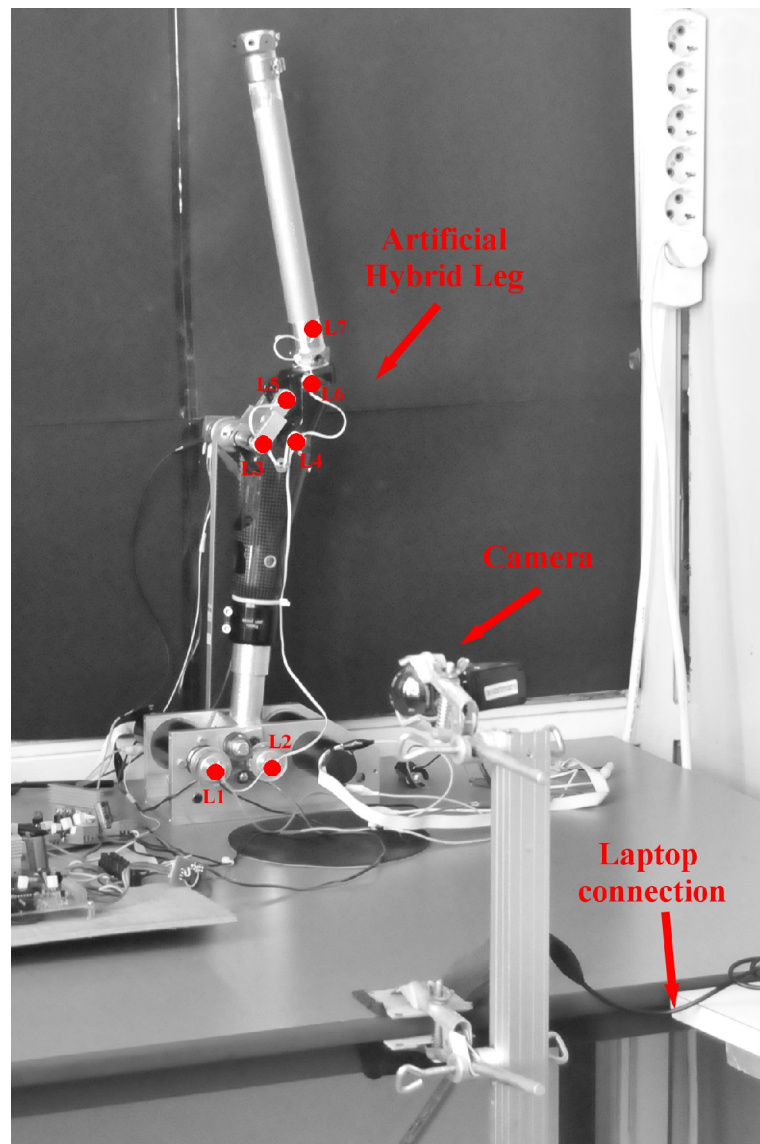


Figure 6.3 Vision-based measuring system. Six LEDs are attached on the six rotating axes of the artificial hybrid leg. The seventh LED is attached on the upper leg and it is used to find the position of the hip joint.

The code for the vision-based measuring system is written as an *m file* and they are executed in MATLAB. The reasoning in the development of the algorithm is quite simple: First step is to mark the seven points on each frame captured by the camera. LEDs attached to the related joints are very useful to separate the locations of the joints from the environment.

Second step is to define the vectors which represent the artificial leg structure. To begin with, the vector \vec{v}_{L2L1} is defined as the horizontal reference vector. This vector is directed from point L1 to L2. After reference vector is obtained, the vectors \vec{v}_{L3L2} , \vec{v}_{L4L3} , \vec{v}_{L5L3} , \vec{v}_{L6L5} , \vec{v}_{L4L1} , \vec{v}_{L6L4} and \vec{v}_{L7L6} are found.

The last step is to measure the angles between these related vectors. By doing so, joint parameters $\theta_t, \theta_1, \theta_2, \theta_3, \theta_4$ and θ_h are calculated for each instant (i.e., for each frame). The resulting group of joint parameter values for the whole walking period are then saved to a file and are plotted in order to compare them with the given reference trajectory.

6.4 Trajectory Generation

Feeding the system with a proper trajectory reference which imitates the hip joint movements of the healthy leg of the amputee in the stance leg phase has a special meaning, since walking characteristic of the amputee is directly related to the hip motion. In the stance leg phase, both hip joints of the healthy and the amputated legs can realize a synchronized motion, if the artificial leg supports a similar hip trajectory for the amputated side like that of the healthy one.

As it is defined in the theoretical introduction to kinematics analysis to obtain the workspace of the artificial leg, in Chapter three, the trajectory reference introduced to the experimental setup must lie within the workspace of the artificial hybrid leg. For this purpose, for each instant of time, a hip joint position which can be provided by the artificial hybrid leg (i.e. which has an inverse kinematics solution) is chosen

among the group of points in the workspace. A parabolic trajectory is considered as a good imitation of healthy hip trajectory and a polynomial of second degree is fitted to the chosen values of hip positions by using the method of least squares. The polynomial coefficients are found as

$$P = [-0.8000 \quad -0.0013 \quad 0.6518] \quad (6.8)$$

Here, P is a row vector of length 3 containing the polynomial coefficients in descending powers.

According to calculated parabolic hip trajectory, inverse kinematic solutions are obtained and joint parameters of the system are derived for each instant of time. These values are then combined together and sequences of joint parameters are obtained.

Here, it must be emphasized that solution of the inverse kinematics problem of the artificial hybrid leg is done iteratively because of the fact that dynamics of the mechanism has a non-linear characteristic. The aim here is to calculate the input variables θ_a and θ_2 from the generated hip trajectory, which are going to be used as the reference inputs to the artificial hybrid leg mechanism. Therefore, arbitrary values of θ_a and θ_2 are introduced to the inverse kinematic model iteratively. The other joint variables are calculated from the four bar geometry and a hip joint position is found for each instant of time. This value is compared with the generated hip position value. If the error between them is small enough ($e < 0.003$), the iteration is stopped. If not, it continues until the desired precision is reached. This iteration is done for the whole walking duration and at the end of iterative inverse kinematic analysis, all the joint variables are calculated for the given trajectory.

Since this iteration process takes time, the code of iterative inverse kinematics is executed offline.

Note that two of these joint parameters, namely θ_a and θ_2 are considered as the inputs to the control system and these input sequences are introduced to the system as trajectory reference through the walking duration. This means that, trajectory reference fed into the controller is in the joint space. For this reason, output of the system is also obtained in the joint space as joint parameters, not as the positions in task space.

6.5 Real-Time Monitoring and Control

In the thesis, real-time monitoring and control of the system is done by a standard PC having Windows XP as the operating system. Interfacing the PC with the system requires the use of PC's microprocessor for regular PC tasks as well as for data acquisition and control tasks. This means that while microprocessor consumes some of its computation capacity to run the system and some other applications, it also provides the control activities.

As it is mentioned in Chapter 5, interfacing the PC with the system is done via Data Acquisition (DAQ) cards and terminals. DAQ terminals are plugged in unused slots of PC and analog input and output signals as well as digital input and output signals can be transmitted according to the specifications of DAQ card used. Although transmission of those signals can be done through serial and/or parallel ports of the PC, capacity of transmitting large number of signals with various ports and high transmission rates make DAQ cards very suitable for monitoring and control applications.

Because of sharing of computer's resources, operating system Windows XP is characterized as a nondeterministic system which is defined as a system the time response of which cannot be guaranteed due to device drivers and interruption priorities (Necsulescu, D., 2002). However, there are some software applications which optimize the usage of computer resources to make the operating system more stable and efficient for the control tasks. MATLAB software of the company

Mathworks and its *Real-Time Windows Target Toolbox* make this optimization automatically for the MATLAB users.

Real-Time Windows Target (RTWT) permits the use of PC as controller by running Simulink models for real-time applications including rapid prototyping, as hardware in the loop simulation of control systems or signal processing tasks. Real-time executable models can be created and they can be controlled through Simulink software. Also, using the Real-Time Workshop product, C codes can be generated, and be compiled; and these real-time codes generated can be executed on Windows-based PC while interfacing to real hardware using PC I/O boards.

All blocks of Simulink can be used in the real-time models, since RTWT toolbox is compatible with Simulink. Simulink scopes, plotters and counters can be used for monitoring the variables of interest during real-time code execution. Also, parameters of the blocks can be changed and these changes directly affect the system response.

The Real-Time Windows Target Toolbox of MATLAB includes a real-time kernel that interfaces with the Windows operating system. The Real-Time Windows Target kernel assigns the highest priority of execution to the real-time executable, which allows it to run without any interference at the selected sample rate. During real-time execution of the assigned model, the kernel intervenes when needed to ensure that the model is given priority to the use of the central processing unit CPU of the PC to execute each model update at the prescribed sample times. Once a model update is completed, the kernel releases the CPU to run any other Windows based application that might need servicing. By doing so, it cloaks the Windows XP operating system and lets MATLAB to behave as a deterministic system using the resources of PC as the processor of the control system.

6.5.1 Controller

As it is mentioned in the previous part of the chapter, a PC is used as the controller unit which is responsible for generating the control output that is the pulse width modulation (P.W.M.) signal (the signal that is used to drive the motors).

Control architecture is constructed in MATLAB as Simulink model using the RTWT toolbox and some other common blocks. Two types of control schemes are prepared, one for position control task, and the other for the velocity control task of artificial hybrid leg.

6.5.1.1 Position Control Architecture

Real-time trajectory control task for the stance-phase control of the artificial hybrid leg starts with the position control scheme. A classical feedback control architecture which is shown in Figure 6.5 is introduced for simplicity. The controller is designed as a Simulink model by using the general library of Simulink as well as RTWT toolbox blocks.

Since real-time application of feed-forward compensation method contains heavy mathematical calculations, it is better to start with a basic control structure, then get the results and compare them with the improved methods. Although position control architecture discussed here leads to some error (it is not designed to reduce the disturbance torques because only feedback control is considered), still the results give some information about the solution of tracking problem.

In the position control task, independent joint control method, in which two PMDC motors are controlled independently, is used. Here, only feedback control is done and torque disturbances are not considered in the control system. Two different controllers (P-PI controller) are used with various controller parameters, in order to optimize the controller for the system response.

Controller software consists of two subsystems: encoder/potentiometer reading subsystem (which is the measuring subsystem) and the controller subsystem.

In measuring subsystem, two types of sensors, an encoder for the ankle joint measurements and a potentiometer for the knee joint measurements, are used. One of the powerful feature of MATLAB and the RTWT toolbox is that the DAQ cards can be automatically recognized by the software. Using the *Digital Input* block of Real-Time Windows Target toolbox, Advantech PCI-1710 DAQ card is introduced to the model and then pulses coming from the ankle encoder are counted. Ankle encoder subsystem model is given in Figure 6.4.

In the encoder reading subsystem, UP signals which come from Index A of the encoder refers to the rotations in *clockwise direction* and DOWN signals which come from Index B of the encoder refers to the rotations in *counter clockwise direction*. UP and DOWN signals are connected to different channels of DAQ card. Angular position information can be obtained by adding these signals algebraically.

Note that, encoder subsystem output gives the number of pulses, not the angular position, so, before proceeding to the construction of the control structure, these pulses are converted to angular values. If it is desired, after obtaining the angular values, angular velocities can be computed by differentiating angular changes with respect to time.

As for the potentiometer, it is interfaced with the controller via analog input port. By using *Analog Input* block which is introduced to the system as the analog input channel of Advantech PCI-170, potentiometer output can be mounted to the controller architecture.

Potentiometer signal is a voltage change and as discussed in the calibration of the potentiometer title, after the calibration process, angular values corresponding to the measured voltage values can be obtained.

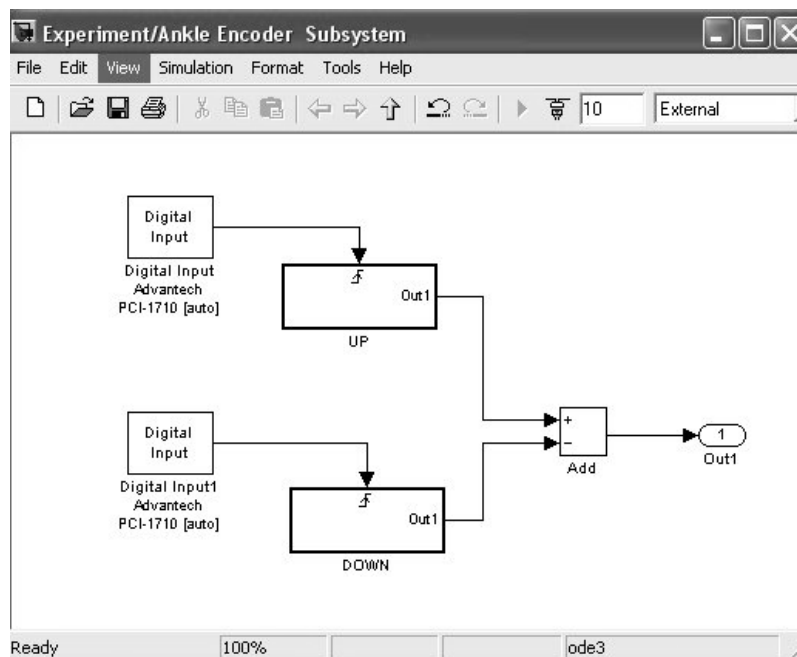


Figure 6.4 Simulink encoder reading subsystem. MATLAB can automatically recognize Advantech PCI-1710 card. By counting UP and DOWN pulses, the angular position of the encoder shaft can be obtained.

In the controller subsystem, classical P and PI controllers are used. Referring to Figure 6.5, desired controller characteristics are achieved by tuning the parameters of the PID controllers properly (adjusting proportional constant equal to K_p , integral and derivative constants equal to 0 in a P controller and proportional and integral constants equal to K_p and K_i respectively, whereas derivative constant equal to 0 in PI controller).

Note that reference inputs to motors are ankle and knee joint variables, which are introduced to the system in degrees. However, voltage values are to be used for all calculations in the control structure. This means that, reference signal which is in degrees must also be converted into corresponding voltage value. *deg to voltage1* and *deg to voltage2* blocks are used to make this conversion.

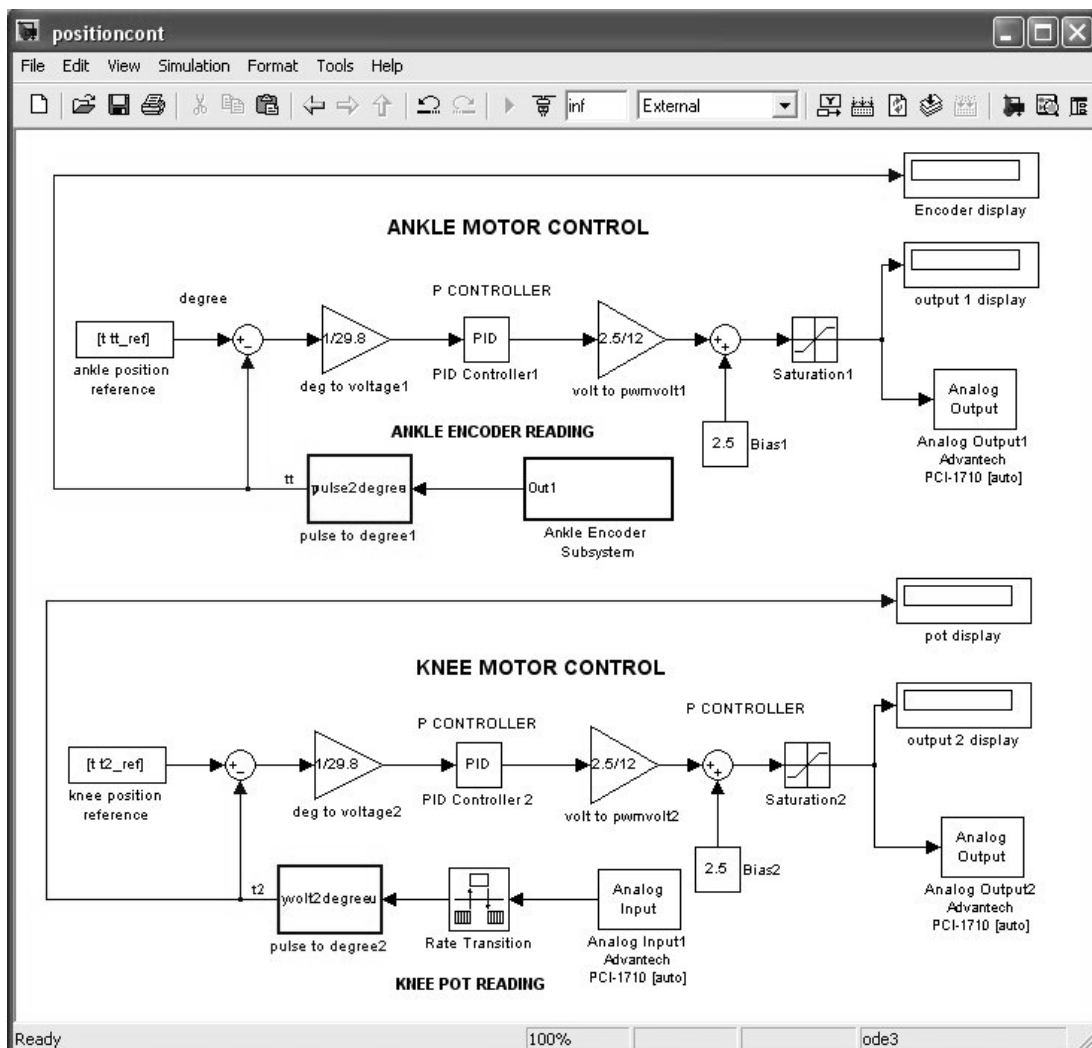


Figure 6.5. Simulink model of position control architecture for artificial knee prosthesis.

In position control methodology, position references are given in sequences. This means that reference signal value changes within a determined time interval and at the end of this time interval, a new reference value is introduced to the system. By doing so, point to point position control is achieved.

As for the output signal of the controller, it is generated in the form of pulse width modulation (PWM) signal which is fed through the related pins of the PIC (pin number is 17) in the electromechanical subsystem. PWM output is also in the range of 0 to 5 Volts; 2.5 Volt corresponding to a duty-cycle of 0%, whereas 0 Volt corresponds to a full duty-cycle in one direction and 5 Volts to a full duty-cycle in the other direction. In Figure 6.5, *Bias1* and *Bias2* block are used to guarantee the

output of the system to be 2.5, when control system starts to run. *Saturation* blocks scales the output of the system have values between 0 and 5 Volts.

The experimental results for the position controller are given in the results and discussions chapter.

6.5.1.2 Velocity Control Architecture for the Tracking Problem

Velocity control theory for the tracking problem of the artificial hybrid leg is discussed in Chapter four. For the real-time applications, a Simulink model is constructed.

Controller can be divided into three main subsystems: measuring subsystem which is composed of encoder and potentiometer reading subsystems, inverse kinematics subsystem in which joint parameters are found and the main controller subsystem which executes the feed-forward compensation codes.

A controller has some inputs and due to these inputs, it generates an output. In the velocity control architecture, similar to position control structure, there are two kinds of input signals: encoder and/or potentiometer reading and the disturbance input due to hybrid leg dynamics. The reading of information transmitted from encoders and potentiometer is done by the computer.

In all input/output (I/O) components of the controller a sample rate of 20 kHz is chosen. This sample rate is suitable for obtaining position and velocity data from the encoders. The measuring system discussed in the position control part system is also used in this controller structure, no additions are made.

As for the inverse kinematics blocks, θ_1 and $\dot{\theta}_1$ which are the encoder readings and θ_2 and $\dot{\theta}_2$ which are the potentiometer readings are the input signals for the dynamic system. Knee joint parameters which are represented briefly in Chapter three in Figure 3.4 are to be found by the Simulink blocks shown in Figure 6.6. First of all,

by pre-calculation block, position and velocity of joint B are found (accelerations are taken as zero). Since position and orientation of the frame attached to the joint B are known, all joint parameters of the multi axis knee joint can be found by using inverse kinematic analysis. It can be seen in Figure 6.6 that, after post calculations, kinematic analysis ends and joint parameters are fed into the main control structure for feed-forward compensation.

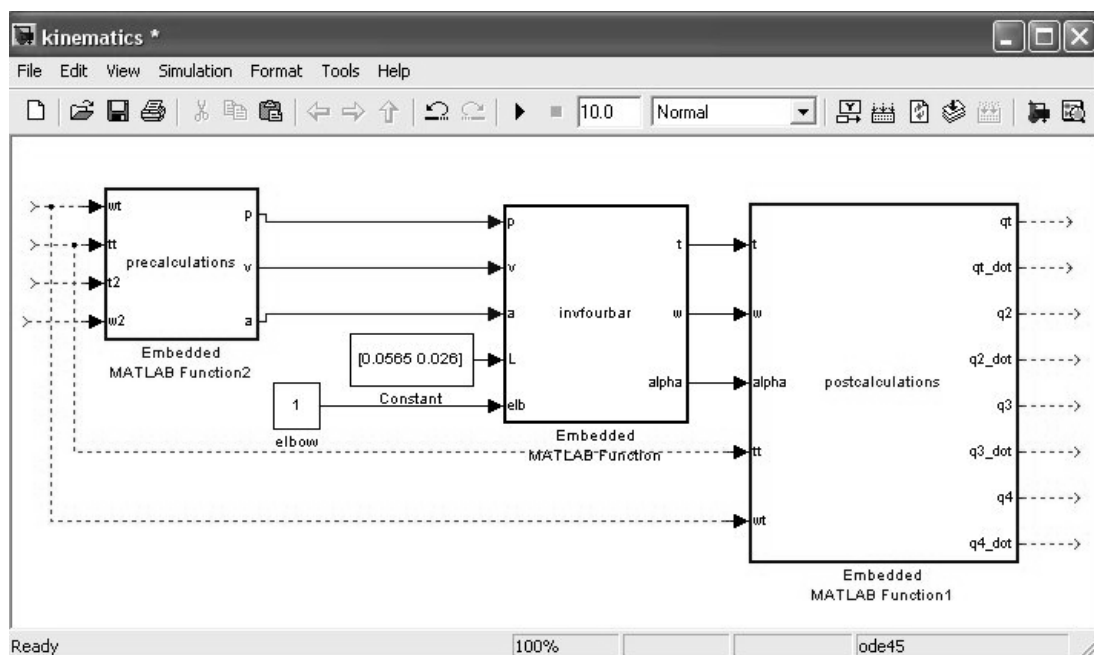


Figure 6.6 Inverse kinematic analysis Simulink blocks of artificial hybrid leg. Taking θ_1, θ_2 and their derivatives as input to the system, all joint variables can be found. These joint parameters are then fed into the main controller to execute feed-forward compensation codes.

As for the main controller, it is aimed to control two permanent magnet direct current motors so that they track the given knee and ankle references for the stance phase. Reference trajectory inputs for related joints are obtained from the workspace of MATLAB (Figure 6.7).

Trajectories used in the real-time applications are derived from the trajectory generation analysis of a bipedal walker, which is discussed in Chapter two. The reason to use these trajectory data is that these data are derived by considering the healthy walking of a human-being. In the hip trajectory control problem, which

means stance-leg control, transfemoral amputees can walk in a comfortable and stable way, if healthy walker trajectories can be followed.

The disturbance torques are computed according to the system dynamics of the hybrid leg, which is given in Chapter three.

Control structure is the application of feed-forward compensation architecture, the theory of which is given in Chapter four. The most important point in the real-time controller application is that, since the output of the controller is PWM voltages which are changed in a range of 0 to 5 Volts, all the other signals which take place in the control action must also be within this range of voltage. Hence, reference input signals (which are angular velocity profiles of the joint variables) and computed disturbance torque values are converted into voltage values. By doing so, dimensions of all input-output signals become the same, and they can be compared with each other without any dimensional error.

The output signal of the controller is again pulse width modulation (PWM) signal, the details of which are given in the previous part. PWM output is in the range of 0 to 5 Volts, 2.5 Volt corresponding to an empty duty-cycle, where 0 Volt corresponds to a full duty-cycle in one direction and 5 Volts to a full duty-cycle in the other direction. Discussions about the performance of velocity control architecture will be discussed in results and discussion chapter.

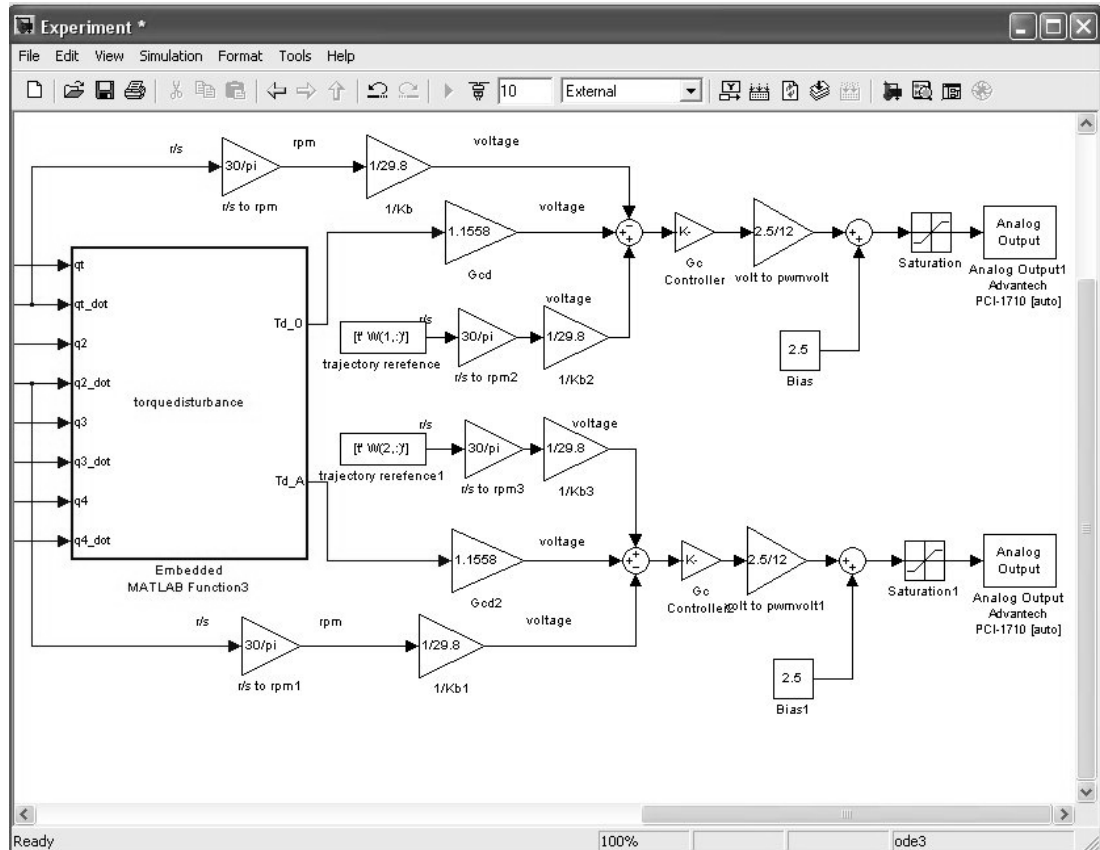


Figure 6.7 Main controller architecture. Trajectory references for both motors are obtained from the workspace. Torque disturbances due to system dynamics are calculated and are fed forward. Output of the system is the P.W.M. signal.

CHAPTER SEVEN

RESULTS AND DISCUSSIONS

7.1 Results

In this work, basic definitions about bipedal walking are given and based on these definitions, mathematical model of a bipedal walker in sagittal plane is derived. Understanding dynamics of this two dimensional model is very important because it contains the synchronized movement of two legs in different walking phases, namely stance and swing phases. After the solutions for the system dynamics are obtained, model based control of the ankle and hip joint trajectories are achieved by using feed forward compensation methodology and simulation results are carried out.

Bipedal walking researches are not limited only with the two-legged walking robots and models. There are many applications which are directly related with the walking of humanoid devices and humans as well. One of these application areas is the artificial walking devices, which aid the people suffering from various walking problems. Artificial hybrid leg with a polycentric knee mechanism is one of these walking aiding devices, which is used for transfemoral amputations. The artificial leg considered here is a hybrid system, since it is composed of a serial manipulator which is an open chain mechanism and of a close chain knee mechanism which is a four bar mechanism used to connect the upper leg with the lower leg.

In this study, dynamics of artificial leg is derived and an experimental setup which is used to test the control algorithms developed is built. The experimental setup is a prototype, so more improvements must be done on the mechanism before it can be ready to be used by the amputees.

Before constructing an experimental setup, some simulations are made in MATLAB. The first group of simulations is related to the model of bipedal walking in sagittal plane. The theory of the mathematical model is given in Chapter two.

After deriving the mathematical model, feed-forward compensation method is applied for the trajectory control problem in both stance and swing leg phases.

In stance leg phase, the trajectory to be followed is the hip trajectory. The other leg which is the swing leg moves synchronously with the stance phase and it is desired that ankle of the swing leg also follows a desired trajectory. Choosing a proper swing leg trajectory is important especially for obstacle avoidance and stair climbing applications. For the given trajectories, simulations are made and results are carried out.

Second group of simulations are made for the purposes of obtaining the workspace of the artificial hybrid leg designed in stance leg phase and for deriving the desired angular positions and velocities of the joint variables, which are going to be used for the computation of joint torques. These simulations give the results to the forward and inverse kinematic problems related to assigned mechanism. Forward kinematic analyses are made to obtain a suitable trajectory for the hip joint, whereas with the inverse kinematic analysis the joint variables which realize this trajectory are calculated. This group of simulation results is also used in the real-time application for the purpose of obtaining a suitable hip joint for the artificial hybrid leg mechanism.

As for the real-time application, position control architecture discussed in Chapter six is applied to the experimental setup, which is a prototype construction of an artificial hybrid leg. Generated trajectories of the hip joint (and also of the knee joint) are introduced to the system as reference inputs, and the outputs of the mechanism which are the joint variables are obtained in joint space configuration as angular positions.

7.1.1 Simulation Results of Bipedal Walker

The first simulation results are obtained from the analysis of bipedal walker in sagittal plane. The bipedal walker model introduced in Chapter two has two degrees of freedom for each walking phase. Rotation of the hip and knee joint in swing leg phase and rotation of the ankle and knee joints in stance leg phase define the degrees of freedom of the system. Note that the walker is excited from these joints with permanent magnet DC motors. All DC motors are assumed to be identical. In Table 7.1 system parameters and parameters of the motors chosen for the simulation are given.

Table 7.1 Assumptions of system and motor parameters in the simulation

System Parameters	Value	Motor Parameters	Value
Length of the leg (L_{leg})	1 m	Armature resistance (R_a)	1 Ohm
Length of lower leg (L_{low})	0.52 m	Armature inductance (L_a)	0.09 H
Max. hip height (h_{max})	%5	Torque constant (K_M)	19 Nm/A ⁻¹
Walking period (T_w)	1 sec	Velocity constant (K_b)	50 min ⁻¹ /V ⁻¹

In Figure 7.1 and 7.2, the control commands for the given velocity references in the stance leg are presented. Note that walking duration is 1 seconds and phase shifting characteristics are not given in the graphs. It is seen from Figure 7.1 and 7.2 that the control command which is generated from feed forward compensation methodology can follow the reference velocities with an admissible error.

As for the control simulation results of the swing leg phase, it can be seen that feed forward compensation leads to a good control performance for the bipedal walker (Figures 7.3 and 7.4). Similar to stance leg simulation results, shifting conditions are not considered here.

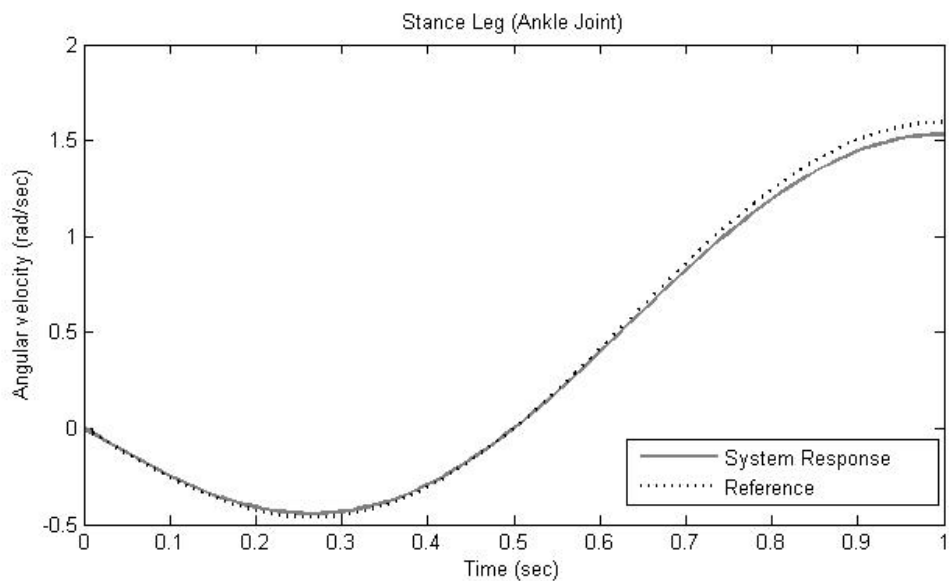


Figure 7.1 Control simulation result for the ankle joint of the stance leg. The system response is compared with the reference ankle velocity.

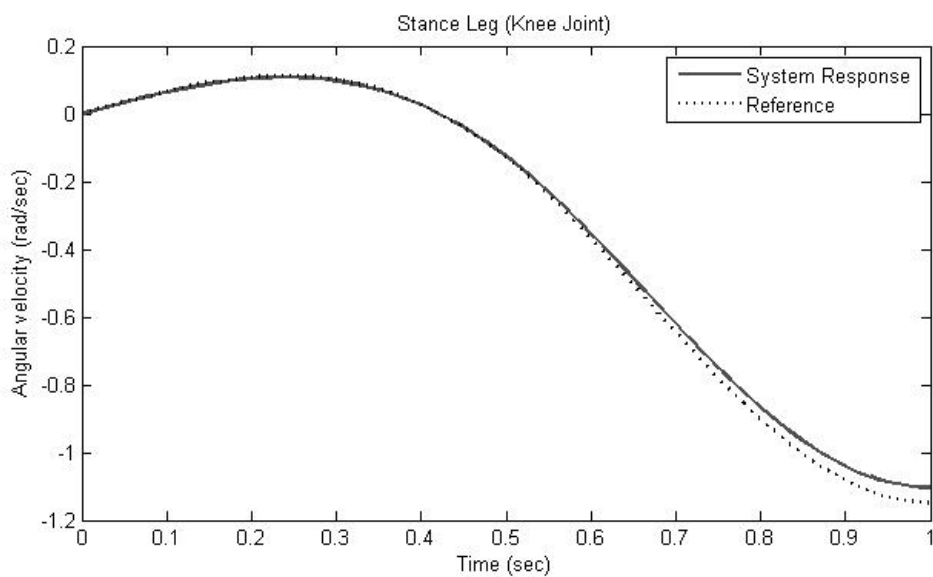


Figure 7.2 Control simulation result for the knee joint of the stance leg. The system response is compared with the reference knee velocity.

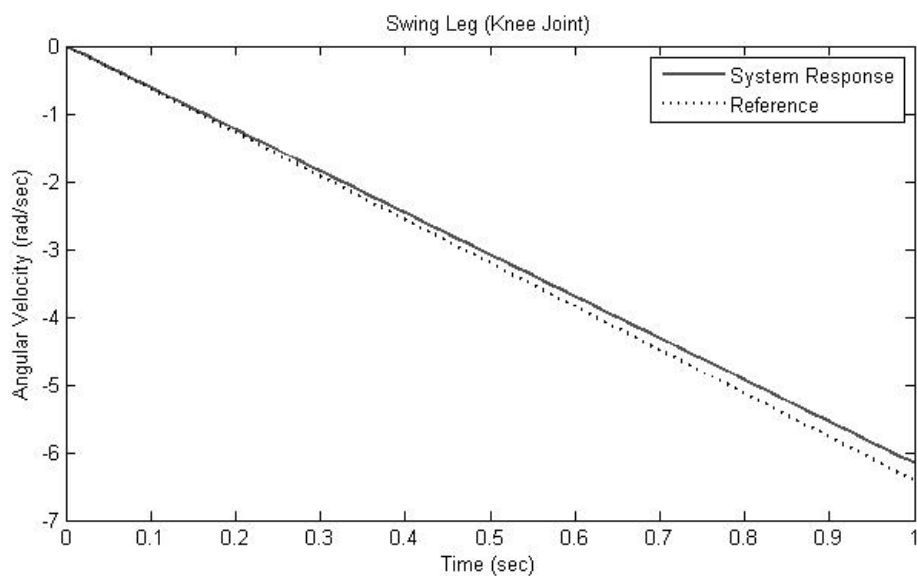


Figure 7.3 Control simulation result for the knee joint of the swing leg. The system response is compared with the reference knee velocity.

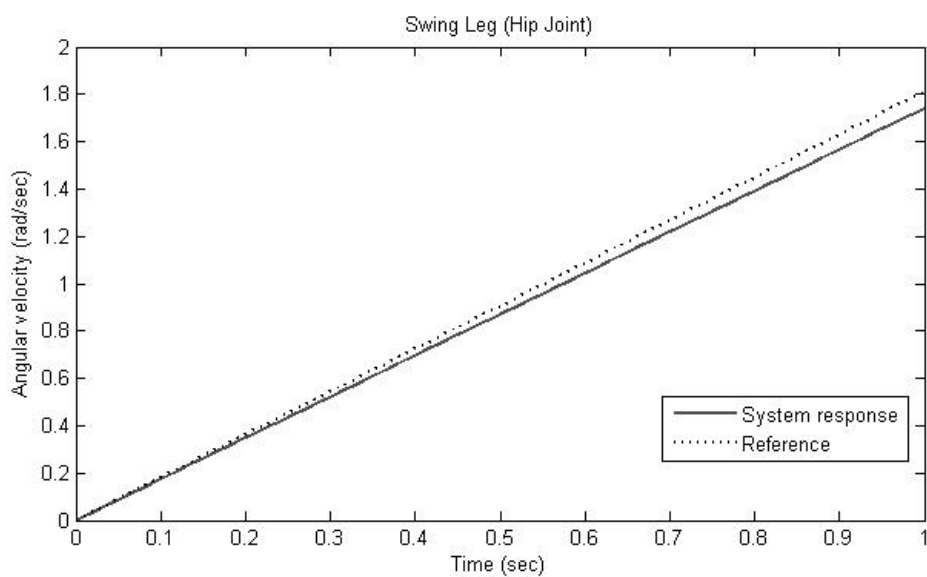


Figure 7.4 Control simulation result for the hip joint of the swing leg. The system response is compared with the reference hip velocity.

7.1.2 Simulation Results of Artificial Hybrid Leg

Satisfactory control performances obtained from simulation results of walking model in sagittal plane has allowed the study to be continued with the analyses on artificial hybrid leg mechanism. In the analyses, only trajectory control of the stance leg has been considered. Hence, mathematical model of the system is derived according to the restrictions of only the stance leg phase. Structural parameters of the artificial leg are given in Table 6.1. According to these parameters, mathematical model is obtained and analyses are carried out.

First step of the analyses includes obtaining the workspace of the artificial leg. This step is very important because without knowing the reachable limits of the mechanism, trajectory cannot be chosen. To find the workspace, forward kinematic analysis is made, which means that for the given joint parameter values, position of hip and those of the four moving points of knee mechanism are to be found in the Cartesian coordinates. In Figure 7.5, grey clouds represent all the possible points of hip joint and those of knee mechanism as calculated from forward kinematic analysis of the system.

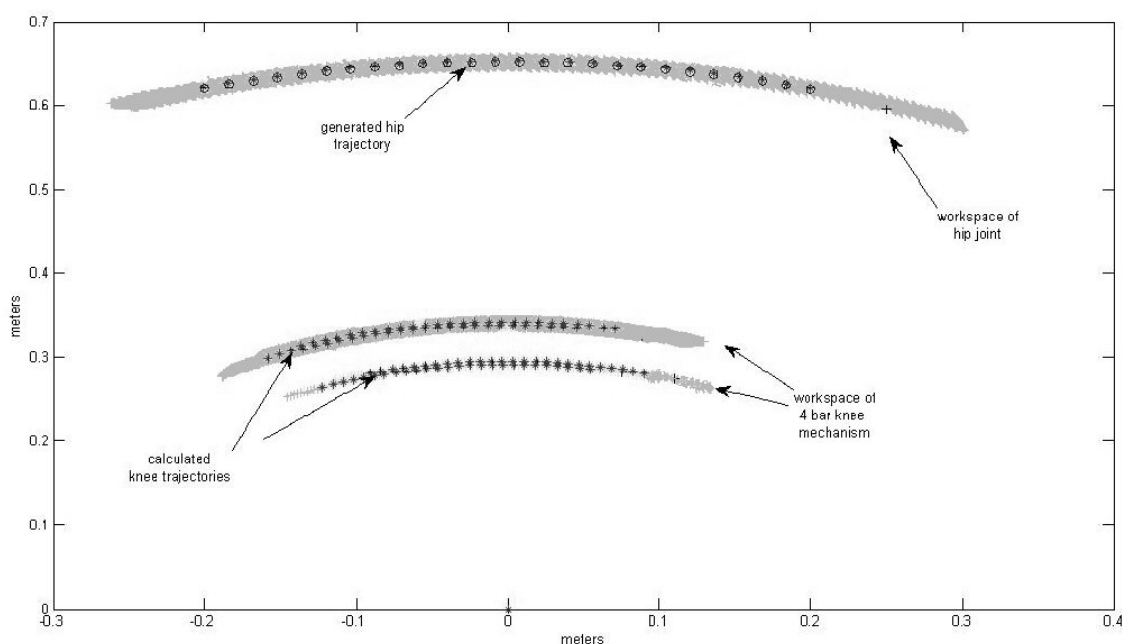


Figure 7.5 Representation of the workspaces and trajectories of artificial hybrid leg.

Second step is to decide the trajectory of the hip joint. A group of points are chosen among the points located within the workspace of the hip joint and a suitable polynomial (in this case a second order polynomial) is fitted to these points shown as + marks in Figure 7.5. In the figure the generated hip joint trajectory is shown by rounded marks. Knee joint trajectories are then calculated from the generated hip joint trajectory by using iterative inverse kinematic analysis method and are displayed in Figure 7.5 in the same way.

Note that while obtaining the joint parameters which realize the desired trajectories, ankle and one of the knee joint parameters (which is θ_2) are chosen as the reference inputs to the system. In Figures 7.6 through 7.14 the reference points *calculated* from the hip trajectory and also the other calculated joint parameters, $\theta_1, \theta_3, \theta_4$ are shown. The graphs are obtained for different walking durations.

Walking durations in the simulations are chosen as three, five and eight seconds. For each duration, graph of five joint parameters, namely $\theta_a, \theta_1, \theta_2, \theta_3$ and θ_4 are obtained. Although the position of the hip joint is not shown, it can be calculated from the equations representing the mathematical model of the artificial hybrid leg; or it can be measured by using vision-based measuring systems.

Simulation results of the artificial hybrid leg are significantly important because as discussed in the above paragraphs, changes in joint parameters θ_a, θ_2 within a time range are employed as the trajectory references to the experimental setup. These reference values are to be compared with the control output of the experimental setup and the control performance will be exposed.

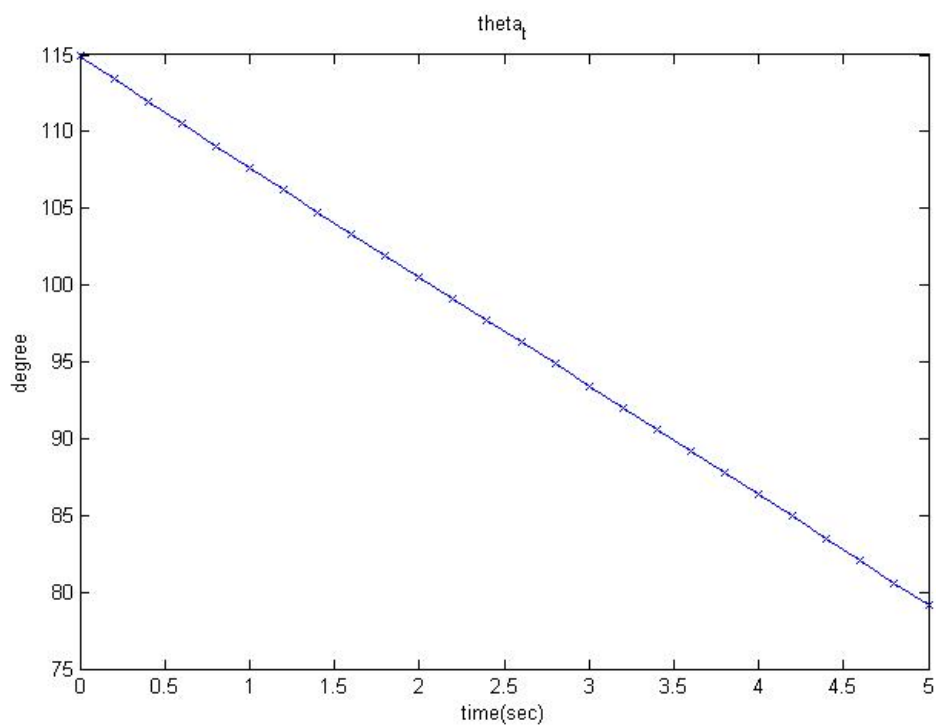


Figure 7.6 Angular change of ankle joint variable, which is the reference input to the ankle motor of the artificial hybrid leg. Walking duration is set to 5 seconds.

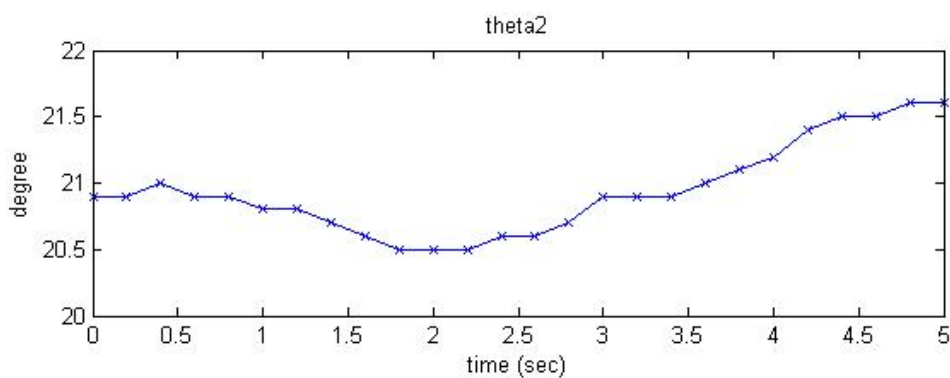
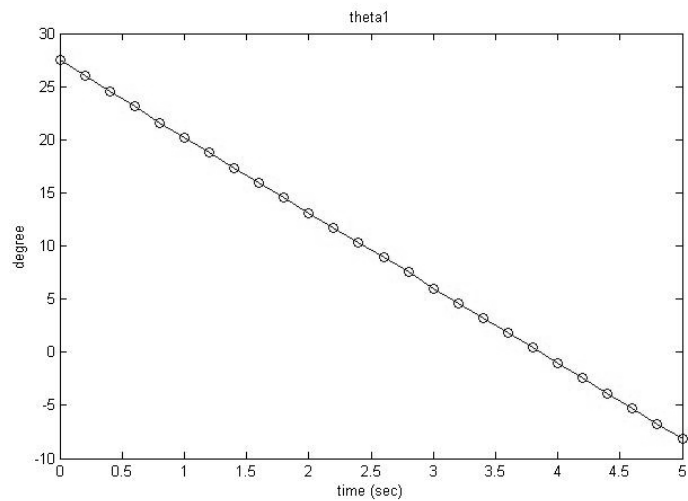
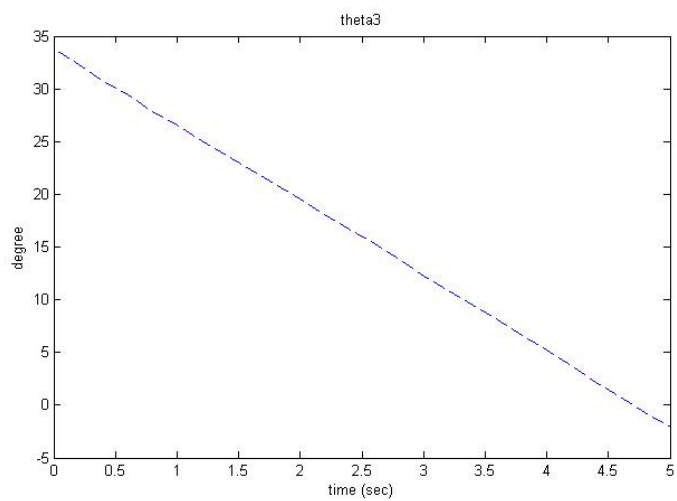


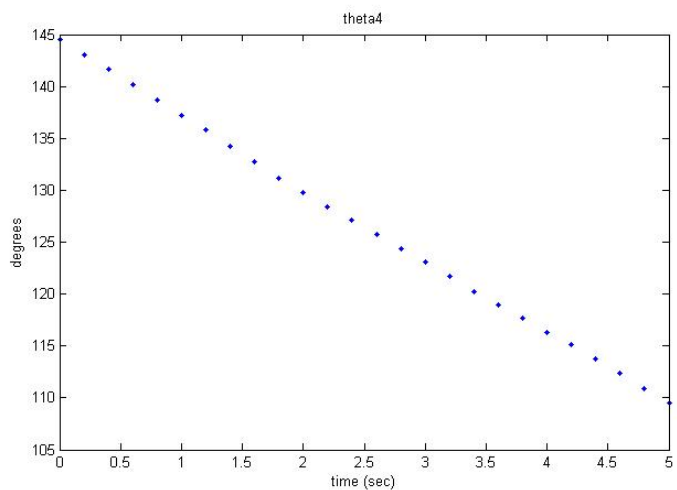
Figure 7.7 Angular change of knee joint variable, which is the reference input to the knee motor of the artificial hybrid leg. Walking duration is set to 5 seconds.



(a)



(b)



(c)

Figure 7.8 Calculated joint variables for the knee mechanism. (a) for θ_1 , (b) for θ_3 and (c) for θ_4 . Walking duration is set to 5 seconds.

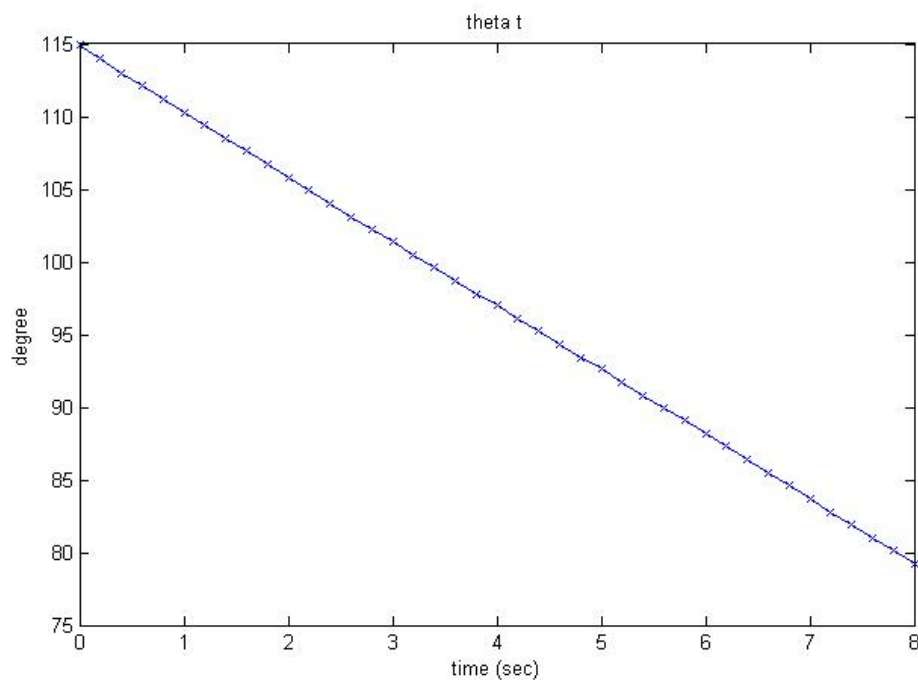


Figure 7.9 Angular change of ankle joint variable, which is the reference input to the ankle motor of the artificial hybrid leg. Walking duration is set to 8 seconds.

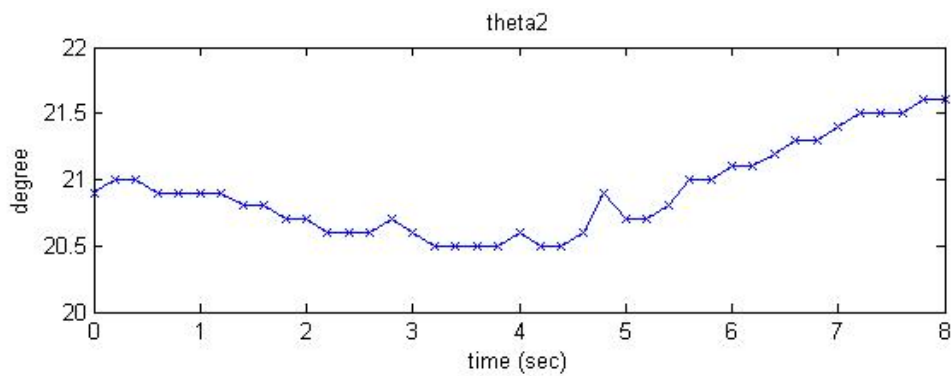
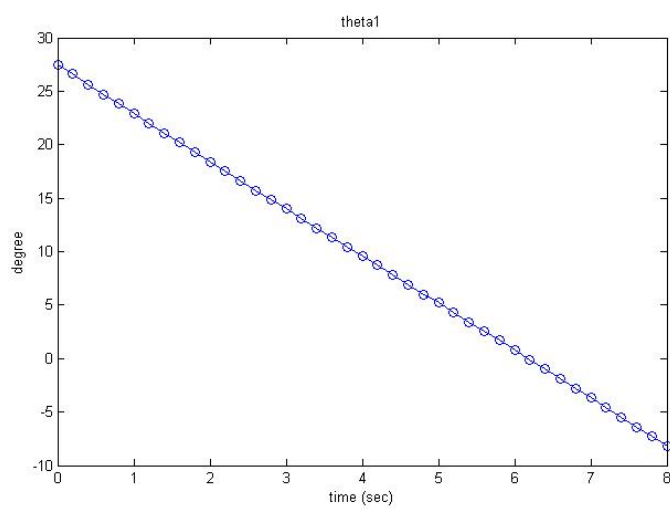
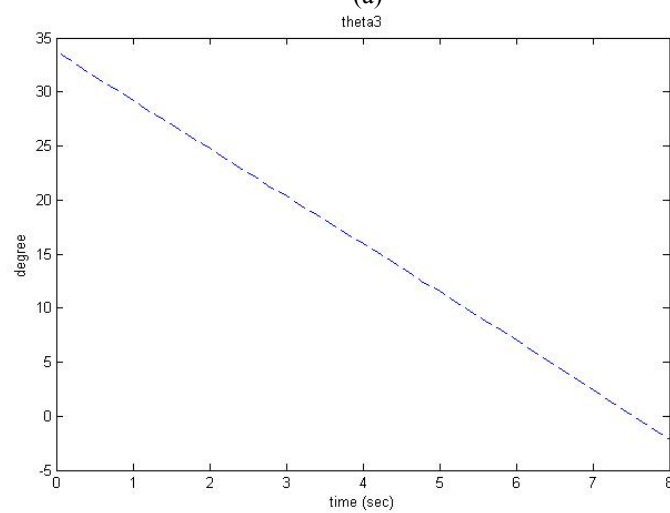


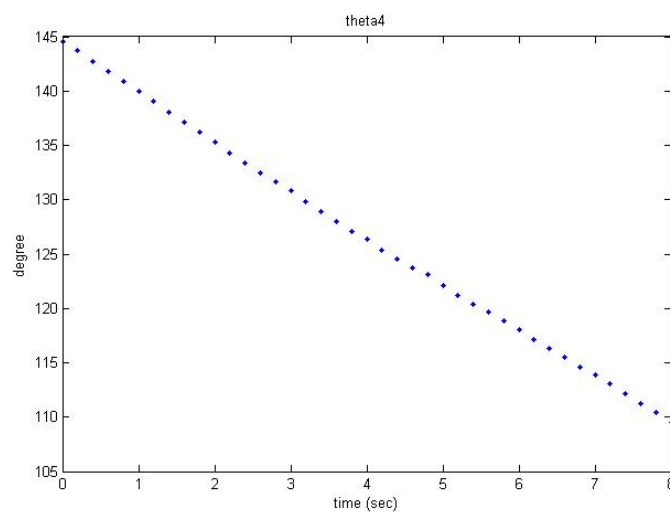
Figure 7.10 Angular change of knee joint variable, which is the reference input to the knee motor of the artificial hybrid leg. Walking duration is set to 8 seconds.



(a)



(b)



(c)

Figure 7.11 Calculated joint variables for the knee mechanism. (a) for θ_1 , (b) for θ_3 and (c) for θ_4 . Walking duration is set to 8 seconds.

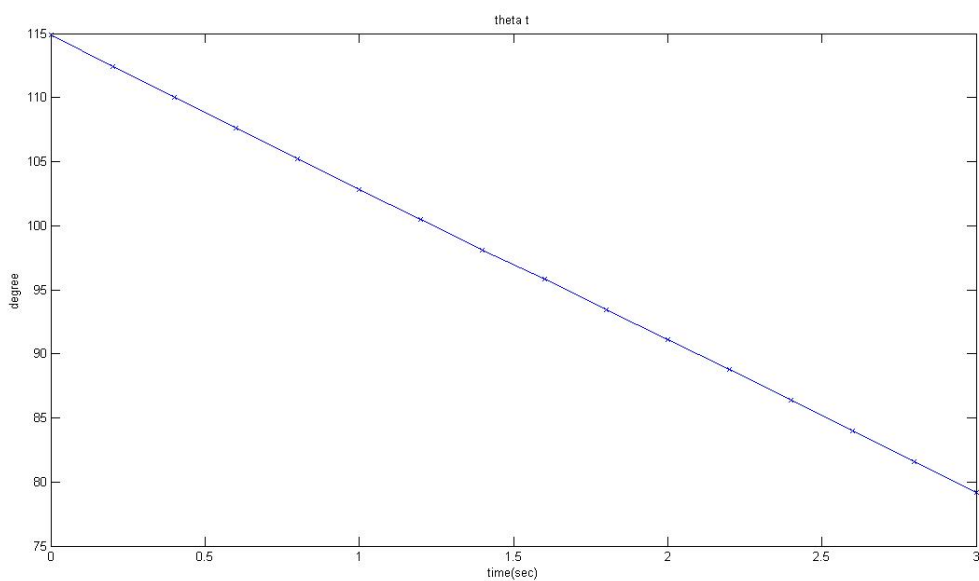


Figure 7.12 Angular change of ankle joint variable, which is the reference input to the ankle motor of the artificial hybrid leg. Walking duration is set to 3 seconds.

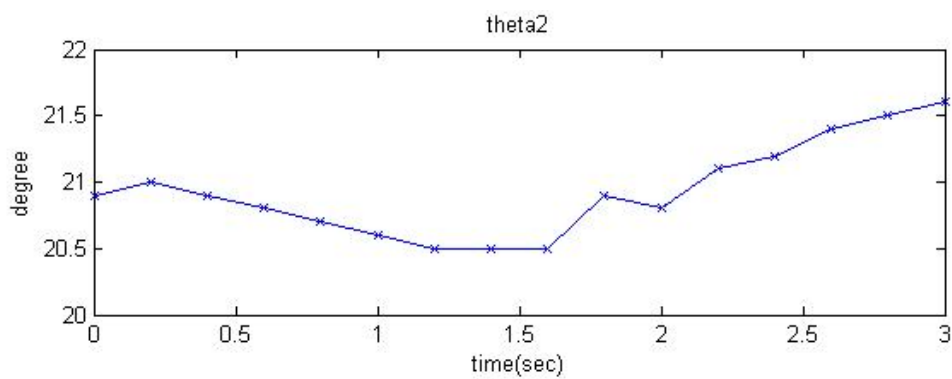
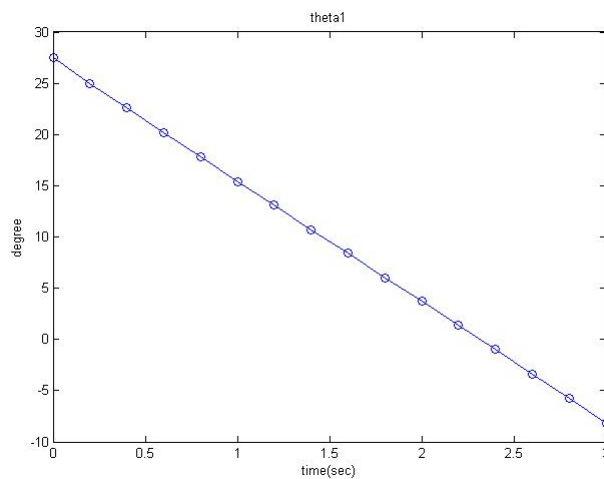
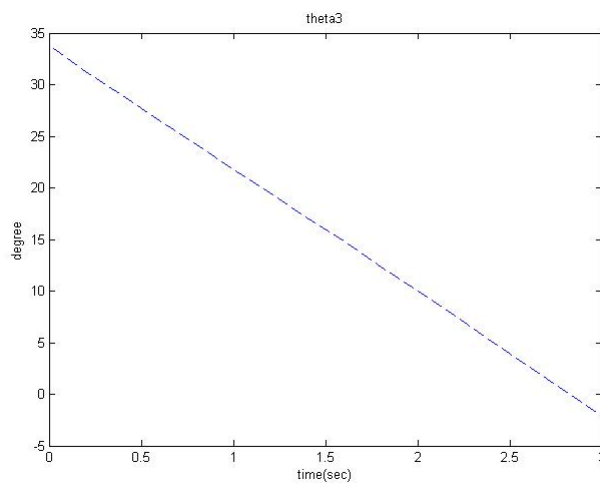


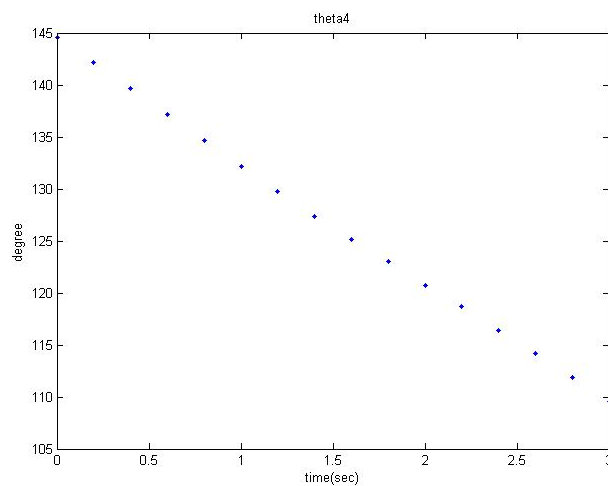
Figure 7.13 Angular change of knee joint variable, which is the reference input to the knee motor of the artificial hybrid leg. Walking duration is set to 3 seconds.



(a)



(b)



(c)

Figure 7.14 Calculated joint variables for the knee mechanism. (a) for θ_1 , (b) for θ_3 and (c) for θ_4 . Walking duration is set to 3 seconds.

7.1.3 Real-Time Point to Point Control Results of Artificial Hybrid Leg

In real-time application, a point to point control structure is introduced in order to control ankle and knee joint variables. In the experiments, only position control of artificial hybrid leg has been achieved according to the ankle and the knee joint trajectories in joint space. If these trajectories defined in the joint space are tracked, then it can be ensured that the hip joint tracks the determined hip trajectories in Cartesian space.

The results of the real-time experiments are given in Figures 7.15 through 7.20. These graphs are the control outputs of the system obtained from the vision-based measuring system in joint space, which are to track the generated ankle, and knee trajectories, i.e references (refer to Figures 7.6, 7.7, 7.9, 7.10, 7.12 and 7.13). Walking duration in Figures 7.15 and 7.16 is five seconds, in 7.17 and 7.18 is 3 seconds whereas in Figures 7.19 and 7.20 is eight seconds.

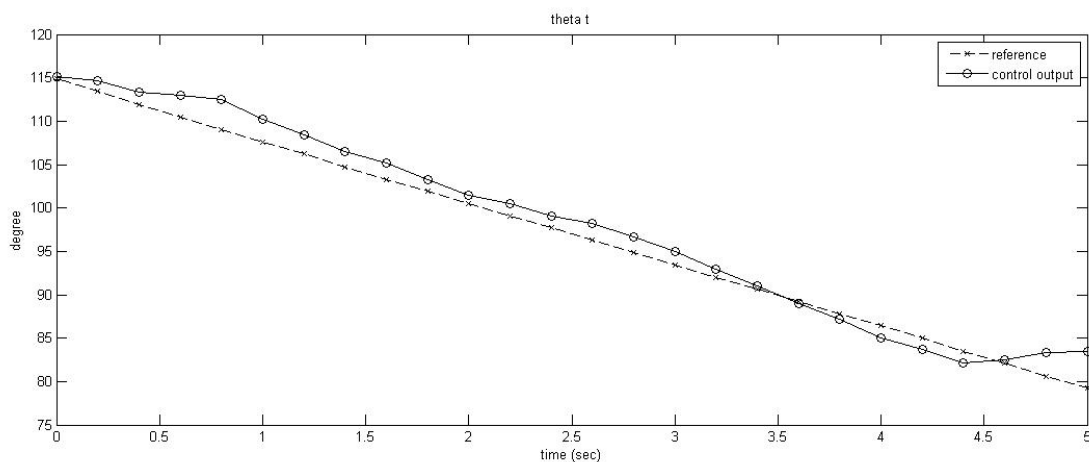


Figure 7.15 Real-time point to point position control output for joint variable θ_1 . Walking duration is 5 seconds.

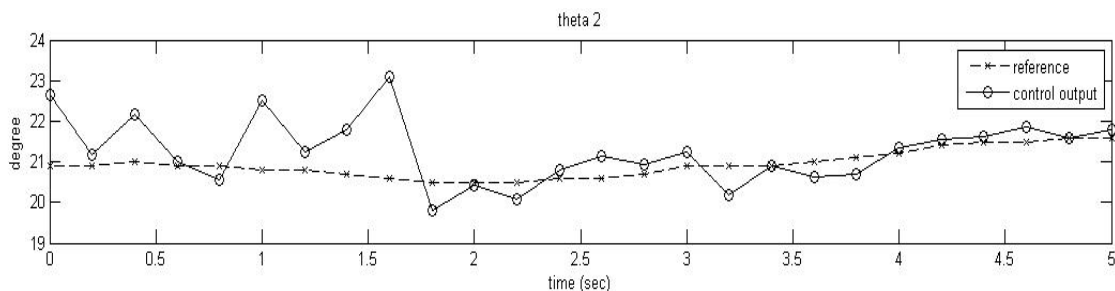


Figure 7.16 Real-time point to point position control output for joint variable θ_2 . Walking duration is 5 seconds.

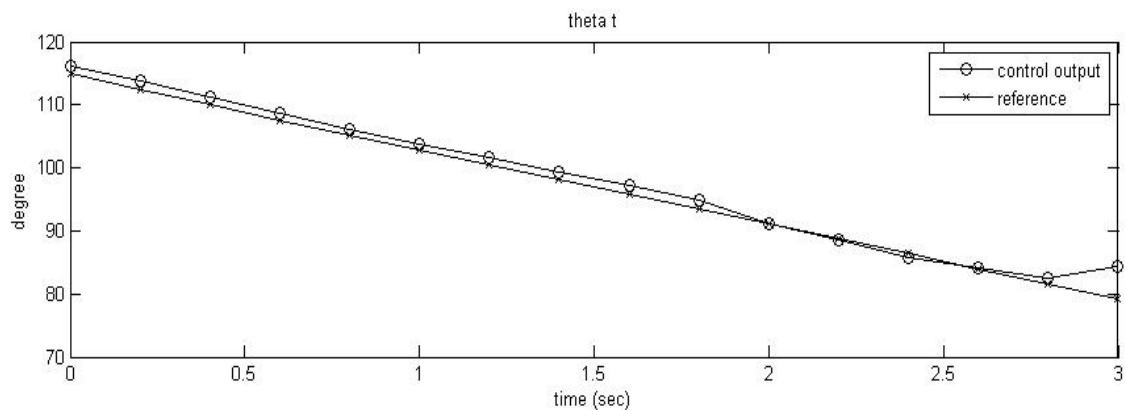


Figure 7.17 Real-time point to point position control output for joint variable θ_t . Walking duration is 3 seconds.

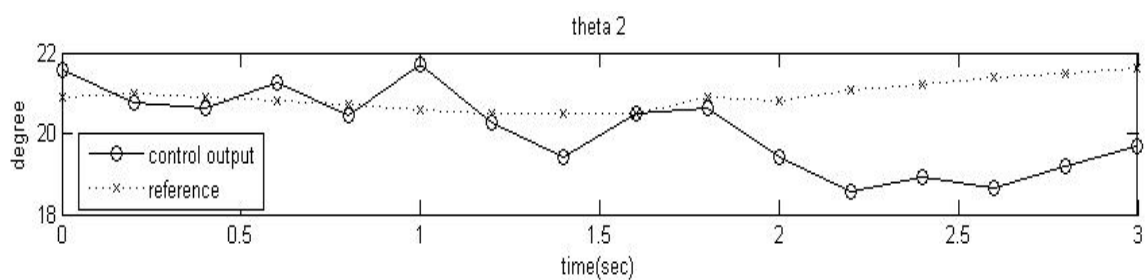


Figure 7.18 Real-time point to point position control output for joint variable θ_2 . Walking duration is 3 seconds.

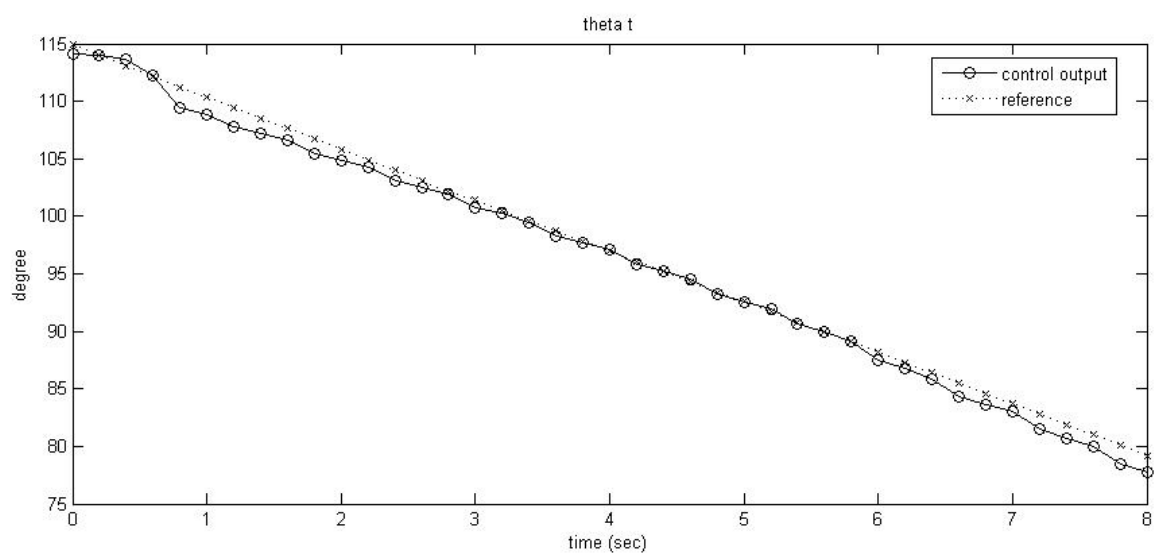


Figure 7.19 Real-time point to point position control output for joint variable θ_t . Walking duration is 8 seconds.

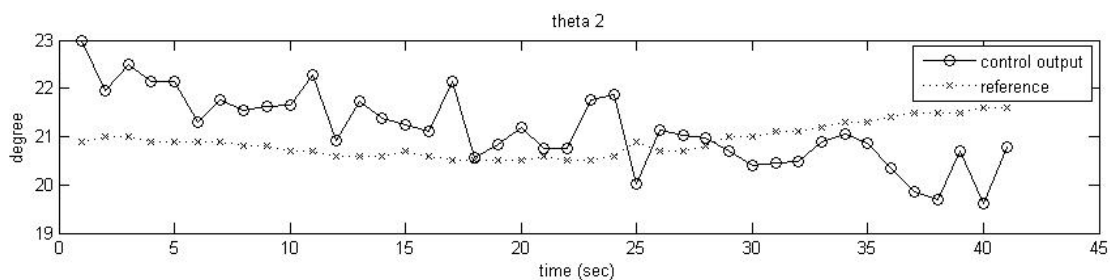


Figure 7.20 Real-Time point to point position control output for joint variable θ_2 . Walking duration is 8 seconds.

7.2 Discussions and Conclusions

In this thesis, studies on bipedal walking phenomenon are separated into two parts: The first part is modelling of bipedal walking which covers deriving the equations of motion for a bipedal walker in 2-D and equations of motion of a walking aiding device (an artificial hybrid leg) as well as developing control methodologies for these two mechanisms. Second part concerns with the application of control algorithms on an experimental setup which is a prototype artificial hybrid leg to be used in transfemoral amputation cases.

In the first part, basic mathematical equations of bipedal walking model are derived. In the mathematical model, it is assumed that walking movement occurs only in sagittal plane, i.e. walking is investigated in two dimensions.

Although, bipedal motion generally takes place in three-dimensional space, the reason to derive the equations of motion in sagittal plane (i.e. in two dimension) is that the main aim of this thesis focuses on the design of an artificial hybrid leg for transfemoral amputees. Since artificial hybrid leg is only responsible for the movements in sagittal plane and that the motion in third dimension is realized by the movement of hip articulation (i.e. control of this movement is achieved by the amputee), equations for sagittal plane motion are adequate to obtain the trajectory of

hip articulation of the amputee which is the reference movement for the artificial hybrid leg.

After obtaining equations of motion of bipedal walking model, dynamics of an artificial hybrid leg to be used on transfemoral amputees is obtained. This system dynamics is very important because as discussed in Chapter 4, feed forward compensation based on disturbance rejection methodology can be achieved by computing the dynamic torques, obtained from system dynamics. These torques are the disturbance inputs to the system being composed of two PMDC motors.

In the second part, explanations about the subsystems of the artificial hybrid leg are given. Also, the experimental setup designed and built for simulating the artificial hybrid leg is described and application of control strategies on this setup is considered.

The results obtained in the simulation of the feed forward compensation strategy with disturbance rejection methodology are given in Figures 7.1 through 7.4. In the simulations, both stance leg and swing leg phases are analyzed. Stance leg response to the given ankle and hip joint reference trajectories are shown in Figures 7.1 and 7.2., whereas swing leg responses are given in Figures 7.3 and 7.4. In the figures, it can be seen that system responses can track the given trajectories with an error of less than 1% which is within the acceptable tolerance boundaries.

Note that these results are taken for a time interval of one step. At the end of first step, the legs exchange the duties; the swing leg becomes the stance leg and stance leg becomes the swing leg. Heel strike and toe-off conditions are not included in these simulations. For this reason the phase exchange conditions are not shown in the figures.

The second group of simulations explained above as very important defines trajectory references for the artificial hybrid leg and are calculated as being based on these simulations. In these simulations, hip trajectory is chosen within the workspace

of the mechanism and by using iterative inverse kinematics techniques, all joint variables are obtained. Since artificial hybrid leg mechanism is a non-linear system, iteration process takes a long time. For this reason, firstly iterative inverse kinematics codes are executed in offline fashion, trajectories are found and after that these trajectories are fed to the controller of the experimental setup in order to realize real-time control application.

Referring to Figure 7.5, it can be seen that the displacement of chosen hip joint trajectory in horizontal direction is rather short, starting from -0.2 meters to 0.2 meters. As for the vertical displacement, it is even shorter (only 0.05 meters). Because of these small position changes in the motion of the joints, angular changes of the joint parameters which are given in Figures 7.6 through 7.14 for different walking speeds seem to have near linear characteristics.

The results of real-time application are given in Figures 7.15 through 7.20. In these Figures, trajectories of ankle and knee joints in joint space are given for different walking durations. As mentioned in the results part, these trajectories are the control output of the system and they are to be compared with the system inputs which are given in Figures 7.6, 7.7, 7.9, 7.10, 7.12 and 7.13.

When the reference and control output trajectories of the ankle joint are compared for different walking durations it can be seen that the control output can track the reference input. Especially when graphs which indicates the walking duration of eight seconds are compared (Figures 7.9 and 7.19), it can be concluded that the output can track the reference input exactly. However, for shorter walking durations, discrepancies can be seen when the system moves from one point to another; but the total error remains within an acceptable range approximately like 1% at the end of the whole walking interval, if $K_p=80$ is chosen for the controller.

As for the control output for the knee joint, there also occur some discrepancies, when the output values are compared with the reference values. The reasons can be given as follows:

The first reason is the working range of the knee joint. For the calculated knee joint trajectory, the angular changes are rather small (total displacement is nearly one degree). When the value for the knee trajectory is changed from one point to another, the variation seems to be even smaller, which cannot be sensed by the potentiometer precisely, even though it is a high precision potentiometer. Thus, potentiometer readings become questionable.

The second reason is the nonlinearities in the system. Since the variation in knee joint is very small compared with the ankle joint, knee joint is more sensible to these nonlinearities. For this reason, sensor attached to the knee joint must have a low margin of error.

The third fact is that, the LEDs used in vision-based measuring system are affected very much from the environmental lightning. The precision of the vision-based measuring system is ± 0.5 degrees which is a large number for the knee joint angular variations.

It can be concluded from the simulation and experimental results obtained in this work that the theory of feed forward compensation methodology with disturbance rejection strategy results with a good control performance. The simulations showed that this control method is applicable to an acceptable degree of accuracy. Different from the studies done by Sciavicco & Siciliano (1996), the torque interface is included in the control structure, which results in a more satisfactory system performance from the point of view of system stability.

Also, it is investigated in the simulation results that a four bar knee mechanism with a longer anterior link allows the amputee to move in a more comfortable and stable way, as mentioned in the studies of Radcliffe (1994), since workspace of the hip joint becomes larger and the artificial leg can realize positions and orientations in a wider range, by extending the anterior link.

As for the real-time application, there appear some problems. The control outputs track the input trajectories with some errors. Thus, improvements must be made in the experimental setup in order to reduce these problems, which follow:

The first improvement proposed is choosing a more convenient hip joint trajectory for the artificial leg. Although the trajectory considered here lets the amputee to walk in a stable way, small variations in the trajectory of knee joint results in the lack of control of the stance phase trajectory. Therefore more suitable trajectories, which can be achieved easily by the artificial leg and which also makes the patient to feel comfortable must be investigated.

The second improvement may be the usage of an encoder for the knee joint measurements. Here, the important point is that the encoder must be attached directly on the knee joint without using any transmission components in order to measure the knee joint variations as precisely as possible.

Lastly, it is proposed that infrared LEDs are to be used in vision-based measuring system. Vision-based measuring system is very sensitive to environmental light which causes disturbances in the measurements. Eliminating light sources from the environment and using the infrared LEDs suppress the disturbances, letting a better measurement.

At the end of this study it can be concluded that the dynamical analysis of bipedal walking undertaken in this work proves to be satisfactory to develop a methodology of control of an artificial hybrid leg as demonstrated by measuring the response of an actual model designed and constructed. If improvements mentioned above are done, the prototype artificial hybrid leg will possibly track a desired hip trajectory in stance leg phase in a more satisfactory way. In the future research work, these improvements are going to be investigated fully and a better control performance will be achieved.

REFERENCES

- Alexander, R.M. (1984). The gaits of bipedal and quadrupedal animals. *International Journal of Robotic Research*, 3(2), 49-59.
- Başer, Ö. (2003). Analysis and Control of Bipedal Human Locomotion, *M.Sc. Thesis*, Dokuz Eylül University, The Graduate School of Natural and Applied Sciences.
- Başer, Ö., Çetin, L., & Uyar, E. (2007). Joint trajectory control of a bipedal robot. In *Proceeding of IFAC Workshop on Technology Transfer in Developing Countries: Automation in Infrastructure Creation- TT*, 215-221, Izmir, Turkey.
- Boonstra, A.M., Schrama, J., Fidler, V., & Eisma, W.H. (1994). The gait of unilateral transfemoral amputees. *Scandinavian Journal of Rehabilitation Medicine*, 26, 217-33.
- Brosilow, C., & Joseph, B. (2002). *Techniques of Model-Based Control*. U.S: Prentice Hall Inc.
- Buckley, J.G., Spence, W.D., & Solomonidis, S.E. (1997). Energy cost of walking: Comparison of “intelligent prosthesis” with conventional mechanism. *Archives of Physical Medicine and Rehabilitation*, 78, 330–333.
- Capek, K. (1921). *R.U.R Rossum’s universal robots*. Theatre play.
- Capi, G., Nasu, Y., Barolli, L. & Mitobe, K. (2003). Real time gait generation for autonomous humanoid robots: A case study for walking. *Robotics and Autonomous Systems*, 42, 107-116.
- Carbone, G., Lim, H., Takanishi, A., & Ceccarelli, M. (2006). Stiffness analysis of biped humanoid robot WABIAN-RIV. *Mechanism and Machine Theory*, 41(1), 17-40.

- Chin T, Sawamura S, Shiba R, Oyabu, H., Nagakura, Y., & Nakagawa, A. (2005). Energy expenditure during walking in amputees after disarticulation of the hip. *Journal of Bone and Joint Surgery*, 87, 117–119.
- Darwin, C. (1871). *The descent of man and selection in relation to sex* (reprinted in 1981). Princeton: Princeton University.
- De Silva, C.W. (2005). *Mechatronics: An integrated approach*. Washington D.C.: CRC Press.
- Frasca, M., Arena, P., & Fortuna, L. (2004). *Bio-inspired emergent control of locomotion systems*. London: World Science.
- Fukuda, T., Michelini, R., Potkonuak, V., Tzafestas, S., Valavanis, K. & Vukobratovic, M. (2001). How far away is “Artificial Man”? *IEEE Robotics & Automation Magazine*, 8 (1), 66-73.
- Grotjahn, M., & Heimann, B. (2002). Model-based feed-forward control in industrial robotics. *The International Journal of Robotics Research*, 21, 45-60.
- Hirai K. (1997). Current and future perspective of Honda humanoid robots. *In Proceedings of International Conference on Intelligent Robots and Systems*, 500-508, Grenoble, France.
- Hirokawa, S. (1989). Normal gait characteristics under temporal and distance constraints. *Journal of Biomedical Engineering*, 11(6), 449–456.
- Hosoda, K., Takuma, T., Nakamoto, A., & Hayashi, S. (2008). Biped robot design powered by antagonistic pneumatic actuators for multi-modal locomotion. *Robotics and Autonomous Systems*, 56(1), 46-53.
- Howe, R.D., & Matsuoka, Y. (1999). Robotics for surgery. *Annual Review of Biomedical Engineering*, 1, 211-240.

- Hurmuzlu, Y., & Moskowitz, G. D. (1986). The role of impact in the stability of bipedal locomotion. *International Journal of Dynamics and Stability of Systems*, 1(3), 217–234.
- Hurmuzlu, Y., & Moskowitz, G. D. (1987). Bipedal locomotion stabilized by impact and switching. I. Two- and three-dimensional, three-element models. *International journal of Dynamics and Stability of Systems*, 2(2), 73–96.
- Juricic, D., & Vukobratovic M. (1972). Mathematical Modeling of a Bipedal Walking System. *ASME Publications*, 72 (13), 26-30.
- Katic, D., & Vukobratovic, M. (2004). Intelligent control of humanoid robots using neural networks. *7th Seminar on Neural Network Applications in Electrical Engineering*, 31-38, Belgrade, Serbia.
- Kirk, N.T. (1943). *Amputations*. Hagerstown, MD: WF Pryor.
- Kwoh, Y.S., Hou, J., & Jonckheere, E.A. (1988). A robot with improved absolute positioning accuracy for CT guided stereotactic brain surgery. *IEEE Transactions on Biomedical Engineering*, 35, 153-161.
- McGeer, T. (1990). Passive dynamic walking. *International Journal of Robotic Research*, 9(2), 62–82.
- McKerrow, P.J. (1991). *Introduction to robotics*. Sydney: Addison-Wesley Publishing Company, Inc.
- Michael, J.W. (1999). Modern prosthetic knee mechanisms. *Journal of Clinical Orthopedics and Related Researches*, 361, 39–47.
- Necsulescu, D. (2002). *Mechatronics*. New Jersey: Prentice Hall Inc.
- Paluska, D., & Herr, H. (2006). The effect of series elasticity on actuator power and work output: Implications for robotic and prosthetic joint design. *Robotics and Autonomous Systems*, 54 (8), 667-673.

- Park, J., & Chung, H. (1999). ZMP compensation by on-line trajectory generation for biped robots. *In Proceedings of IEEE Conference on Systems, Man and Cybernetics (SMC'99)*, 960-965, Tokyo, Japan.
- Perry, J., Burnfield, J.M., Newsam, J.C. & Conley, P. (2004). Energy Expenditure and gait characteristics of a bilateral amputee walking with “C-Leg” prostheses compared with stubby and conventional articulating prostheses. *Archives of Physical Medicine and Rehabilitation*, 85, 1711-1718.
- Pinzur, M.S., & Bowker, J.H. (1999). Knee disarticulation. *Journal of Clinical Orthopedics and Related Researches*, 361, 23-28.
- Pinzur, M.S., Gold, J., Schwartz, D., & Gross, N. (1992). Energy demands for walking in dysvascular amputees as related to level of amputation. *Orthopedics*, 15, 1033–1037.
- Pinzur, M.S., Slosar, P.J., Jr, Reddy, N.K., & Osterman, H. (1992). Through knee amputation in peripheral vascular insufficiency: functional outcome. *Contemporary Orthopedics*, 24, 157–160.
- Radcliffe, C.W. (1994). Four-bar linkage prosthetic knee mechanism: Kinematics, alignment and prescription criteria. *Journal of Prosthetics and Orthotics International*, 18, 159-173.
- Raibert, M., Chepponis, M., & Brown Jr., H. (1986). Running on four legs as though they were one. *IEEE Transactions on Robotics and Automation*, 2 (2), 70-82.
- Raibert, M., Tzafestas, S., & Tzafestas, C. (1993). Comparative simulation study of three control techniques applied to a biped robot. *In Proceedings of the IEEE International Conference on Systems, Man and Cybernetics*, 494-502, Washington D.C., U.S.A.
- Sciavicco, L., & Siciliano, B. (1996). *Modeling and control of robot manipulators*. New York: McGraw Hill.

- Seo, Y.J., & Yoon, Y.S. (1994). Design of a robust dynamic gait of the biped using the concept of dynamic stability margin. *Robotica*, 13, 461-468.
- Stepanenko, Y. (1970). Method of analysis of spatial lever mechanism. *Mechanics of Machines*, 23, 117-124.
- Sugihara, T., Nakamura, Y., & Inoue, H. (2002). Real-time humanoid motion generation through ZMP manipulation based on inverted pendulum control. *In Proceedings of the 2002 IEEE International Conference on Robotics and Automation*, 1404-1409, Washington D.C. U.S.A.
- Tang, P.C.Y, Ravji, K., Key, J.J., Mahler, D.B., Blume, P.A & Sumpio, B. (2008). Let them walk! Current prosthesis options for leg and foot amputees. *Journal of the American College of Surgeons*, 206 (3), 548-560.
- Vukobratovic, M. (1975). *Legged locomotion robots and anthropomorphic mechanisms*. Belgrade: Mihailo Pupin Institute.
- Vukobratovic, M., Brovac, B., Surla, D., & Stokic, D. (1990). *Biped Locomotion – Dynamics, Stability Control and Applications*. New York: Springer Verlag.
- Vukobratovic, M., Frank, A.A., & Juricic, D. (1970). On the stability of biped locomotion. *IEEE Transactions on Biomedical Engineering*, 17 (1), 25-36.
- Vukobratovic, M., Juricic, D. (1969). Contribution to the synthesis of biped gait. *IEEE Transactions on Biomedical Engineering*, 16(1), 1-6.
- Vukobratovic, M., & Stepanenko, Y. (1973). Mathematical models of general anthropomorphic systems. *Mathematical Biosciences*, 17, 191-242.
- Webb, B., & Consi, T. R. (2001). *Biorobotics*, Cambridge: MIT Press.
- Yamashita, T. (1987). A study of dynamics in initiation and stopping of human gait. *In Proceedings of the 7th World Congress: Theory of Machines and Mechanisms*, 1837–1840, Sevilla, Spain.

Zheng, Y.-F., & Hemami, H. (1984). Impact effects of biped contact with the environment. *IEEE Transactions on System, Man, and Cybernetics*, 14(3), 437–443.